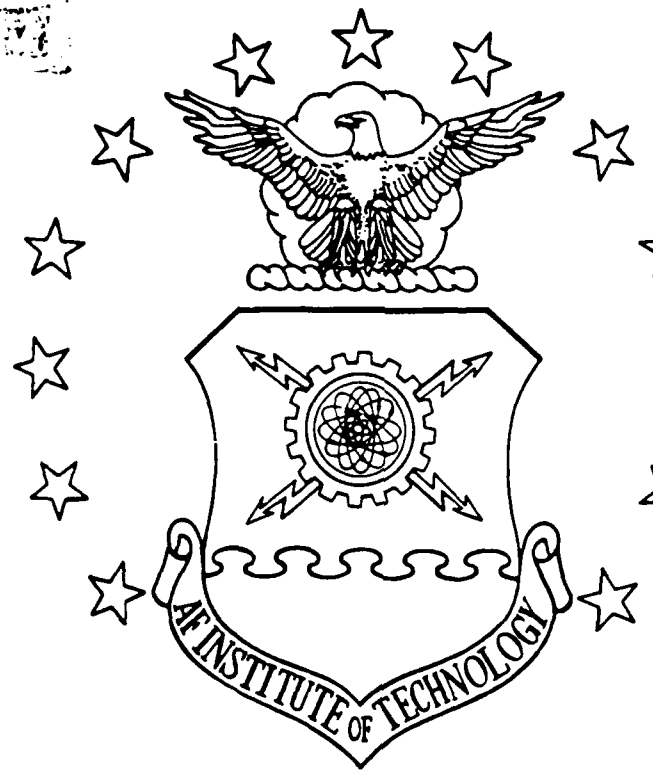

THE EFFECT OF LOADING ON THE LASER ABLATION OF GRAPHITE/ EPOXY COMPOSITE MATERIAL

THESIS

Joseph L. Hamrick, II
Captain, USAF

AFIT/GAE/ENY/89D-12

DEPARTMENT OF THE AIR FORCE
AIR UNIVERSITY
AIR FORCE INSTITUTE OF TECHNOLOGY

Wright-Patterson Air Force Base, Ohio

AFIT/GAE/ENY/89D-12

THE EFFECT OF LOADING ON THE LASER ABLATION OF GRAPHITE/EPOXY COMPOSITE MATERIAL

THESIS

Presented to the Faculty of the School of Engineering
of the Air Force Institute of Technology
Air University
in Partial Fulfillment of the
Requirements for the Degree of
Master of Science in Aeronautical Engineering

Joseph L. Hamrick,II, BS
Captain, USAF

December 1989

Preface

This research was initiated to fill a gap in existing knowledge about the mechanical processes which cause the removal of solid matter from fiber-reinforced composite materials during ablation. The effect these processes have upon the energy required to remove the mass is of interest to anyone trying to predict the effect of thermal radiation on load-bearing composite structures.

Dr. George Sendeckyj of the Wright Research and Development Center's Flight Dynamics Laboratory suggested the problem, and has provided valuable assistance to me in this research. Mr. F. E. Barnett of WRDC Materials Laboratory provided important financial and facility support to the work. 1st Lt Dave Felker and his coworkers in WRDC/FIBCA were essential in the fabrication of the experimental specimens.

I'm especially indebted to Capt Jerry R. Couick and the Rockwell Power Services contractors at the Air Force Weapons Laboratory for their test facility support.

Thanks also to my thesis committee; Dr. Peter J. Torvik, Lt Col Ronald L. Bagley and Dr. Shanker Mall. And also to Jay Anderson and Dan Rioux for much needed technical support. The technicians in WRDC/FIBTA were also very helpful.

Most importantly, all praise and honor to my Saviour Jesus Christ for (among many things) the fact that I was selected for this program and given the strength to complete it.

Table of Contents

List of Figures

List of Tables

Notation

A Coefficient of elastic line solution in section AB

B " " " " " " " "

C' " " " " " " " BC

D' " " " " " " " "

$\vec{q}$ → heat flux $\left[\frac{W}{m^2}\right]$

$\hat{n}$ → outward normal unit vector

dA → element of surface area (m^2)

g → heat generation (W/m^3)

dV → element of volume (m^3)

ρ → mass density (kg/m^3)

ρ_t → radius of curvature due to temperature gradient (cm)

C_p → specific heat at constant pressure ($J/kg \cdot K$)

T → temperature (degrees Kelvin)

t → time (seconds)

$K_{ij}, \overline{K}$ → conductivity tensor

I,J,K → row, column and layer of volume element and/or temperature node

L,M,N → number of rows, columns and layers used to divide region V

Q^* → effective enthalpy of ablation $\left[\frac{kJ}{gm}\right]$

I → laser irradiance $\left[kW/cm^2\right]$

η_d → efficiency of discrete mass removal

m → mass (gm)

α → layup angle

σ_x → axial stress (psi, MPa)

M → bending moment (in·lb, N·m)

d → diameter of graphite fiber (cm)

E_i → Young's moduli (psi, MPa)

ε° → strain of laminate midsurface

Q_{ij}, $\bar{Q}_{ij}$ → anisotropic stiffnesses (psi, MPa)

z → depth below laminate midsurface (cm)

N_x → axial load per unit width (lb/in, N/m)

$\varepsilon_{f_{ult}}$ → strain at failure for a fiber

$\mathcal{E}$ → energy (kJ)

K_I → mode 1 stress intensity factor ($lb \cdot in^{3/2}$, $kg/mm^{3/2}$)

V_i → volume fraction of component i

χ_i → mass fraction of component i

Abstract

The purpose of this investigation was to quantify the effect initial structural loading of a graphite/epoxy member has upon the mass removal rate during laser ablation. The effective heat of ablation (Q^*_{eff} = energy absorbed/mass removed) was used as a measure of this efficiency. A simple physical model of the important factors affecting the graphite/epoxy was developed, and predictions were made of the effect of loading on Q^*_{eff} .

A three-dimensional finite difference heat transfer code was written to predict the temperature distribution in the composite. The orthotropic nature of the thermal conductivity tensor in the plys was modeled, to accurately model the heat flow from the irradiated region.

The effect of thermal and mechanical loads upon the stress distribution in a single fiber was calculated, and a linear decrease in Q^*_{eff} with increasing stress was predicted. The coefficient of increasing ablation efficiency, (η_d), was postulated to increase linearly with axial stress σ_x. This was based upon the hypothesis that fracture of individual fibers will be a process linearly dependent upon applied stress, and will remove a fraction of the composite's mass without requiring the absorption of laser energy.

Uniaxial tensile coupons were fabricated from Hercules AS4/3502 graphite/epoxy prepreg, in balanced, symmetric laminates laid up in a pattern of $(0/+60/-60)_{ns}$. These specimens were place under tensile loads between 0% and 50% of the laminate's fracture strength. While under fixed grip loading conditions, they were irradiated with a 10.6 μm device at irradiances between 5 and 26 kW/cm^2.

Linear regression of data taken at ~15kW/cm^2 calculated η_d = 0.013 kJ/gm + 1.74(kJ/gm)/GPa*σ_x. At 26 kW/cm^2, η_d = 0.087 kJ/gm + 3.36(kJ/gm)/GPa*σ_x. Therefore, it may be concluded that axial fiber stress does linearly decrease the 10.6 μm laser energy needed to ablate AS4/3502 graphite/epoxy. The total effect seen in this study was less than 20 percent of the unloaded value.

It is recommended that further analytic modeling of the interaction between applied load and fiber fracture be undertaken to allow prediction of η_d values for different materials without the collection of experimental data.

THE EFFECT OF LOADING ON THE LASER ABLATION OF GRAPHITE/EPOXY COMPOSITE MATERIAL

I. Introduction

The laser-induced ablation of fiber-reinforced composite materials has been studied extensively. However, the majority of experiments performed have been on samples of material without any externally applied loads (5,19). Since most structures of interest do bear loads, the effect of these loads on the phenomenon of ablation is important in understanding the interaction between laser radiation and structures.

Although load enhancement of mass removal rates has been observed experimentally (17), little, if any, analytical modeling of laser ablation phenomena has included appropriate mechanical processes to explain this observation (19).

Also, global structural instability has typically been modeled as simple degradation of material strength properties at elevated temperatures (19). This approach is clearly not applicable to simple mass removal, which takes place under no load in materials needing no structural strength (2).

Examination of solid particles ejected from ablating graphite/epoxy composite during the Very High Irradiance (HI-I) and Screening Test Series (STS-1) tests (2,18) indicated that 'rafts' of solid laminae, on the order of 1000-5000 microns were ejected from ablating samples. This was under conditions of no pre-loading. It is conjectured that if the state of the ablation surface is such that discrete volumes of material can be broken off and ejected without being vaporized by laser radiation, any increased stress due to applied loads will increase the rate of material fracture. This would have the effect of allowing more mass to be removed discretely, and lower the apparent heat of ablation (Q^*_{eff}).

II. Theoretical Analysis

Temperature Distribution

The prediction of stress states in the sample requires a knowledge of the temperature distribution created in the sample due to laser heating as well as the loading distribution. Various one- (1D) and two-dimensional (2D) finite difference schemes have been used in the past (5,13-16). However, the detailed knowledge of temperature gradients needed to predict the fracture mechanics of the fibers suggests a three-dimensional (3D) model is needed. The anisotropic nature of the composite material also contributes to this necessity.

The conservation of energy on a infinitesimal control volume leads to the differential equation of heat conduction in a solid (10:5). Left in terms of a finite control volume it is

$$-\int_A \vec{q} \cdot \hat{n}\, dA + \int_V g\, dV = \int_V \rho C_p \frac{\partial T}{\partial t}\, dV \qquad (1)$$

where

$$-\int_A \vec{q} \cdot \hat{n}\, dA = \text{heat flux through boundaries of V} \qquad (2)$$

$$\int g\, dV = \text{heat generation in V} \qquad (3)$$

$$\int \rho C_p \, \partial T/\partial t \, dV = \text{rate of energy storage within volume V} \qquad (4)$$

The heat flux term, $\vec{q}$, for an isotropic solid, is proportional to the temperature gradient, $\vec{q} = -k\vec{\nabla}T$. For the anisotropic case, k is not a constant, but a second order tensor (10:612)

$$q_i = - K_{ij} \frac{\partial T}{\partial x_j} \qquad (5)$$

A discretization of the volume of interest into small elements (rectangular prisms were used for simplicity in this case, although other schemes are possible) yields an explicit value for the temperature rise, dT, at each element during a small interval of time, dt. This rise is added to the existing temperature of the element, and then the process is repeated for the next time interval. Phase changes, ablation and temperature dependent properties may be incorporated for each element.

Neglecting heat generation and substituting Equation (5) into Equation (2), and approximating derivatives with first order terms, yields the following equations for the energy flux into an element of volume V_{IJK}.

$$q_{x_{I,J,K}} = K_{11} \left[\frac{T_{I,J,K} - T_{I+1,J,K}}{\Delta x}\right] \Delta y \, \Delta z + K_{12} \left[T_{I,J,K} - T_{I,J+1,K}\right] \Delta z \qquad (6a)$$

$$q_{y_{I,J,K}} = K_{12}\left(T_{I,J,K} - T_{I+1,J,K}\right)\Delta z + K_{22}\frac{\left(T_{IJK} - T_{I,J+1,K}\right)}{\Delta y}\Delta x\ \Delta z \quad (6b)$$

$$q_{z_{I,J,K}} = K_{33}\frac{\left(T_{I,J,K} - T_{I,J,K+1}\right)}{\Delta z}\ \Delta x \Delta y \quad (6c)$$

where the zero elements of $\overline{\overline{K}}$ have been left out.

To compute the temperatures in a region divided into L rows, M columns and N layers, an (L+2) x (M+2) x (N+2) array of temperature nodes was created. Nodes on the extremities were set identically equal to their closest neighbors on the inside. This ensured zero flux (due to zero temperature gradient) on all boundaries, creating insulated boundary conditions.

The only energy input into the volume came from absorbed laser flux, which was added to each face exposed to the irradiance.

Like 1D and 2D explicit schemes the size of time interval, dt, is constrained to be less than a critical value for stability. As suggested by Torvik (13:13), a conservatively stable time increment was chosen by using the smallest dt necessary. That is, the smallest distance increment of the three possible was used to calculate dt.

Existing data on high temperature thermal properties of AS4/3502 are extremely scarce. Data for similar materials were collected and applied (3,5,8,19). Thermal property

data on AS4/3501-6 composite is much more prevalent, and has been used interchangeably with that available on AS4/3502 in this work. The computer code applies these properties as a function of temperature through the point where data are available. For temperatures above those where data exist, the last recorded value of the property is maintained.

In a one dimensional fiber reinforced epoxy laminae, the principal directions of thermal conductivity are obviously along the fiber, normal to the fiber in the plane of the laminae, and normal to the plane of the laminae (Figure 1). The conductivity , K_{11} , in the direction along the fiber, $\hat{e}_1$, is dominated by the conductivity of the fiber itself. Data for this conductivity are approximated by the High Temperature Materials Information Analysis Center (HTMIAC) (8). The data is calculated by a parallel conductor analysis using 13 W/m*°K for fiber conductivity, and an isotropic conductivity value for the matrix resin.

It is assumed that in the cured laminate, fiber to matrix ratios will be similar in the laminae plane, $\hat{e}_2$, and normal to them, $\hat{e}_3$. Therefore, laminate conductivities K_{22} and K_{33} are assumed to be equal.

In the layers laid at $\pm \alpha$ (60 degrees in this case), the principal directions no longer coincide with the global axes, and the conductivity tensor is no longer diagonal.

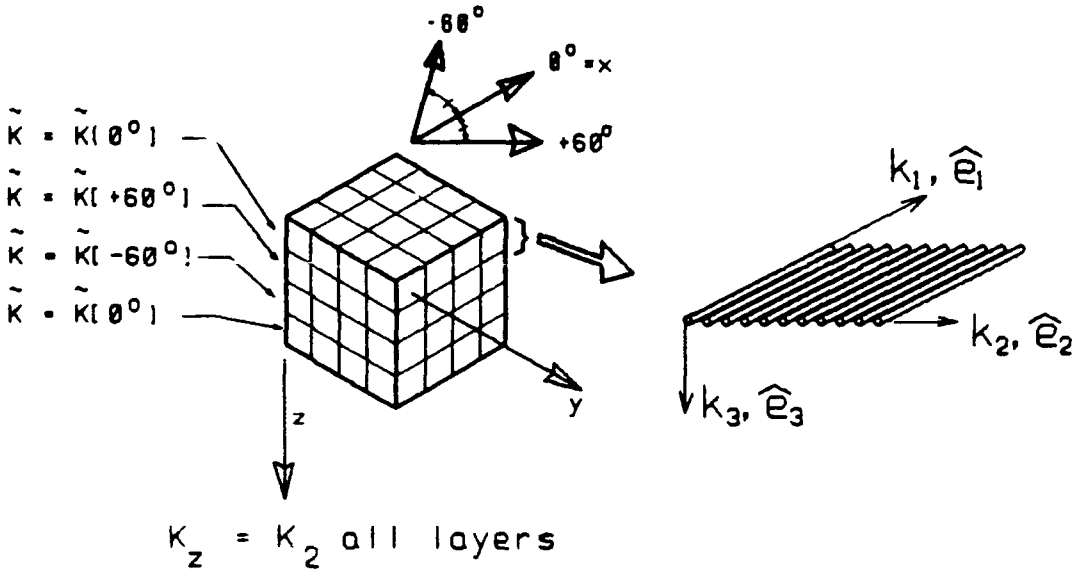

Figure 1. Thermal Conductivity in Orthotropic Laminae

The conductivity values in the rotated layers are found by the second order tensor transformation (11).

$$K'_{ij} = a_{ik}\, a_{jl}\, K_{kl} \tag{7}$$

where

K'_{ij} is the tensor in the rotated axes $\hat{e}'_1, \hat{e}'_2, \hat{e}'_3$

K_{kl} is the tensor in the principal axes $\hat{e}_1, \hat{e}_2, \hat{e}_3$

a_{ik} is the direction cosine between the $\hat{e}_k$ and $\hat{e}'_i$ axes

Letting A_{ik} be a matrix of the direction cosines a_{ik}, Equation (7) can be written:

$$K'_{ij} = A_{ik} K_{kl} A^{T}_{jl} \tag{8}$$

For the rotation of the sample in the laminate described, this leads to two non-diagonal values:

$$K_{12} = K_{21} = (K_{11} - K_{22}) \cos\alpha \sin\alpha \qquad (9)$$

The only conductivity terms calculated in the computer code used for this project are these and terms on the diagonal. It would be a simple matter to calculate and include the remaining terms if necessary, to provide for totally anisotropic constructions.

The material properties of each element in the region are calculated for the current temperature. The flux components are then estimated from the current temperature distribution, using Equations (6). Equation (1) is then solved for the incremental temperature change, ΔT. This increase in temperature is then added to the cell's current value, and the region is checked for the onset of phase change.

This phase change is ablation in this case, but it might also be melting or sublimation in the case of other materials. When the phase change temperature is exceeded, the amount of energy absorbed is subtracted from the cell's total phase-change energy, and the temperature is set back to the phase change temperature. If the cell's energy of phase change is exceeded during this check in later iterations, the cell is 'removed' from the calculations by

having its conductivities multiplied by zero in the following iterations.

The current code using this algorithm is listed in Appendix A. It remains predominately stable by the criterion that temperatures monotonically decrease from the irradiated regions toward insulated boundaries. This is the case for all but one or two cells, which remain 5 or 6 degrees below the initial temperature imposed upon the region; but no adjacent cells suffer this anomaly, and the remainder of the region's temperature values increase as expected even at long run times (high iteration count).

No further investigation was made into this difficulty since the code agrees within 5 percent with simple 1D and closed-form analytic predictions of the temperature profile through the thickness (Figure 2). It also predicts experimental results (Figure 3) and the reverse temperature gradient was found to decrease with increasing mesh refinement.

Stress Distribution in a Single Fiber

Once the temperature distribution has been calculated, the mechanical response of the fibers will be determined. It is expected that fracture of the fibers will occur at stresses below their ultimate strength due to growth of cracks. Initial cracks in the fiber exist in some distribution. Thermal expansion stresses may cause fracture of some fraction of the fibers by forcing unstable

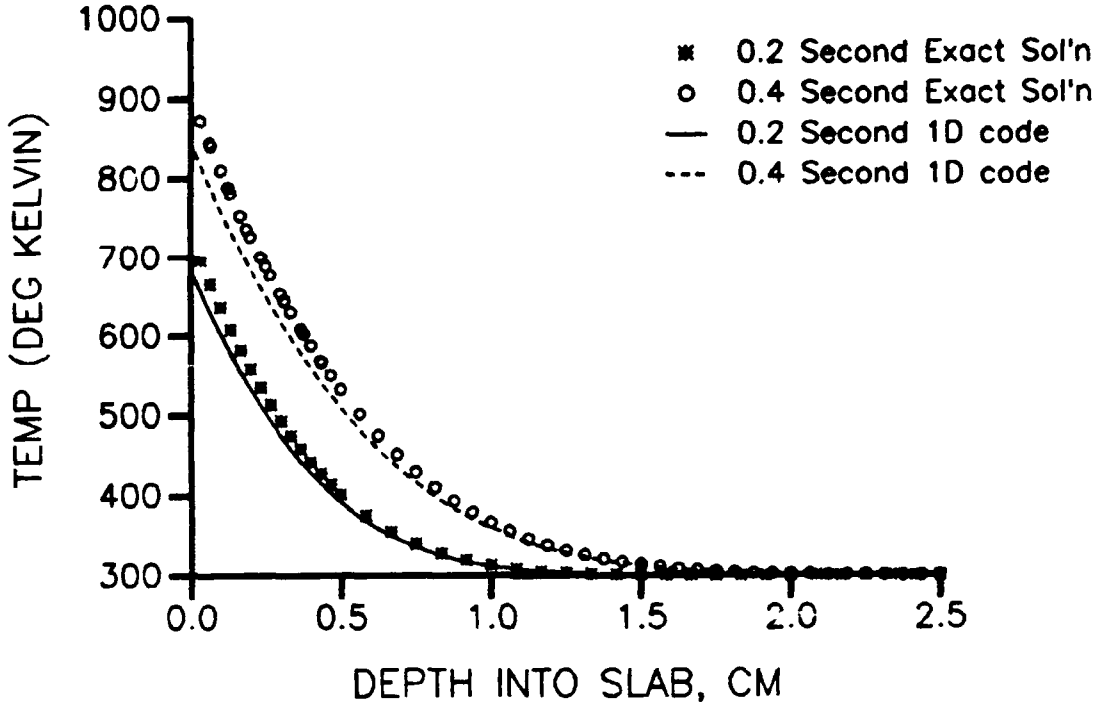

(a) Semi-Infinite Solution vs. 98 Node 1D Code

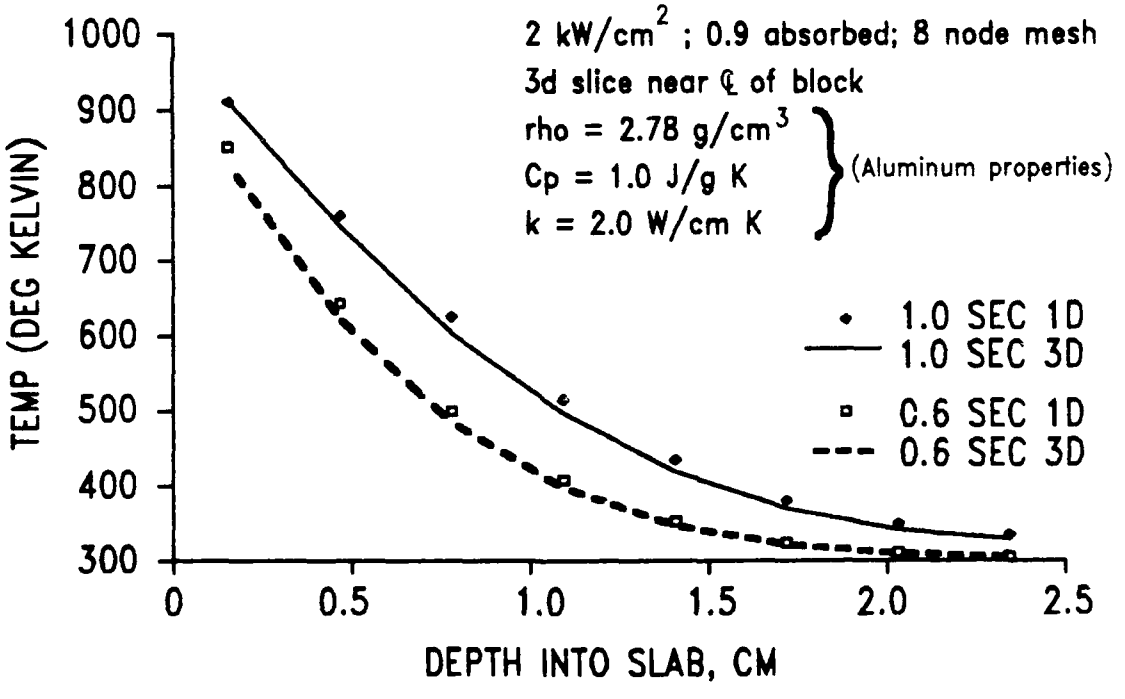

(b) 1D Code vs. 3D Code

Figure 2. Comparison of Various Finite Difference Temperature Predictions

growth of these cracks. This is assumed because of the evidence of discrete fiber removal from various composite materials with no applied loads (2).

To calcu'ate the stress growing the cracks, σ_x, (Figure 4) the fibers will be modeled as single beams laying on an elastic foundation (Figure 5). This is to include the influence of the resin layer beneath the fibers.

Modeling of Single Graphite Fiber

Elementary beam theory provides the following equations for stresses in a prismatic bar (4:214):

$$\sigma_x = \frac{M \cdot z}{I} \tag{10}$$

To find this moment, a single graphite fiber will be modeled as a round Bernoulli-Euler beam with two distinct regions. One region extends from the centerline to the edge of the laser beam. The next region extends beyond the edge of the laser beam into the unheated remainder. This region is many orders of magnitude longer than the fiber diameter, d, so that the fiber may be considered to extend semi-infinitely (Figure 6).

The axial stress in a fiber due to an axial load is simply the load divided by the fiber cross-sectional area,

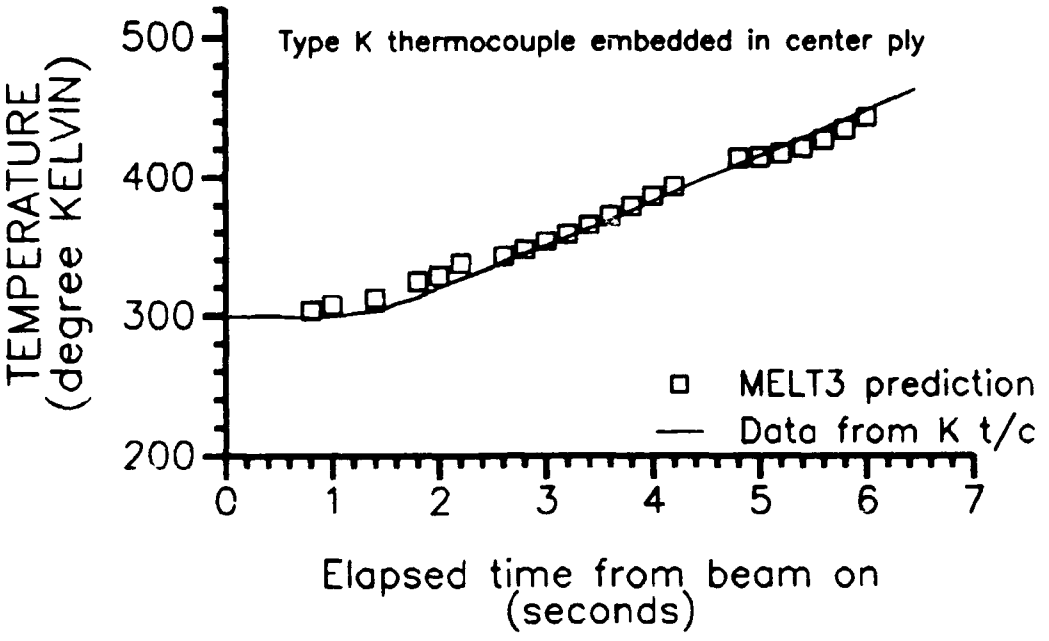

Figure 3. Comparison of MELT3D Predictions with Experimental Data

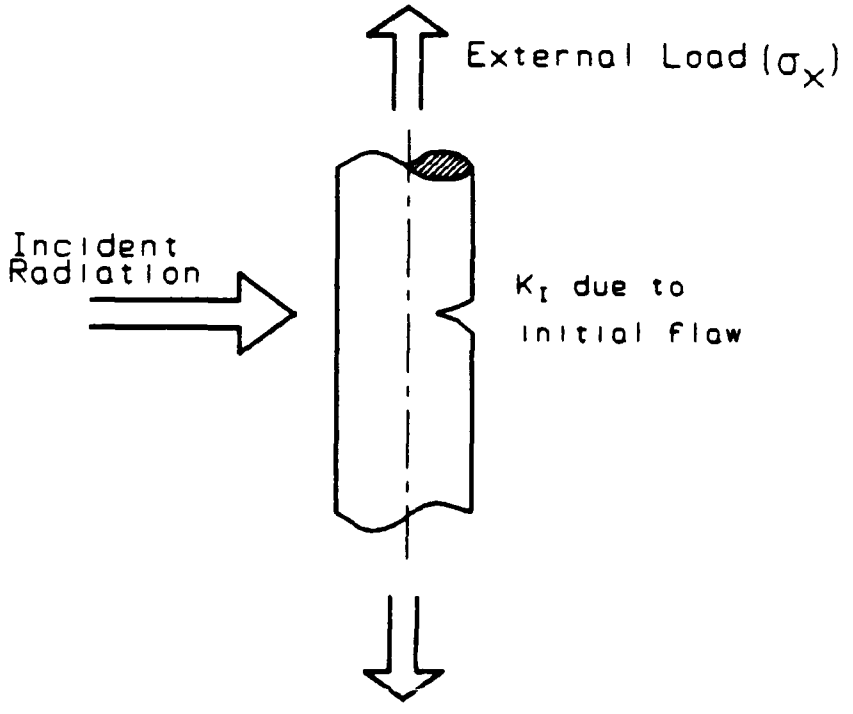

Figure 4. Single Graphite Fiber

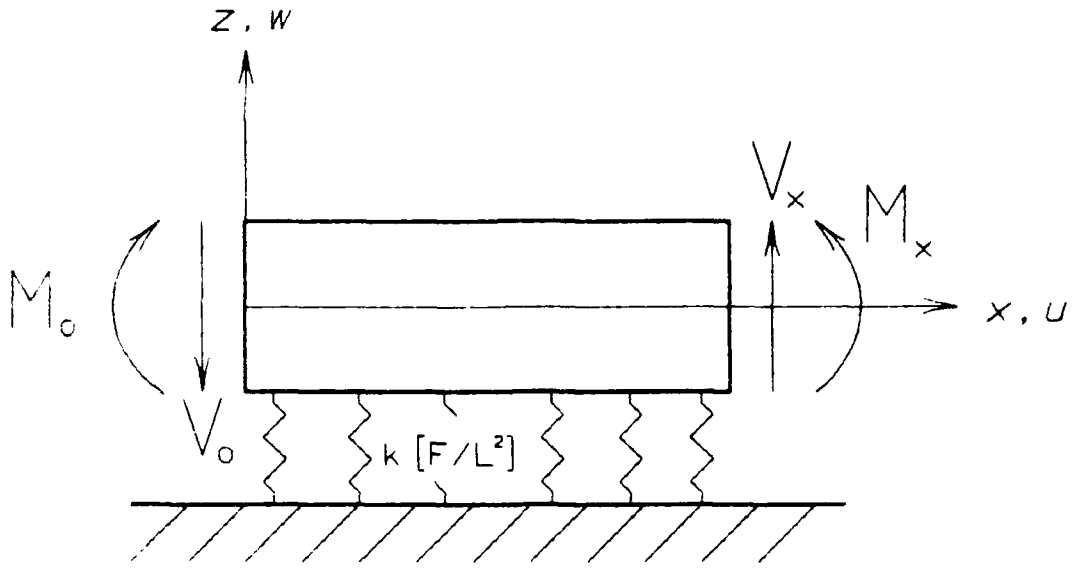

Figure 5. Beam Element on Elastic Foundation

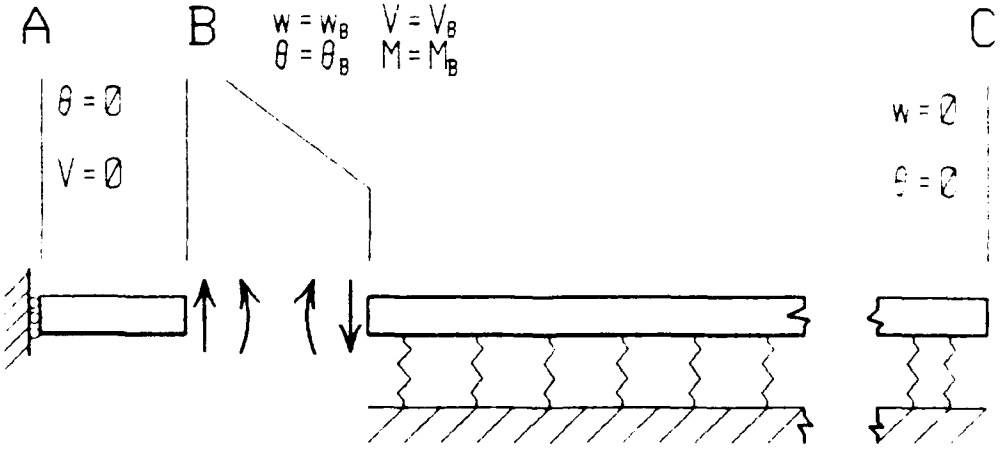

Figure 6. End Conditions for Beams AB and BC

if shearing on the matrix/fiber surface interface is ignored. While this shear is the only physical mechanism for transfering load to the fiber, the remainder of the analysis will be concerned with the heated region after the matrix may be considered to have been removed by pyrolysis. This means all the load will be transferred to a fiber by interaction with the matrix in the region away from the actual laser spot, so simple uniaxial stress is assumed.

The actual value of this stress in a single fiber is found by calculating the total strain the laminate will experience, and imposing this strain on a single fiber

$$\sigma_x = E_{fiber}\ \varepsilon^{\circ} \qquad (11)$$

where ε° is the strain of the mid-surface (which is the strain everywhere in the cross section, because balanced, symmetric laminates do not couple axial strains and midplane bending).

Although the stresses in the direction of the fiber, σ_x, will actually be the sum of axial and bending moment components, for the conditions being explored in this effort, the stresses due to bending are insignificant compared to stresses due to axial loads. See Appendix B for details of this analysis.

Stress Distribution in the Laminate (9)

In a given ply of the laminate, the plane stress $\left(\sigma_z = \tau_{xz} = \tau_{yz} = 0\right)$ constituitive law can be written as

$$\begin{Bmatrix} \sigma_1 \\ \sigma_2 \\ \tau_{12} \end{Bmatrix} = \begin{bmatrix} Q_{11} & Q_{12} & 0 \\ Q_{12} & Q_{22} & 0 \\ 0 & 0 & Q_{66} \end{bmatrix} \begin{Bmatrix} \varepsilon_1 \\ \varepsilon_2 \\ \gamma_{12} \end{Bmatrix}$$

where the reduced stiffnesses Q_{ij} are

$$Q_{11} = \frac{E_1}{1 - \nu_{12}\nu_{21}}$$

$$Q_{12} = \frac{\nu_{12}E_2}{1 - \nu_{12}\nu_{21}} = \frac{\nu_{21}E_1}{1 - \nu_{12}\nu_{21}}$$

$$Q_{22} = \frac{E_2}{1 - \nu_{12}\nu_{21}}$$

$$Q_{66} = G_{12}$$

and for a lamina at an angle θ with respect to the structural axes, the stress-strain relations in terms of "transformed reduced stiffnesses" $\bar{Q}_{ij}$ are

$$\begin{Bmatrix} \sigma_1 \\ \sigma_2 \\ \tau_{12} \end{Bmatrix} = \left[\bar{Q}\right] \begin{Bmatrix} \varepsilon_x \\ \varepsilon_y \\ \gamma_{xy} \end{Bmatrix} = \begin{bmatrix} \bar{Q}_{11} & \bar{Q}_{12} & \bar{Q}_{16} \\ \bar{Q}_{12} & \bar{Q}_{22} & \bar{Q}_{26} \\ \bar{Q}_{16} & \bar{Q}_{26} & \bar{Q}_{66} \end{bmatrix} \begin{Bmatrix} \varepsilon_x \\ \varepsilon_y \\ \gamma_{xy} \end{Bmatrix} \quad (12)$$

in which (13)

$$\bar{Q}_{11} = Q_{11}\cos^4\theta + 2\left(Q_{12} + 2Q_{66}\right)\sin^2\theta\cos^2\theta + Q_{22}\sin^4\theta$$

$$\bar{Q}_{12} = \left(Q_{11} + Q_{22} - 4Q_{66}\right)\sin^2\theta\cos^2\theta + Q_{12}\left(\sin^4\theta + \cos^4\theta\right)$$

$$\bar{Q}_{22} = Q_{11}\cos^4\theta + 2\left(Q_{12} + 2Q_{66}\right)\sin^2\theta\cos^2\theta + Q_{22}\sin^4\theta$$

$$\bar{Q}_{16} = \left(Q_{11}+Q_{12}-2Q_{66}\right)\sin\theta\cos^3\theta + \left(Q_{12}-Q_{22}+2Q_{66}\right)\sin^3\theta\cos\theta$$

$$\bar{Q}_{26} = \left(Q_{11}+Q_{12}-2Q_{66}\right)\sin^3\theta\cos\theta + \left(Q_{12}-Q_{22}+2Q_{66}\right)\sin\theta\cos^3\theta$$

$$\bar{Q}_{66} = \left(Q_{11}+Q_{22}-2Q_{12}-2Q_{66}\right)\sin^2\theta\cos^2\theta + Q_{66}\left(\sin^4\theta + \cos^4\theta\right)$$

The strains anywhere through the thickness of the laminate may be expressed in terms of the mid-surface's strain $\left\{\varepsilon_x^\circ,\ \varepsilon_y^\circ,\ \gamma_{xy}^\circ\right\}^T$ and curvature $\left\{\kappa_x,\ \kappa_y,\ \kappa_{xy}\right\}^T$ such that for any given lamina

$$\begin{Bmatrix} \sigma_x \\ \sigma_y \\ \tau_{xy} \end{Bmatrix}_k = \begin{bmatrix} \bar{Q}_{11} & \bar{Q}_{12} & \bar{Q}_{16} \\ \bar{Q}_{12} & \bar{Q}_{22} & \bar{Q}_{26} \\ \bar{Q}_{16} & \bar{Q}_{26} & \bar{Q}_{66} \end{bmatrix}_k \left\{ \begin{Bmatrix} \varepsilon_x^\circ \\ \varepsilon_y^\circ \\ \gamma_{xy}^\circ \end{Bmatrix} + z \begin{Bmatrix} \kappa_x \\ \kappa_y \\ \kappa_{xy} \end{Bmatrix} \right\}$$

Integrating these stresses over the thickness produces the following expressions for force per unit width and moment per unit width

$$\begin{Bmatrix} N_x \\ N_y \\ N_{xy} \end{Bmatrix} = \int_{-t/2}^{t/2} \begin{Bmatrix} \sigma_x \\ \sigma_y \\ \tau_{xy} \end{Bmatrix} dz = \sum_{k=1}^{N} \int_{z_{k-1}}^{z_k} \begin{Bmatrix} \sigma_x \\ \sigma_y \\ \tau_{xy} \end{Bmatrix}_k dz$$

$$\begin{Bmatrix} M_x \\ M_y \\ M_{xy} \end{Bmatrix} = \int_{-t/2}^{t/2} \begin{Bmatrix} \sigma_x \\ \sigma_y \\ \tau_{xy} \end{Bmatrix} z dz = \sum_{k=1}^{N} \int_{z_{k-1}}^{z_k} \begin{Bmatrix} \sigma_x \\ \sigma_y \\ \tau_{xy} \end{Bmatrix}_k z dz$$

where z_k and z_{k-1} are defined in Figure 7. This can be expressed as

$$\begin{Bmatrix} N_x \\ N_y \\ N_{xy} \end{Bmatrix}_k = \begin{bmatrix} A_{11} & A_{12} & A_{16} \\ A_{12} & A_{22} & A_{26} \\ A_{16} & A_{26} & A_{66} \end{bmatrix} \begin{Bmatrix} \varepsilon_x^o \\ \varepsilon_y^o \\ \gamma_{xy}^o \end{Bmatrix} + \begin{bmatrix} B_{11} & B_{12} & B_{16} \\ B_{12} & B_{22} & B_{26} \\ B_{16} & B_{26} & B_{66} \end{bmatrix} \begin{Bmatrix} \kappa_x \\ \kappa_y \\ \kappa_{xy} \end{Bmatrix}$$

$$\begin{Bmatrix} M_x \\ M_y \\ M_{xy} \end{Bmatrix}_k = \begin{bmatrix} B_{11} & B_{12} & B_{16} \\ B_{12} & B_{22} & B_{26} \\ B_{16} & B_{26} & B_{66} \end{bmatrix} \begin{Bmatrix} \varepsilon_x^o \\ \varepsilon_y^o \\ \gamma_{xy}^o \end{Bmatrix} + \begin{bmatrix} D_{11} & D_{12} & D_{16} \\ D_{12} & D_{22} & D_{26} \\ D_{16} & D_{26} & D_{66} \end{bmatrix} \begin{Bmatrix} \kappa_x \\ \kappa_y \\ \kappa_{xy} \end{Bmatrix}$$

where

$$A_{ij} = \sum_{k=1}^{N} \left(\bar{Q}_{ij} \right)_k \left(z_k - z_{k-1} \right)$$

$$B_{ij} = \frac{1}{2} \sum_{k=1}^{N} \left[\bar{Q}_{ij} \right]_k \left[z_k^2 - z_{k-1}^2 \right]$$

$$D_{ij} = \frac{1}{3} \sum_{k=1}^{N} \left[\bar{Q}_{ij} \right]_k \left[z_k^3 - z_{k-1}^3 \right]$$

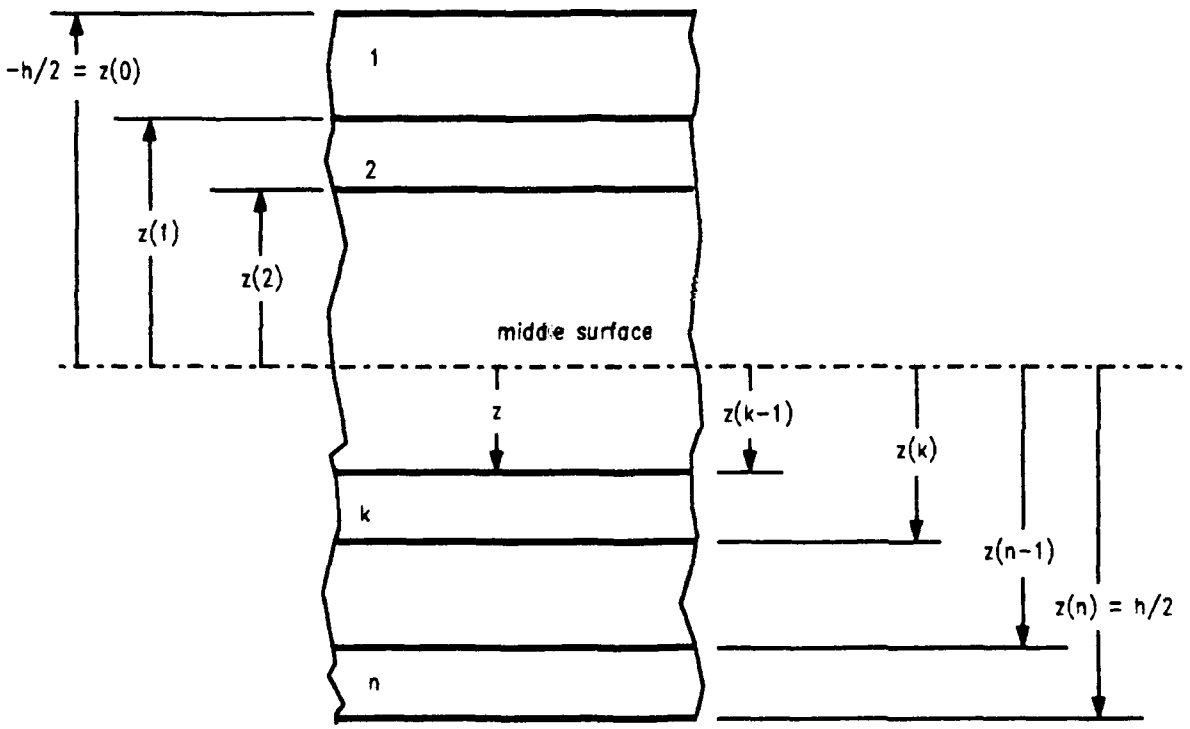

Figure 7. Geometry of an n-layered laminate (9:154)

In (9) it is shown that for a laminate cured at a temperature other than the service temperature, 'thermal forces and moments' may be defined by

$$\begin{Bmatrix} N_x^T \\ N_y^T \\ N_{xy}^T \end{Bmatrix}_k = \int \begin{bmatrix} \bar{Q}_{11} & \bar{Q}_{12} & \bar{Q}_{16} \\ \bar{Q}_{12} & \bar{Q}_{22} & \bar{Q}_{26} \\ \bar{Q}_{16} & \bar{Q}_{26} & \bar{Q}_{66} \end{bmatrix}_k \begin{Bmatrix} \alpha_x^o \\ \alpha_y^o \\ \alpha_{xy}^o \end{Bmatrix}_k \Delta T \, dz$$

$$\begin{Bmatrix} M_x^T \\ M_y^T \\ M_{xy}^T \end{Bmatrix}_k = \int \begin{bmatrix} \bar{Q}_{11} & \bar{Q}_{12} & \bar{Q}_{16} \\ \bar{Q}_{12} & \bar{Q}_{22} & \bar{Q}_{26} \\ \bar{Q}_{16} & \bar{Q}_{26} & \bar{Q}_{66} \end{bmatrix}_k \begin{Bmatrix} \alpha_x^o \\ \alpha_y^o \\ \alpha_{xy}^o \end{Bmatrix}_k \Delta T \, z \, dz$$

where the thermal expansion coefficients for an arbitrary lamina at angle 0, $\{\alpha_x, \alpha_y, \alpha_{xy}\}^T$, are given by vector transformation of the two coefficents in the lamina's coordinates, $\{\alpha_1, \alpha_2, 0\}^T$.

Finally, by defining effective forces and moments

$$\begin{Bmatrix} \bar{N}_x \\ \bar{N}_y \\ \bar{N}_{xy} \end{Bmatrix} = \begin{bmatrix} N_x + N_x^T \\ N_y + N_y^T \\ N_{xy} + N_{xy}^T \end{bmatrix} = \begin{bmatrix} A_{11} A_{12} A_{16} \\ A_{12} A_{22} A_{26} \\ A_{16} A_{26} A_{66} \end{bmatrix} \begin{Bmatrix} \varepsilon_x^o \\ \varepsilon_y^o \\ \gamma_{xy}^o \end{Bmatrix} + \begin{bmatrix} B_{11} B_{12} B_{16} \\ B_{12} B_{22} B_{26} \\ B_{16} B_{26} B_{66} \end{bmatrix} \begin{Bmatrix} \varkappa_x \\ \varkappa_y \\ \varkappa_{xy} \end{Bmatrix}$$

$$\begin{Bmatrix} \bar{M}_x \\ \bar{M}_y \\ \bar{M}_{xy} \end{Bmatrix} = \begin{bmatrix} M_x + M_x^T \\ M_y + M_y^T \\ M_{xy} + M_{xy}^T \end{bmatrix} = \begin{bmatrix} B_{11} B_{12} B_{16} \\ B_{12} B_{22} B_{26} \\ B_{16} B_{26} B_{66} \end{bmatrix} \begin{Bmatrix} \varepsilon_x^o \\ \varepsilon_y^o \\ \gamma_{xy}^o \end{Bmatrix} + \begin{bmatrix} D_{11} D_{12} D_{16} \\ D_{12} D_{22} D_{26} \\ D_{16} D_{26} D_{66} \end{bmatrix} \begin{Bmatrix} \varkappa_x \\ \varkappa_y \\ \varkappa_{xy} \end{Bmatrix}$$

or

$$\left\{\begin{array}{c}\bar{N}\\ \bar{M}\end{array}\right\} = \left[\begin{array}{c|c}A & B\\ \hline B & D\end{array}\right] \left\{\begin{array}{c}\varepsilon^{\circ}\\ \kappa\end{array}\right\} \qquad (17)$$

we can invert the stiffness matrices A,B and D and express the strains and curvatures as

$$\left\{\begin{array}{c}\varepsilon^{\circ}\\ \kappa\end{array}\right\} = \left[\begin{array}{c|c}A' & B'\\ \hline H' & D'\end{array}\right] \left\{\begin{array}{c}\bar{N}\\ \bar{M}\end{array}\right\} .$$

With the layup used, effective engineering properties can be defined

$$E_x = \frac{A_{11}A_{22} - A_{12}^2}{h\, A_{22}}$$

where h is total laminate thickness such that

$$\varepsilon_x^{\circ} = \sigma_x / E_x \qquad (19)$$

With the properties of the laminae used here being

$E_1 = 20.8 \times 10^6$ psi (143.0 GPa)

$E_2 = 1.38 \times 10^6$ psi (9.51 GPa)

$\nu_{12} = 0.31$

$G = 0.85 \times 10^6$ psi (5.86 GPa)

$\varepsilon_{1_{ult}} = 1.42\%$

it follows that the effective modulus of the total laminate is E_x = 8.1 x 10^6 psi (55.8 GPa). Therefore, $\varepsilon_x^o = \sigma_x/E_x$ is the mid-surface strain which will be assumed for each fiber in the laminate. The stress in any lamina will be assumed to be this strain multiplied by the lamina's stiffness in the x direction. This is a simplifying assumption, since once ablation occurs symmetry and balance are destroyed, creating a laminate with different stiffness coefficients. These differences will be assumed to have negligible effect upon the axial stresses in the test samples.

Interaction of Thermal and Mechanical Loads

The matrix epoxy absorbs little of the total energy of ablation, and practically no evidence of discrete removal of the matrix exists (2). Therefore, the discrete mass removal model will only consider fracture and discrete removal of the fibers. This leads to a formulation of the form

$$\mathcal{E}_{total} = V_m \mathcal{E}_m + V_f \mathcal{E}_f \qquad (20)$$

where V_m = volume fraction of matrix

V_f = volume fraction of fibers

But $\mathcal{E}_f$ is only the energy absorbed by that fraction of the fibers which ablate, η_a. A fraction η_d (= 1-η_a) will be removed intact, absorbing essentially no energy.

Although Q^*_{eff} is an empirical measure of all the energy delivered to a material divided by the mass removed during irradiation, it is a reasonable approximation to the actual ablation energy.

From Figure A2, C_p is less than 2000 J/kg·K. From 300 °K to ablation at 3800 °K, the energy absorbed will be:

$$\mathcal{E} = C_p \Delta T$$

$$= 2000 \frac{J}{kg\ K} \cdot 3500\ ^\circ K$$

$$= 7 \frac{kJ}{gm}$$

$$\approx 20\% \cdot Q^*_{eff}$$

The total energies of temperature rise to the ablation point plus the ablation phase change energy will both be considered in Q^*_{eff}.

So we have

Projected - Reflected - Radiated - Conducted =

Energy of Temperature Rise + Energy of Phase Change

$$Q^*_{eff} = \frac{\text{Reflected + Radiated + Conducted + Energy of Temperature Rise + Energy of Phase Change}}{\text{Material Lost as Solid + Material Lost as Vapor}}$$

The true Q would be the ratio of the last two terms.

Looking more closely at Equation (20), the energy absorbed will be examined on a layer by layer basis. Each layer is assumed to be either entirely fiber or entirely

matrix, with thicknesses divided in the same ratio as the composite's fiber-to-matrix distribution. The energy absorbed during the ablation will be

$$\mathcal{E}_{abs} = \eta_a Q_f^* \Delta m_f = \eta_a Q_f^* \rho_f A_{laser} \Delta h_f$$

where

Q_f^* = effective enthalpy of ablation of fibers alone

Δh_f = thickness of a fiber layer

$A_{laser} = A_l$ = laser spot area

Δh_f = thickness of a fiber layer

and the other symbols have their previous definitions. In the next layer of matrix, the energy absorbed is simply

$$\mathcal{E}_{abs} = Q_m^* \Delta m_m = Q_m^* \rho_m A_{laser} \Delta h_m$$

The effective Q^* calculated during the ablation of all these layers would be

$$Q_{eff}^* = \frac{\Sigma \mathcal{E}_{abs}}{\Sigma \Delta m}$$

$$= \frac{N_f \left[\eta_a Q_f^* \rho_f A_l \Delta h_f \right] + N_m \left[Q_m^* \rho_m A_l \Delta h_m \right]}{N_f \rho_f A_l \Delta h_f + N_m \rho_m A_l \Delta h_m} \qquad (21)$$

where N_f = total number of fiber layers

N_m = total number of matrix layers

$N_f \Delta h_f = h_f$, total fiber thickness

$N_m \Delta h_m = h_m$, total matrix thickness

and note that the total thickness ablated is

$$h = h_f + h_m$$

where

$$h_m = h\ V_m$$

$$h_f = h\ V_f \qquad (22)$$

Substituting Equations (22) back into Equation (21) results in

$$Q^*_{eff} = \frac{\eta_a \rho_f V_f Q^*_f + \rho_m V_m Q^*_m}{\rho_f V_f + \rho_m V_m} = \frac{(1-\eta_d)\rho_f V_f Q^*_f + \rho_m V_m Q^*_m}{\rho_f V_f + \rho_m V_m} \qquad (23)$$

$$= \frac{\left(1-\eta_d\right)\rho_f V_f Q^*_f + \rho_m V_m Q^*_m}{\rho}$$ where ρ is total composite density

$$= \left(1 - \eta_d\right) \chi_f Q^*_f + \chi_m Q^*_m \qquad (24)$$

where $\chi_f = \rho_f V_f / \rho$ = mass fraction of fibers

$\chi_m = \rho_m V_m / \rho$ = mass fraction of matrix

It can be seen when η_d is zero, Q^*_{eff} becomes simply $Q^*_{eff} = Q^*_f \chi_f + Q^*_m \chi_m$, which is the limiting case that would have been arrived at by simple intuition.

The form of relationship between applied stress σ_x and discrete removal efficiency η_d is suggested by the fracture mechanics of a single fiber. The mass of discrete fibers removed will be

$$\eta_d M_f = \rho_f \frac{\pi d^2}{4} \bar{L} N_d \qquad (25)$$

where

N_d = number of discrete fibers removed

$\bar{L}$ = average length of a removed fiber

The brittle fracture of a given fiber will be governed by the applied stress intensity factor (SIF) K_I. When this applied SIF exceeds the critical SIF K_{IC} crack growth will occur. If additional energy is available to allow K_I to remain above K_{IC}, unstable crack growth will fracture the fiber (1). The applied SIF is calculated from

$$K_I = \frac{\sigma_x}{f\sqrt{\pi a}} \qquad (26)$$

where f is a function of the crack geometry. For a given constant distribution of initial cracks of length a, K_I is

simply proportional to applied stress σ_x. If damage is assumed to be proportional to K_I, this suggests a linear variation of η_d with the applied stress σ_x. To account for the possibility of some threshold stress, σ_{xo}, below which no discrete mass removal by fracture occurs, a variation will be assumed of the form

$$\eta_d = \eta_{d0} + \eta_{d\sigma} \cdot \sigma_x \tag{27}$$

Available data on this phenomenon is too sparse to be conclusive, but it does support the assumption of a monotonically increasing function of σ_x (17). A small amount of additional data collected in preparation for the primary set of experiments also lends credibility to the form of Equation (27). See Appendix D for details.

Substituting Equation (27) into Equation (24) yields

$$Q^*_{eff} = \left[1-\eta_{d0} - \eta_{d\sigma}\sigma_x\right] \chi_f Q^*_f + \chi_m Q^*_m \tag{28}$$

The values of Q^*_f and Q^*_m could be deduced from experiments conducted at $\sigma_x = 0$, or assumed to be (5)

$$Q^*_f \approx 43 \text{ kJ/gm}$$

$$Q^*_m \approx 4 \text{ kJ/gm} \tag{29}$$

Using the mass fractions measured for the particular specimens used in this thesis, and the values in Equation (29), the predicted effect of loading on Q^*_{eff} will have a form like that shown in Figure 8.

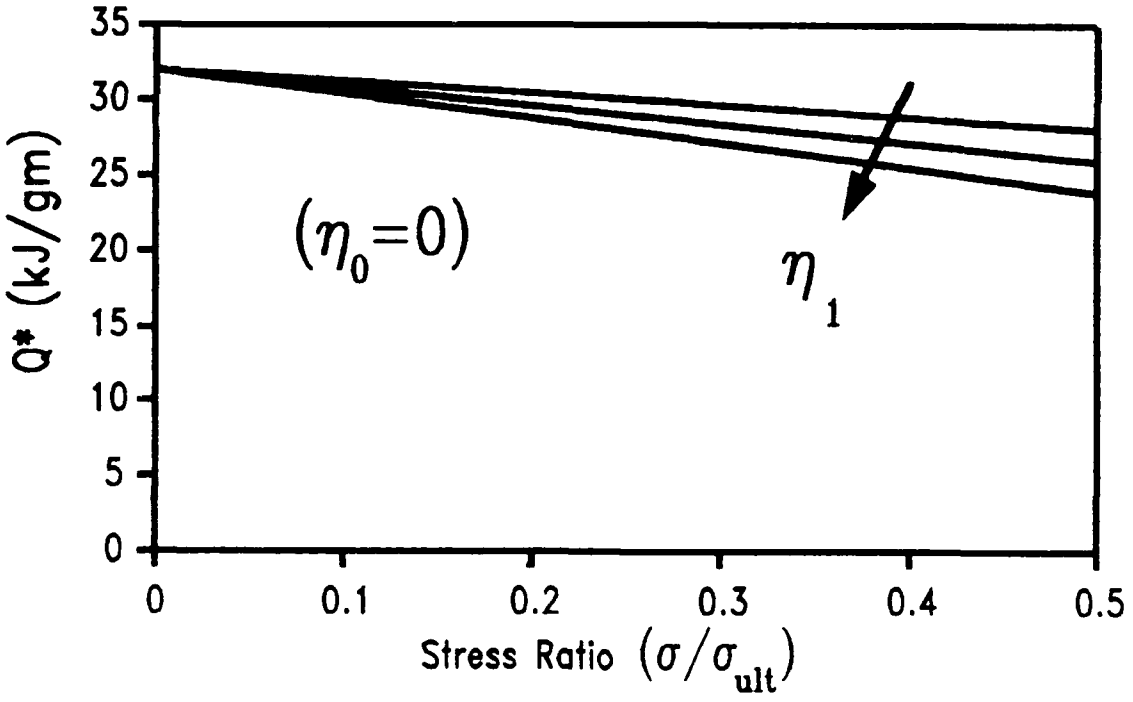

Figure 8. Predicted Q* Behaviour Under Loading

III. Experimental Apparatus

Test Specimens

Fabrication of the test specimens is detailed in Appendix C. A listing of the specimens fabricated and pertinent pre-test data is given in Table I. All specimens were laid up as balanced, symmetric laminates. The thinner (0.244" = 0.620 cm) samples were $[0,\pm 60]_{6s}$. The thicker samples (0.367" = 0.932 cm) were $[0,\pm 60]_{12s}$.

Specimen Instrumentation

Type K (chromel/alumel) thermocouples and/or strain gauges were attached to some specimens (Figure C1b). All samples were weighed before being tested to determine their mass.

Tensile Loading Machine

The device used to load the samples in tension was a hydraulically actuated frame built by the Air Force Weapons Laboratory's Directed Energy Weapon Effects Branch (WL/TALE). A schematic diagram is shown in Figure 9a, and a photograph of the grips holding a sample follows in Figure 9b. Loads of up to 30000 pounds of force (133400 N) were applied in this program. The force was measured

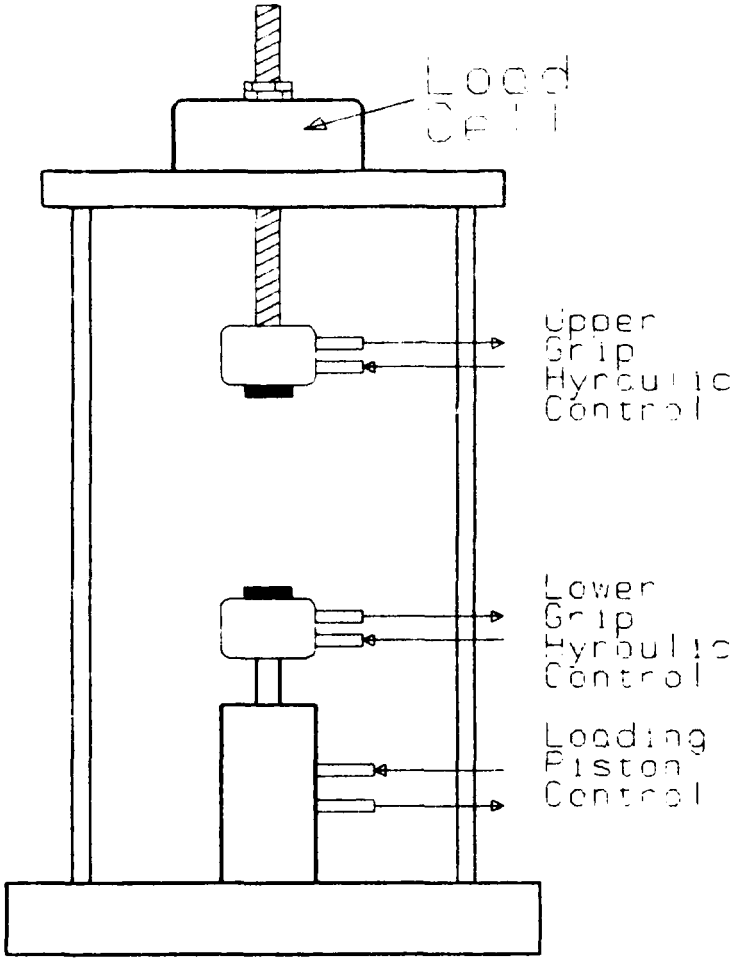

(a)

(b)

Figure 9. Tensile Loading Machine

by a Strainsert Universal Flat Load Cell, Model FL5OU-3DPKD, SN 06669-1 (50000 lb capacity) located above the top hyraulic grip of the machine.

TABLE I
Test Specimen Specifications

		Beam Diameter		Spot	Average Panel Properties		
		Minor	Major	Area	Density	Resin	Voids
Shot#	SampleID#	(cm)	(cm)	(cm^2)	(gm/cm^3)	(Wt%)	(Wt%)
1	CH13989-1#5	2.7	2.9	6.15	NA	NA	NA
2	CH13989-1#3	2.7	2.9	6.15	NA	NA	NA
3	CH13989-4#1	2.5	2.7	5.30	NA	NA	NA
4	CH13989-4#2	2.5	2.8	5.50	NA	NA	NA
5	CH13989-4#3	2.6	2.8	5.72	NA	NA	NA
6	CH13989-4#5	2.6	2.8	5.72	NA	NA	NA
7	CH13989-5#1	2.6	2.8	5.72	NA	NA	NA
8	JH13189-1#3	2.6	2.8	5.72	1.59	27.75	1.32
9	JH13189-1#4	2.6	2.8	5.72	1.59	27.75	1.32
10	JH13189-2#3	1.65	1.8	2.33	1.59	28.13	0.92
11	JH13189-2#4	1.65	1.8	2.33	1.59	28.13	0.92
12	JH13189-2#5	1.65	1.8	2.33	1.59	28.13	0.92
13	JH13189-2#6	1.65	1.8	2.33	1.59	28.13	0.92
14	JH13189-2#7	1.65	1.8	2.33	1.59	28.13	0.92
15	JH13189-2#8	1.65	1.8	2.33	1.59	28.13	0.92
16	JH13189-1#3	1.65	1.8	2.33	1.59	27.75	1.32
17	CH13989-2#1	1.2	1.3	1.23	NA	NA	NA
18	CH13989-2#2	1.2	1.3	1.23	NA	NA	NA
19	JH13189-2#9	1.2	1.3	1.23	1.59	28.13	0.92
20	CH13989-3#1	1.2	1.3	1.23	NA	NA	NA
21	JH13189-1#4	1.2	1.3	1.23	1.59	27.75	1.32
22	CH13989-3#2	1.2	1.3	1.23	NA	NA	NA
23	CH13989-3#3	1.2	1.3	1.23	NA	NA	NA
24	CH13989-3#4	1.2	1.3	1.23	NA	NA	NA
25	CH13989-3#6	1.2	1.3	1.23	NA	NA	NA
26	JH13189-2#10	1.2	1.3	1.23	1.59	28.13	0.92
27	JH13189-1#6	1.2	1.3	1.23	1.59	27.75	1.32
28	CH13989-2#7	1.5	1.7	2.00	NA	NA	NA
29	JH13189-1#7	1.5	1.7	2.00	1.59	27.75	1.32
30	JH13189-1#5	1.5	1.7	2.00	1.59	27.75	1.32
31	CH13989-3#8	1.5	1.7	2.00	NA	NA	NA
32	CH13989-3#9	1.5	1.7	2.00	NA	NA	NA
33	CH13989-3#7	1.5	1.7	2.00	NA	NA	NA
34	CH13989-3#10	1.5	1.7	2.00	NA	NA	NA
35	JH13189-2#11	1.5	1.7	2.00	1.59	28.13	0.92
36	JH13189-2#12	1.5	1.7	2.00	1.59	28.13	0.92

Continuous Wave (CW) 10.6 um Laser and Associated Diagnostics

The Electric Discharge Coaxial Laser II (EDCL-II) is a 10.6 μm infrared carbon dioxide laser capable of 40 kW of output power. As shown in Figure 10, in the test program described here a fraction of this power was removed by a sodium chloride beam splitter to be measured by a Coherent Model 213 power meter (SN B0H375). Diamond-lathed copper mirrors are used to take the remaining power and focus it on the target plane in the shape and intensity desired.

At the target, infrared emission from the target is detected by a Thermogage Model 8000-1A germanium pyrometer (SN 3247). This data provided information on the surface temperature of the ablating samples.

16mm motion pictures are also recorded at 500 frames per second (fps), using a Redlake Hycam II Model 41-0064 (SN333). Video tape of the ablating samples was recorded with a Sony DXC-M3 Color Video Camera and a Panasonic AG6200 VHS tape recorder. Placement of the camera and recorder made recording their serial numbers impossible.

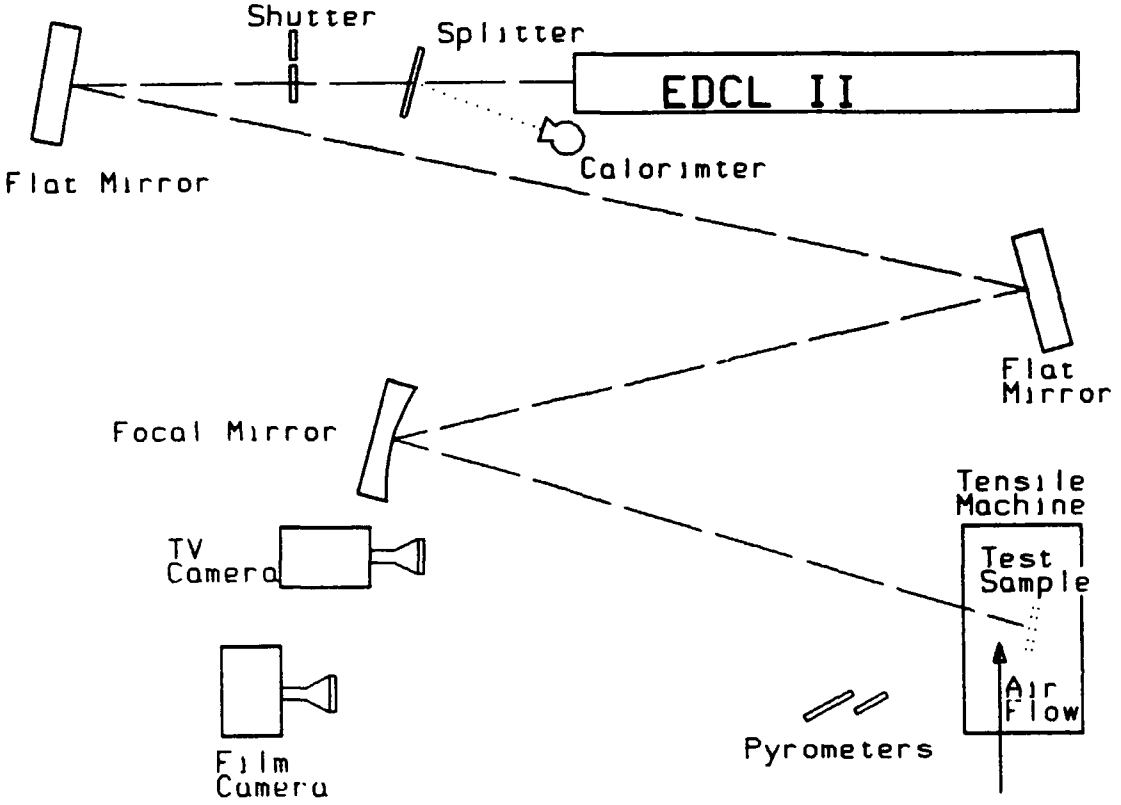

(a)

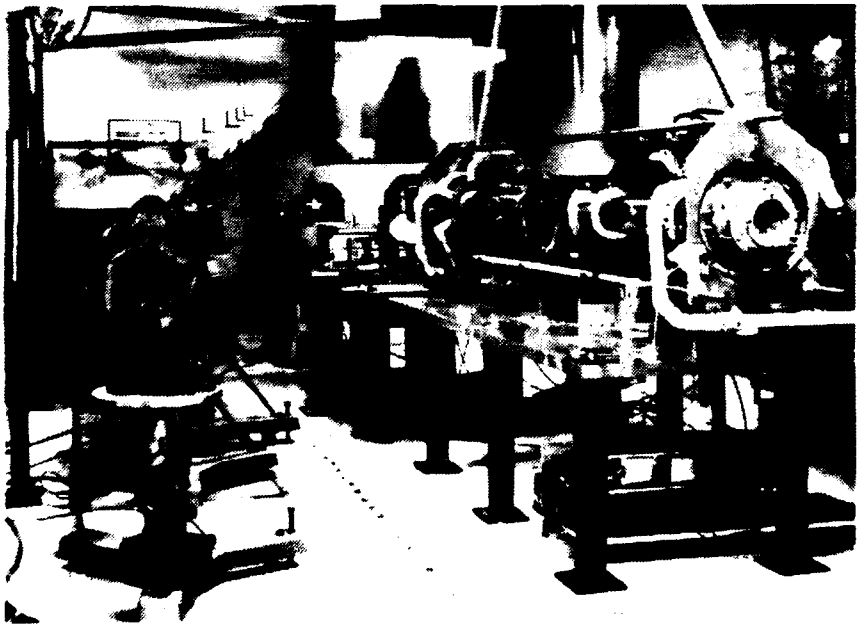

(b)

Figure 10. Laser Optical Train

IV. Experimental Procedure

Specimen Preparation

The sample to be tested is placed in the upper hyraulic grip and positioned to be perpendicular to both the axis of loading and the incident laser beam. The lower grip is placed around the bottom of the sample and any instrumentation wires are routed away toward their respective recording devices (Figure 9b). 1600 psi (11 MPa) hyraulic pressure was supplied to the grips to secure the specimen. Data recording devices are checked to see that proper readings are being received from each of the instruments.

Laser Optical Train

The optical train is adjusted to produce a desired spot size upon the target. Accounting for the expected device output power, this adjustment controls the irradiance on target. Aberrations in the irradiance profile which might be encountered include ellipticity of an otherwise circular beam, irradiance flucuations at various locations within the spot area, and power fluctuations with time during the test.

The first difficulty, a non-circular beam, occurs when magnifying mirrors reflect the beam at a finite angle with respect to their centerline. Since it is impossible to reflect the laser energy perpendicular to the mirror and still usefully propagate it, some ellipticity must remain in the beam, unless two or more mirrors can be used to offset each others effects. Major and minor diameters are recorded in Table I.

The next problem is affected by the ellipticity, by alignment of the laser resonator cavity, and by inherent design of the EDCL-II. Both ellipticity and spacial power variations can be quantified by measuring the burn profile in a soft material like plexiglass before testing the sample, or to a less accurate degree, by the shape of the sample's burn craters.

The last problem, temporal fluctuations in power, can only be measured during the test by a fast response power meter measuring scattered radiation from some part of the optical train. If the variations seen are significant, then they must be accounted for after the fact in the analysis of the test data. As shown in a typical plot of this reading (Figure 11), there were no significant fluctuations during these tests.

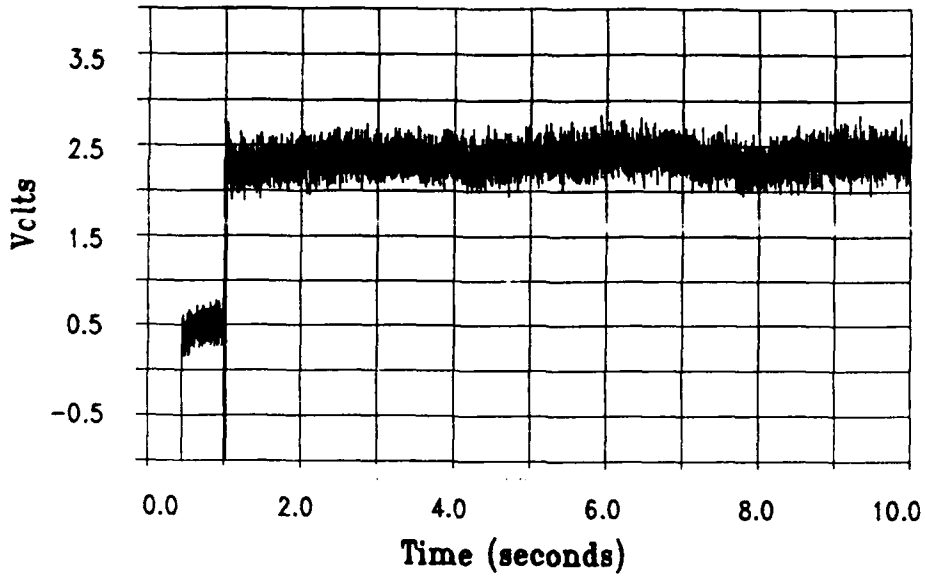

(a) AFIT Shot #4 EDCL II P(t)

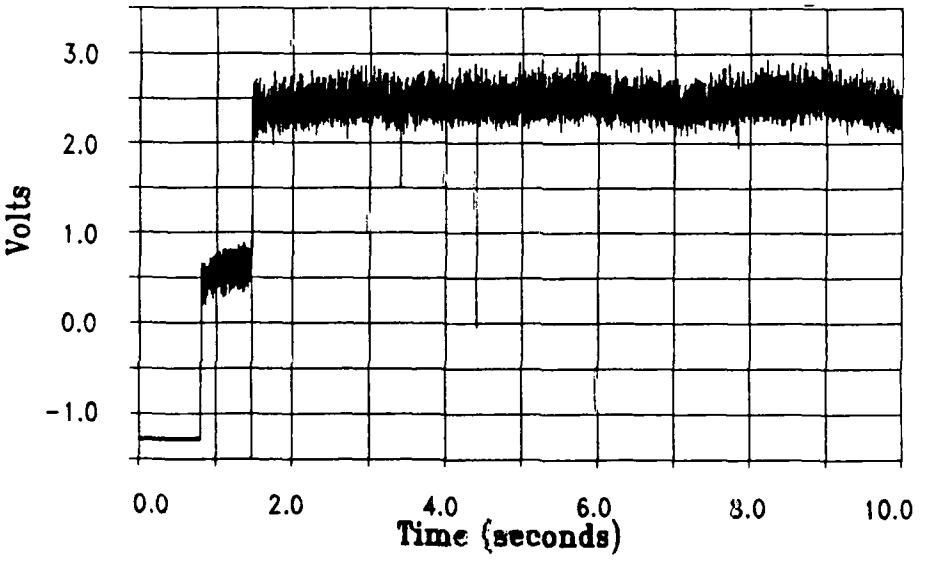

(b) AFIT Shot #5 EDCL II P(t)

Figure 11. Typical Power vs. Time Curves

Data Collection During Irradiation

Once all instruments are connected and operating properly, recording of the various signals is begun, the load on the tensile machine is raised to the level desired, and the laser is turned on.

After 1 to 2 seconds are allowed for the laser power output to stabilize, opaque shutters keeping the beam from going to the target are removed. The time allowed for the shutter to eclipse the beam is kept well below 5 percent of the total irradiation time to ensure the variation in intensity profile is insignificant to the sample's total interaction with the radiation.

After a predetermined amount of time, the shutter is returned to its initial position, removing the radiation from the target. The laser is then shut down.

Post-test Data Collection

Any significant fibers broken off during the test which can be seen downwind of the purging air flow are collected. The sample is then weighed to determine its mass loss. It is then placed in a plastic bag and kept from further handling until photomicrographs can be taken.

After the photography of the sample's ablation surface, the depth of the crater ablated in the sample is measured with a depth gauge or other micrometer.

V. Experimental Data

Table II and Figures 12, 13, and 14 summarize the results obtained on the EDCL-II device. Sample calculations showing equations used to reduce the data are shown in the following paragraphs.

Before irradiation tests occurred, two samples 'A' and 'B' were pulled in tension to failure in the tensile machine. Sample A's load/strain curve is shown in Figure 12. Sample B is similar. Compare the effective modulus E_x = 8.1 msi (55.9 GPa) to that obtained on similar samples tested on an AFIT MTS tensile testing machine (also ~8.1 msi (55.9 GPa) from Figure C5). This is in excellent agreement with the effective modulus calculated in Chapter II.

The strength of the laminate was calculated by finding the stress which places the ultimate strain, ϵ_{ult}, on the laminate

$$\sigma_{ult} = E_x \epsilon_{ult} = 8.1 \times 10^6 \text{psi} * 0.0142$$

$$= 115020 \text{ psi} = 793 \text{ MPa}$$

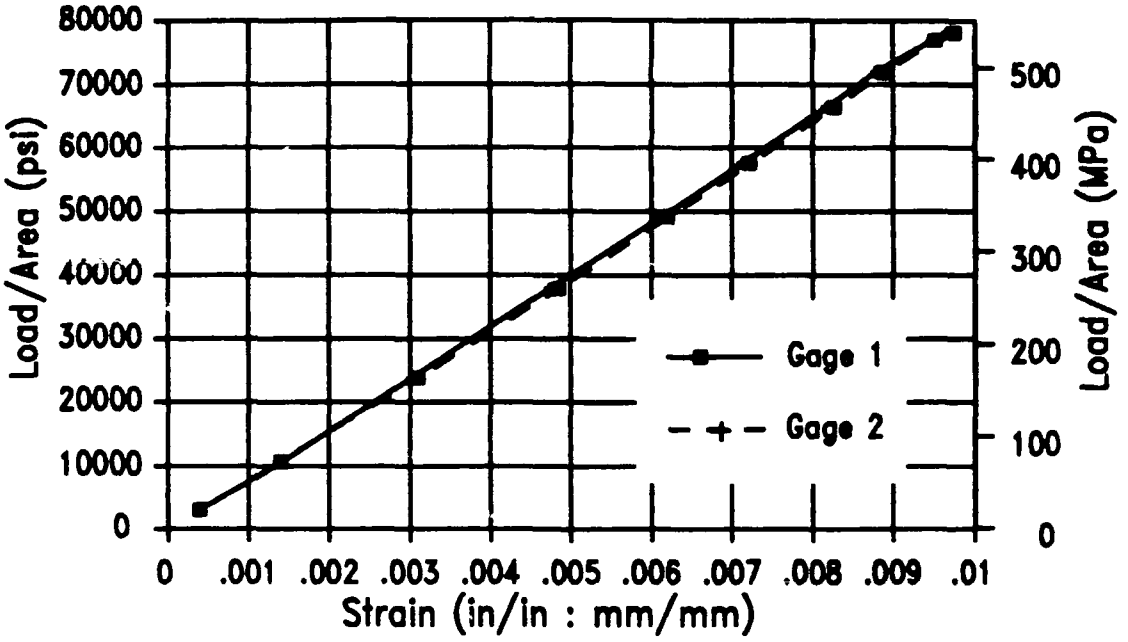

Figure 12. Stress vs. Strain Curve for Test Sample A

The load which applies this stress to the laminate is the 'ultimate load' used to normalize the data in the Stress Ratio column of Table II. For 0.247" (0.627 cm) thick samples, it is approximately 28400lb$_f$ (126300 N). For 0.370" (0.939 cm) thick samples, 42500lb$_f$ (189000 N).

It was found that the mass losses achieved on the samples used in tests 1 to 9 were too small to allow accurate measurements. The analytic balances available could weigh samples less than 160 grams to within 0.1 milligram, but heavier samples had to be weighed on a device with only 0.1 gram resolution. The 2" (5.08 cm)

TABLE II.

Laser Interaction Parameters and Results

Shot #	POWER on TARGET (kW)	IRRADIANCE $\left[\frac{kW}{cm^2}\right]$	TENSILE LOAD (lbm)	TENSILE LOAD (kN)	STRESS RATIO	LASER TIME (sec)	MASS LOSS (gm)	Q^*_{mass} $\left[\frac{kJ}{gm}\right]$
10	31.77	13.6	0	0	0.00	2.02	1.95	32.99
11	30.64	13.1	9400	41.8	0.22	2.02	1.98	31.12
12	30.73	13.2	14800	65.8	0.35	1.77	1.82	29.95
13	32.72	14.0	19000	84.5	0.44	1.43	1.56	30.07
14*	31.68	13.6	18700	83.1	0.44	1.61	1.71	29.90
15	31.60	13.5	14400	64.1	0.34	1.76	1.81	30.65
16	31.60	13.5	9500	42.3	0.33	1.51	1.50	31.89
17	31.77	25.9	0	0	0.00	2.02	2.28	28.13
18	32.72	26.7	0	0	0.00	1.27	1.45	28.64
19	31.25	25.5	5300	23.6	0.12	1.02	1.07	29.84
20	31.51	25.7	4500	20.0	0.11	1.01	1.09	29.30
21	31.68	25.9	5000	22.2	0.17	0.63	0.63	31.83
22	31.68	25.9	9700	43.2	0.23	1.03	1.17	27.99
23	31.51	25.7	9800	43.6	0.23	1.11	1.42	24.61
24	31.25	25.5	14600	64.9	0.34	1.24	1.45	26.72
25*	32.38	26.4	19000	84.5	0.44	1.02	1.45	22.76
26	32.03	26.1	15000	66.7	0.35	1.02	1.18	27.59
27	31.60	25.8	4700	20.9	0.16	0.78	0.80	30.96
28	31.68	15.8	0	0	0.00	2.01	1.95	32.64
29	31.25	15.6	0	0	0.00	1.27	1.20	33.15
30	31.51	15.7	2800	12.5	0.10	1.01	0.94	33.68
31	30.99	15.5	2900	12.9	0.07	1.76	1.80	30.16
32	31.25	15.6	5300	23.6	0.12	1.51	1.48	31.92
33	32.29	16.1	7600	33.8	0.18	1.52	1.50	32.74
34	31.77	15.9	9700	43.2	0.23	1.28	1.23	32.93
35	31.60	15.8	11900	52.9	0.28	1.01	0.95	33.56
36	31.77	15.9	14500	64.5	0.34	1.01	1.06	30.09

* Samples #14 and #25 broke in half during testing

wide samples used for the first 9 tests were all greater than 160 grams. The 0.1 gram resolution was more than 10% of the achieved mass losses. This poor accuracy makes the data unusable, and the values won't be reported here.

The first column in Table II, Power on Target (kW) was found by taking power out of the EDCL-II device, measured as described in Chapter III, and plotted on a laser printer. The laser plot was then redigitized to record the final value representative of the total laser power. This number was multiplied by 0.868. This number was suppled by the WL/TALE personnel as the factor of mirror losses.

$$P_{target} = P_{device} * 0.868.$$

This number has an uncertainty of ± 15%, a typical value accepted by the laser effects research community for ballistic calorimeters. The next column, Irradiance (kW/cm^2) is obtained by measuring the major and minor axes of the burn spot, with an uncertainty of ± 0.05 cm, calculating the burn area, and dividing this area into the Power on Target.

$$I = \frac{P_{target}}{\pi/4\ (d_{minor})(d_{major})}$$

The tensile load from the load cell is also plotted on a laser printer and redigitized. Definite bounds on the uncertainty associated with this number are unavailable. The stress ratio was found by taking the load and dividing by the calculated fracture load for the sample.

Laser time on target, obtained from an infrared detector viewing a mirror down the beam train from the laser shutter, was also plotted and redigitized. This uncertainty is no larger than the resolution of placing the digitizer cursor on the plot. The uncertainty in time values will therefore be ignored.

Mass loss values came from weighing the samples on a analytic balance before and after testing. Uncertainty here is ± 0.2 milligrams. This is less than 0.06 percent for all samples reported and will also be ignored.

The effective enthalpy of ablation becomes

$$Q^*_{eff} = \frac{\text{Energy}}{\text{mass loss}} = \frac{P_{target} \cdot t}{\Delta m}$$

$$= \frac{P_{target}\left[\pm 15\%\right] \cdot t \left[\pm 0\%\right]}{\Delta m \left[\pm 0\%\right]}$$

$$Q^*_{eff} = 15\% + 0\% + 0\% = \pm 15\%$$

Although this uncertainty is larger than the ordinate change for the 15 kW/cm^2 data, this will not invalidate the

conclusions stated in Chapter VI. For the data taken at 26 kW/cm^2, changes larger than 15 percent are seen.

As stated in Chapter II, the effective enthalpy of ablation, Q^*_{eff}, is based upon the energy delivered to the target. Energy lost to the surroundings will not contribute to material ablation, making the value, of Q^*_{eff} higher tha, the actual enthalpy value of the ablating material. The most significant loss mechanism for material ablating at 3800°K will be reradiation of energy away from the target and conduction away from the ablation surface. This first value may be approximated by calculating the energy flux of a body at temperature T with an emissivity ε (assumed to be equal to the absorptivity α)

$$q = \varepsilon\sigma T^4 = \alpha\sigma T^4$$

$$= 0.9 \left[5.67 \times 10^{-8} \frac{W}{m^2\ {}^\circ k^4}\right]\left[3800\ {}^\circ k\right]^4$$

where σ is the Stefan-Boltzman constant

$$= 10.6 \times 10^{6}\ W/m^2$$

$$= 1.06\ kW/cm^2 \approx 8\% \cdot \left[13\ kW/cm^2\right]$$

$$\approx 4\% \cdot \left[26\ kW/cm^2\right]$$

The second loss, conduction away from the ablation surface, will be estimated as conduction into the depth of the sample and radially from the ply being ablated. From Figure B6, the average thermal gradient through the thickness is approximately 1.5×10^3 °K/cm at the ablation surface. From Figure A2, $K_{zz} \approx 1$ W/m·K.

$$q_{cond} = K \nabla T$$

$$= 1 \frac{W}{m^\circ K} \cdot 1.5 \times 10^3 \frac{^\circ K}{cm}$$

$$= 1.5 \text{ kW/cm}^2$$

$$\approx 12\% \cdot \left[13 \text{ kW/cm}^2\right]$$

$$\approx 6\% \cdot \left[26 \text{ kW/cm}^2\right]$$

Radial conduction will also remove energy from the ablation surface. A conservative bound on this loss is estimated by taking the maximum gradient $\left[1.5 \times 10^3 \text{ °K/cm}\right]$, maximum conductivity (10 W/m·°K from Figure A2) and calculating the power lost in the ply being ablated. For a 1cm diameter spot and 0.0132 cm thick plys

$$P_{radial} = 10 \frac{W}{m \cdot K} \cdot 1.5 \times 10^3 \frac{^\circ K}{cm} \cdot \pi \cdot 1 \text{ cm} \cdot 0.0132 \text{ cm}$$

$$= 0.622 \text{ kW}$$

$$\approx 2\% \cdot P_{laser}$$

Therefore, the reported values of Q^*_{eff} are too high by a figure on the order of 22 percent, compared to values computed by accounting for energy losses.

Figure 13 is a plot of the data for 26 kW/cm^2. Figure 14 shows 13 kW/cm^2 and 16 kW/cm^2 data on the same plot. This was done because of the close agreement of the unloaded Q* values at both intensities. The magnitude of the correlation coefficient of Figure 14, being higher than that of the 26 kW/cm^2 data alone (0.627 vs. 0.599), justifies this method of presentation.

The lines fit to Figures 13 and 14 are least squares linear regressions of Q^*_{eff} on stress ratio yielding lines of the form

$$Q^*_{eff} = A + B \cdot \frac{\sigma}{\sigma_{ult}}$$

Equations (28) and (29) are solved for η_o and η_1 using the values for A and B above. It was calculated that

$$\eta_d = \eta_o + \eta_1 \cdot \frac{\sigma}{\sigma_{ult}}$$

$$= 0.013 \frac{kJ}{gm} + 1.74 \frac{kJ/gm}{GPa} \sigma$$

for data taken at 15kW/cm^2.

$$\eta_d = 0.087 \frac{kJ}{gm} + 3.36 \frac{kJ/gm}{GPa} \sigma$$

for data taken at 26 kW/cm^2.

The small value of η_o in both cases raises the question of its significance. To discern this, the

average value of Q^*_{eff} taken at zero load was subtracted from each data set. A straight line was fit through the origin, and the sums of the residuals squared associated with each fit were compared to those from the two parameter slope, B.

For 15 kW/cm^2

$$Q^*_{eff} = 32.96 \frac{kJ}{gm} - 5.80 \frac{kJ}{gm} \cdot \left(\frac{\sigma}{\sigma_{ult}}\right)$$

$$\text{residuals squared} = 18.2 \left(\frac{kJ}{gm}\right)$$

for one parameter fit

$$\left(Q^*_{eff} - 32.93 \frac{kJ}{gm}\right) = -5.71 \frac{kJ}{gm} \cdot \left(\frac{\sigma}{\sigma_{ult}}\right)$$

$$\text{residuals squared} = 23.0 \left(\frac{kJ}{gm}\right)^2$$

For 26 kW/cm^2

$$Q^*_{eff} = 30.23 \frac{kJ}{gm} - 11.2 \frac{kJ}{gm} \cdot \left(\frac{\sigma}{\sigma_{ult}}\right)$$

$$\text{residuals squared} = 44.7 \left(\frac{kJ}{gm}\right)^2$$

and for one parameter fit

$$\left(Q^*_{eff} - 32.00 \frac{kJ}{gm}\right) = -17.30 \frac{kJ}{gm} \cdot \left(\frac{\sigma}{\sigma_{ult}}\right)$$

$$\text{residuals squared} = 55.7 \left(\frac{kJ}{gm}\right)^2$$

Fitting a one parameter fit to the data to account for an offset, η_o, does not give any better representation of the data collected here.

Figures 15a through 15g show representative photographs of the test samples. In addition to ply

separation and loose fibers hanging from the ablation crater surfaces, global structural damage is obvious at the higher load levels. This type of damage obviously contributed (in an unknown degree) to the mass loss enhancement. Macroscopic fiber removal occurred during many of the tests, as shown by fiber bundles seen on the floor of the test area. A typical bundle would be on the order of 2mm wide by 5mm to 7mm long. No attempt was made to systematically collect these bundles, but many were found downstream of the nitrogen sample purge.

Figures 16a and 16b show scenes from the video tape taken during the irradiation of sample #5. The darker bands and regions are areas of lower temperature. The orientation of these bands, which coincide with ply orientation, is taken as evidence of discrete ply removal. A solid ply breaking off and being carried away by the purge gas would expose a ply beneath it at lower temperature. This was seen in MELT3D.FOR predictions, and has been observed in other laser effects tests. If all plys were ablated entirely, without discrete removal, new plys will not be exposed until the layer beneath had heated up to the ablation temperature, and no darker bands would be visible on film or video.

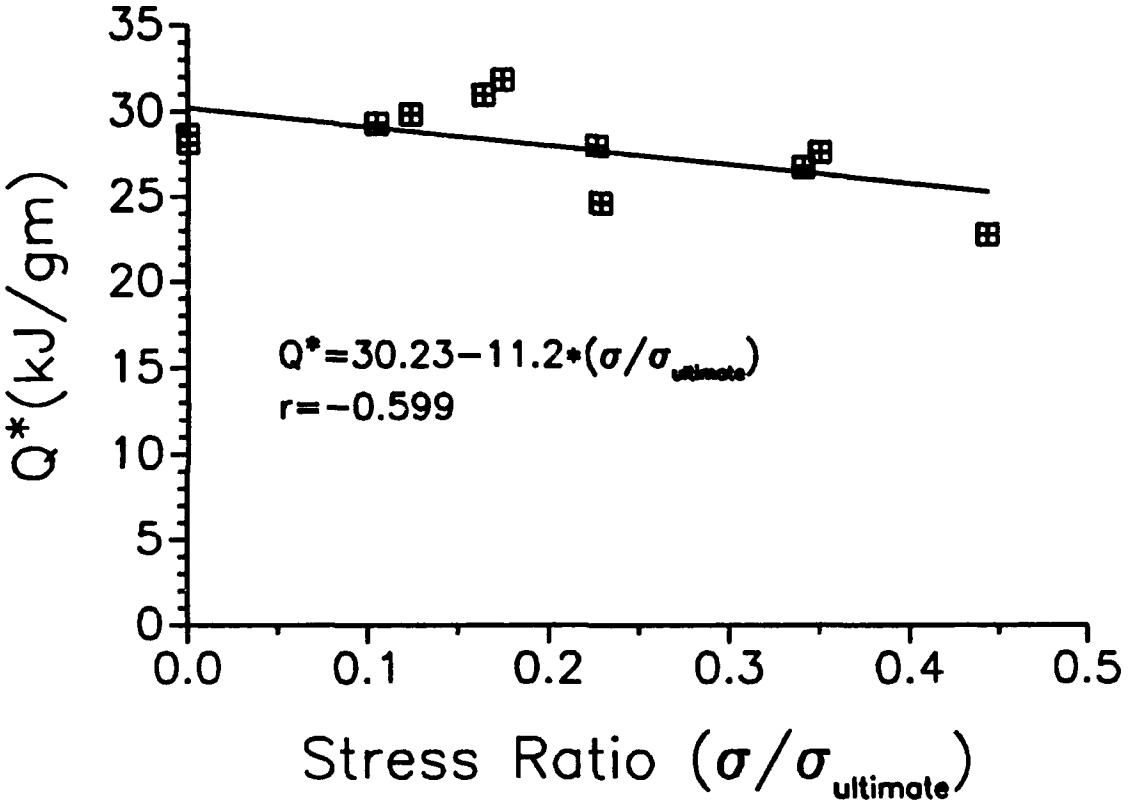

Figure 13. Q* versus Stress Ratio for 26 kW/cm^2

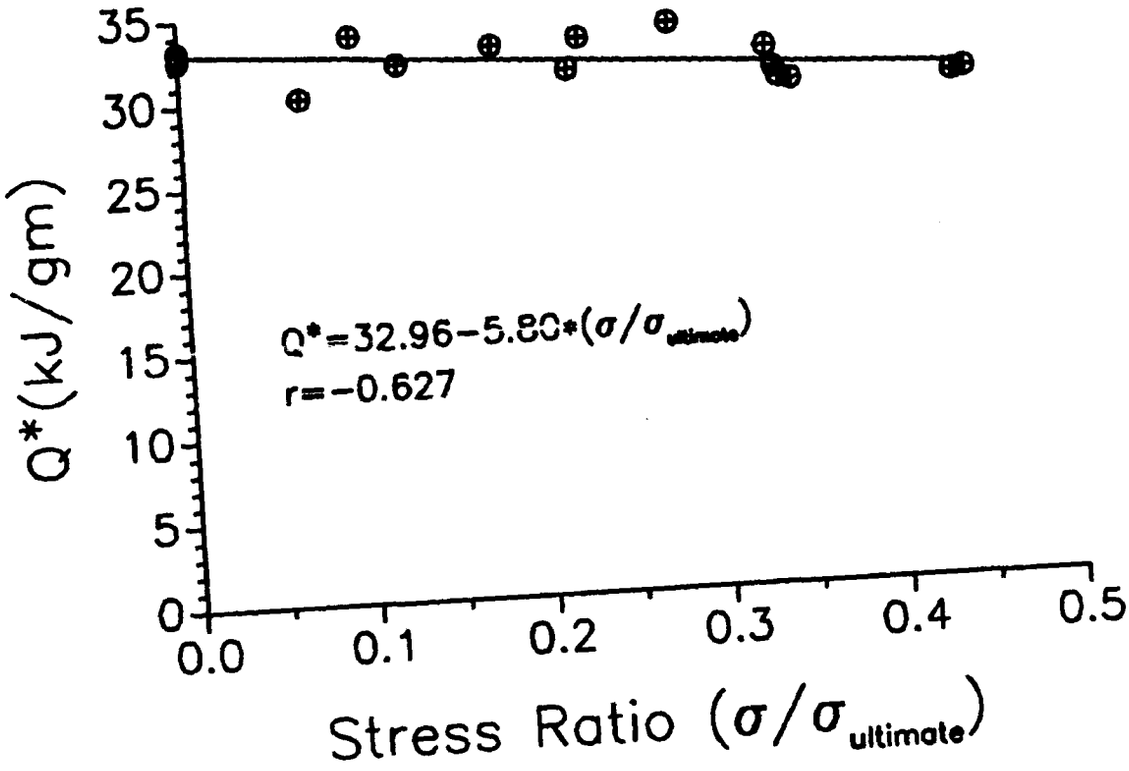

Figure 14. Q* versus Stress Ratio for 13 & 16 kW/cm^2

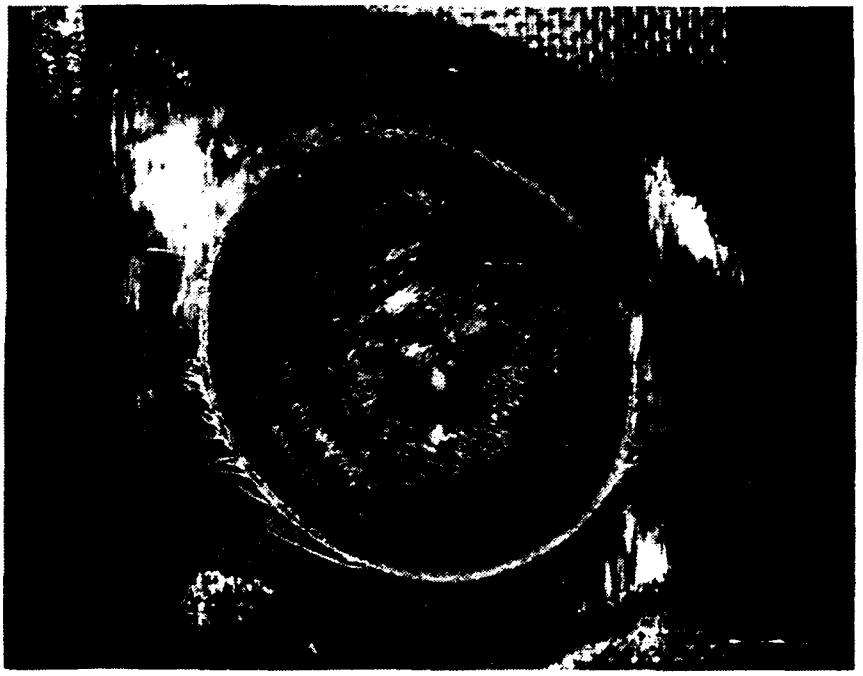

(a) Shot #10; I = 13 kW/cm^2; Stress Ratio = 0.0

Figure 15. Representative Test Sample Photographs

(b) Shot #11; I = 13 kW/cm^2; Stress Ratio = 0.22

(c) Shot #12; I = 13 kW/cm^2; Stress Ratio = 0.35

Figure 15. Representative Test Sample Photographs (Cont'd)

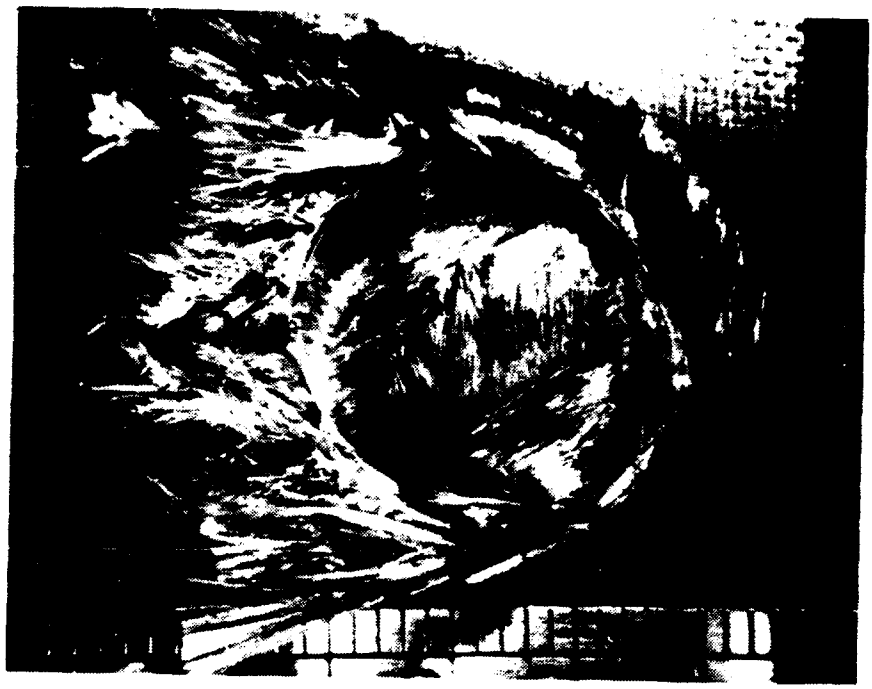

(d) Shot #13; I = 13 kW/cm ; Stress Ratio = 0.44

(e) Shot #13; Close Up

Figure 15. Representative Test Sample Photographs (Cont'd)

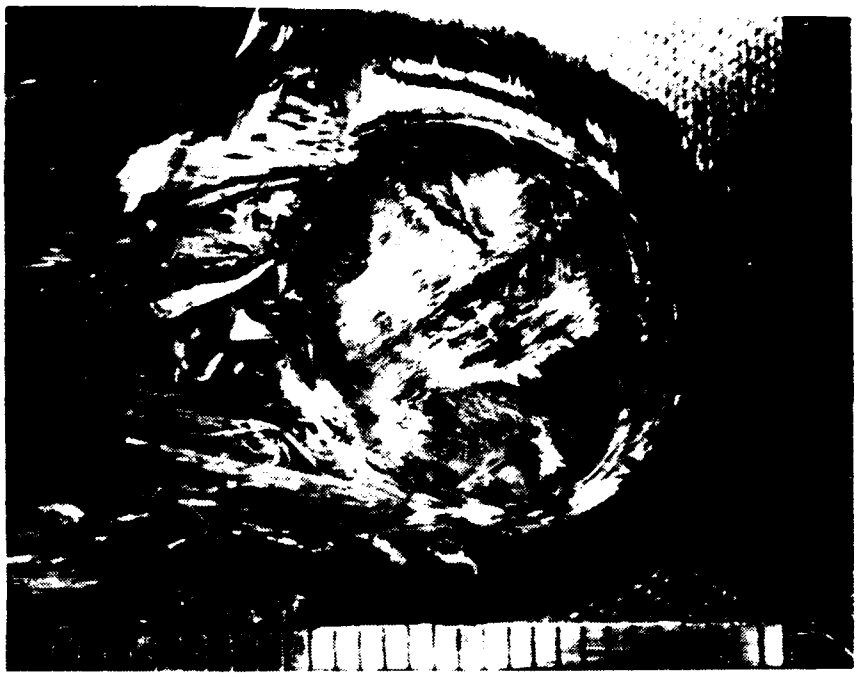

(f) Shot #15; I = 13 kW/cm^2; Stress Ratio = 0.34

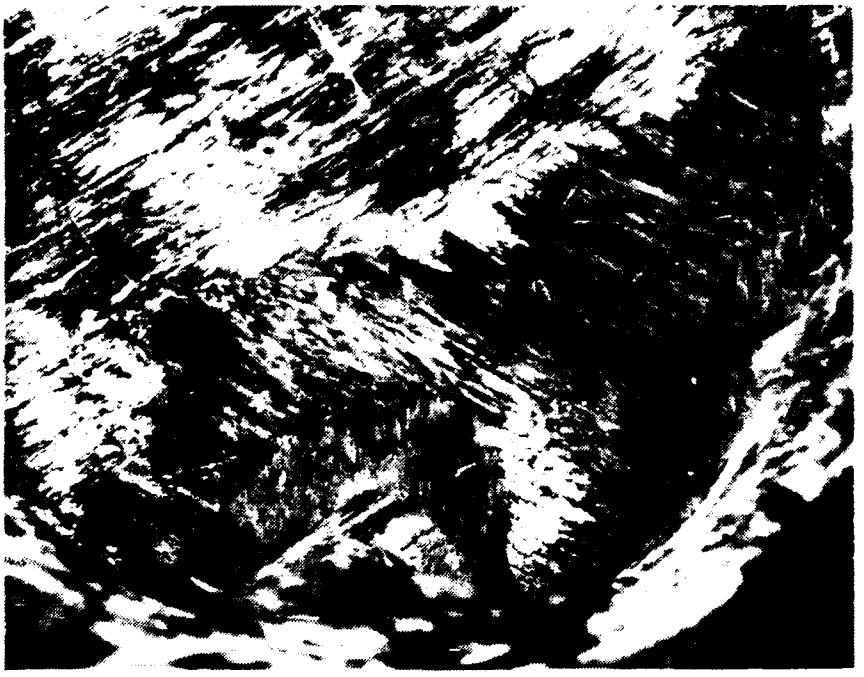

(g) Shot #15; Close Up

Figure 15. Representative Test Sample Photographs (Concl'd)

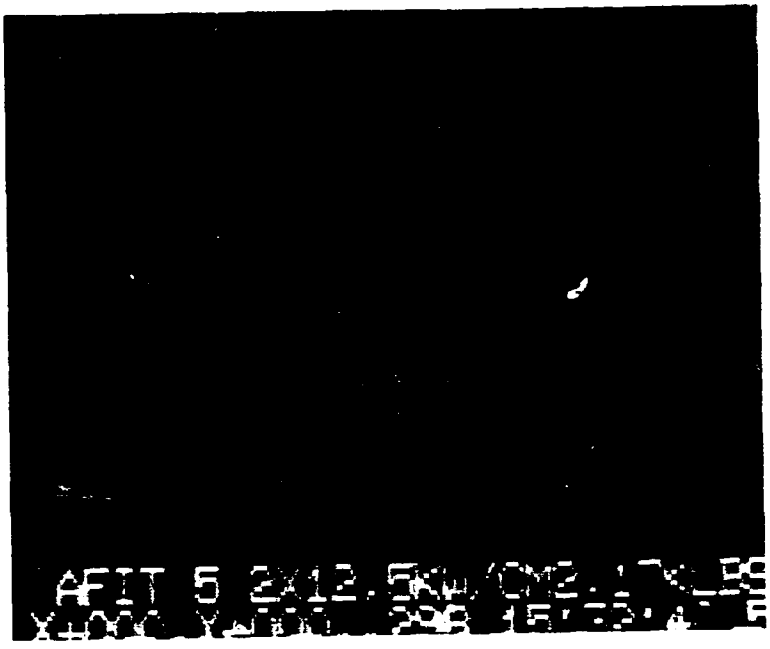

(a)

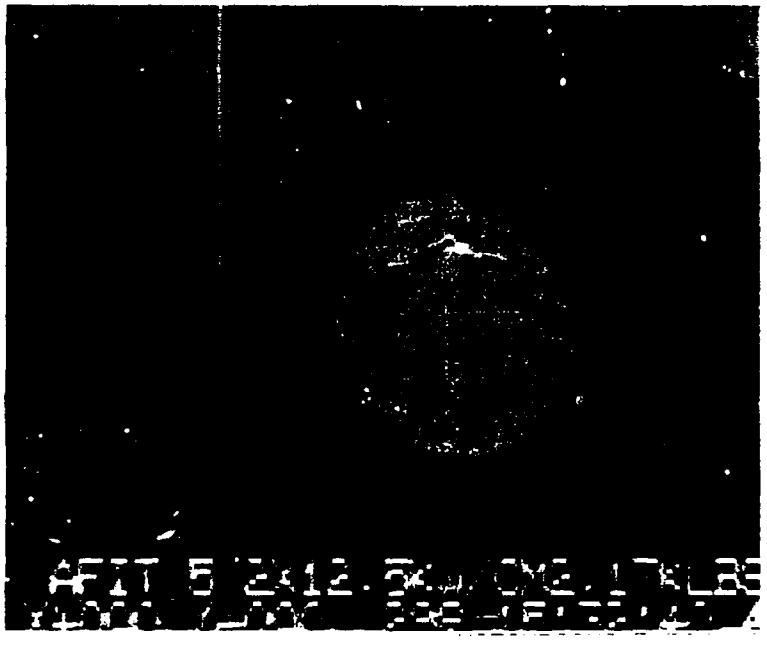

(b)

Figure 16. Video Camera Images of Shot #5

VI. Conclusions and Recommendations

As Figures 13 and 14 show, there is a slight trend toward decreasing Q* at higher stresses. The data indicate that at stress ratios explored, only a 9% decrease in Q* was seen at 13-16 kW/cm^2 and 19.8% decrease at 26 kW/cm^2.

This shows that the initial postulate is essentially correct. That is, discrete fiber removal occurs during ablation. The removal by a fracture mechanism which appears to be a linear function of applied stress (or some linear mechanism) also appears to be verified by the experimental data collected.

Therefore it is concluded that graphite/epoxy will ablate at rates that increase linearly with applied axial stress. This will continue until the applied load is so high that the tensile specimen will fracture due to the creation of an initial flaw by burning off one or two plys on the surface (12). One sample did this during the tests at LHMEL-1 (Appendix D) and two samples broke midway during irradiation (likely at the point when the cross section became too small to carry the applied load) in the EDCL-II test series.

No specific experimental efforts in this area are recommended for the immediate future. For the stress ratios seen here, ablation efficiency increase is small

enough that it may neglected for many engineering purposes, and the unloaded ablation enthalpy values may be used.

More sophisticated analytic modeling might be undertaken to explore what factors might be affecting the particular size of broken fibers. The work might be yield some insight to the rise in Q^*_{eff} seen at 16 kW/cm^2 between σ/σ_{ult} = 0.12 and 0.28.

It might also prove useful to explore the change in stiffness of a laminate as a cylindrical hole is ablated from the sample. Integrating the mass loss as a function of instantaneous stress (instead of assuming constant stress) is a likely next step.

If any further experiments are conducted, collection of the ablated particles must be attempted. Differing ply layups may also be interesting to explore. More care needs to be taken when designing test samples; as mentioned in Chapter IV, analytic balances capable of weighing larger masses are more coarse. It is imperative to build samples light enough to have their mass loss weighed to high precision. A conflicting desire, unfortunately, is the recommendation to test samples much wider than the laser beam diameter, to eliminate effects of the laminate's edges.

More sophisticated modeling of the boundary conditions on a fiber might be undertaken; specifically the effect, if

any, of layers above the plane of the ablation surface upon the fracture characteristics of the fiber. Also, a less empirical model of η_d might be found by measuring the distribution of initial cracks in the virgin fiber, and using that distribution to account for different lengths of removed fibers.

Appendix A: MELT3D.FOR, Three Dimensional Heat Conduction and Ablation Program

This appendix shows the flow of logic for this program in Figure A1. A listing of the code follows. Graphs showing the temperature dependance of thermal properties computed in this program are given in Figure A2. A listing of the subroutines called by MELT3D.FOR concludes the appendix.

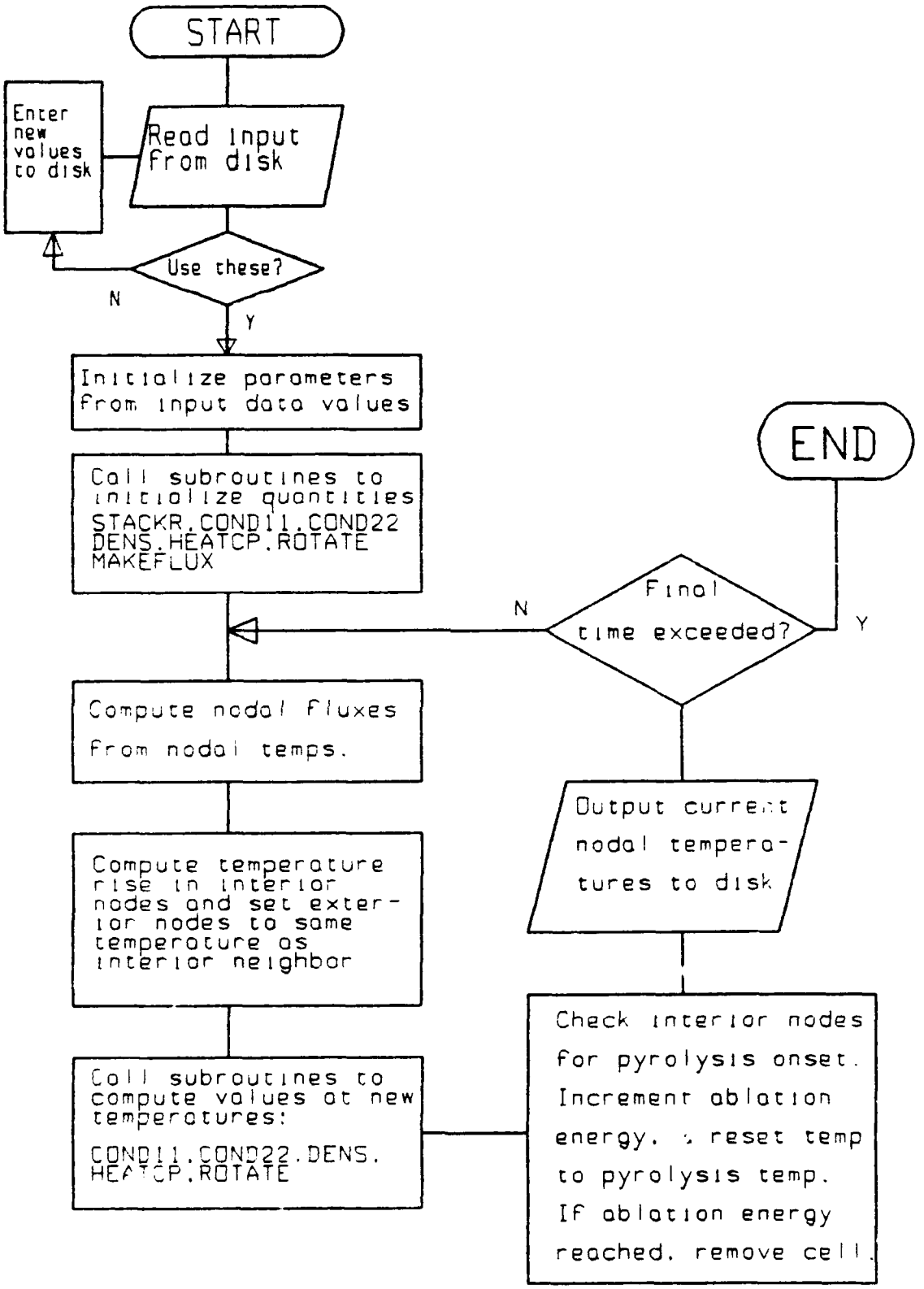

Figure A1. Flowchart for MELT3D.FOR

```
      PROGRAM MELT3D
C*************************************************************************
C
C          LAST EDIT 17 October 1989, 21:40
C     Created 2 August 1989 by Capt Joseph L. Hamrick,II  GAE-89D
C          This is a 3 dimensional transient heat conduction solving
C     program created to solve for the temperature distribution in an
C     anisotropic solid by finite summation of the heat balance on
c     a finite control volume.  The differential
C     equation of heat conduction is left in integral form for a
C     differential element of volume.  The heat fluxes through each
C     face of the cubic elements are summed algebraically, and the net
C     rate of increase of heat in the element ( in Watts) is equated to
C     the right hand side of the equation, (density*heat capacity*rate
C     of temperature change*volume of element; or rho * specheat *
C     dtemp/dt * vol).  This is solved for the temperature rise, dtemp,
C     and added to the existing temperature at one reference node of
C     the cube.
C          The heat fluxes are discretized in terms of the differences
C     in temperatures at discrete nodal points, and for a non-diagonal
C     conductivity tensor, the flux through any side is simply the sum
C     of the proper tensor terms and appropriate temperature
C     differences.
C          This program is only intended to solve for the instance of
C     prescribe laser flux on the 'top' surface (z=0) and INSULATED
C     boundarys everywhere else.  This is justified from references in
C     the thesis which show convection and reradiation to be
C     neglibible for the interaction regimes of interest here.
C
C                                 ------------
C                                /            / 1
C                               /            /  1
c                              /            /   1
C                             /____________/    1
C          qx(i,j,k)====> 1             1  ======>qx(i+1,j,k)
C                         1 qy(i,j+1,k) 1    /
c                         1    //       1   /
c                         1   //        1  /
c                         1 \//_        1 /
c                         1____________1/
C
C
C     THE VARIABLES USED IN THIS PROGRAM ARE:
C
C
C     LOOP = CRITERIA TO READ DATA INTERACTIVELY OR FROM A FILE
C
C     TEMP(I,J,K) = TEMPERATURE AT NODE (I,J,K); APPROXIMATELY
C                   EQUAL TO AVERAGE TEMP IN CELL I,J,K (deg Kelvin)
C     QX(I,J,K) = FLUX IN POSITIVE X DIRECTION THROUGH THE FRONT FACE
C                 OF CUBE I,J,K (Watts)
```

```
C     QY(I,J,K) = FLUX IN POSITIVE Y DIRECTION THRU THE LEFT SIDE FACE
C                 OF CUBE I,J,K (Watts)
C     QZ(I,J,K) = FLUX IN POSITIVE Z DIRECTION (DOWN) THRU TOP FACE OF
C                 CUBE I,J,K (Watts)
C     FLUX(I,J,K) = LASER FLUX INTO TOP FACE OF CUBES EXPOSED TO THE
C                   BEAM (Watts; [= IRRAD(I,J,K)*DX*DY])
C     RK11(I,J,K,) = CONDUCTIVITY TENSOR ELEMENT 1,1 AT I,J,K,(W/m*K)
C     RK22(I,J,K,) = CONDUCTIVITY TENSOR ELEMENT 2,2 AT I,J,K,(W/m*K)
C     RK12(I,J,K,) = CONDUCTIVITY TENSOR ELEMENT 1,2 AT I,J,K,(W/m*K)
C     RHO(I,J,K) = DENSITY OF BULK MATERIAL, kg/m**3, IN CELL I,J,K
C     SPECHEAT(I,J,K) = HEAT CAPACITY, W*s/kg*K, IN CELL I,J,K
C
C     XMAX = LENGTH OF REGION, cm
C     YMAX = WIDTH OF REGION, cm
C     ZMAX = THICKNESS OF REGION, cm
C     NUMX = NUMBER OF CELLS IN X DIRECTION
C     NUMY = "      "  "     "  Y "
C     NUMZ = "      "  "     "  Z  DIRECTION, = (# PLYS )
C
C     DX,DY,DZ = LENGTHS OF INCREMENTAL DISTANCES, meters
C     VOL = DX*DY*DZ , I.E. VOLUME OF INCREMENTAL CELL
C
C     COND??(TEMP(I,J,K),RK?)  = SUBROUTINES TO
C          COMPUTE TEMPERATURE VARIATION IN PRINCIPLE CONDUCUTIVITIES
C          RK1 AND RK2
C     DENS(TEMP,RHO)         = SUBROUTINE TO COMPUTE RHO(TEMP)
C     HEATCP(TEMP,SPECHEAT) = "          "  "       SPECHEAT(TEMP)
C     MAKEFLUX = SUBROUTINE TO COMPUTE IRRAD VALUES AND EXPOSED CELLS
C
C*******************************************************************************
C*******************************************************************************
      INTEGER FLAG(10,10,10)
      CHARACTER*70 LABTXT
      CHARACTER*10 OUTFILE
      REAL IRRAD
C
      DIMENSION TEMP(10,10,10), FLUX(10,10,10), RK11(10,10,10)
      DIMENSION RK12(10,10,10),RK22(10,10,10),NSTACK(100)
      DIMENSION RHO(10,10,10), SPECHEAT(10,10,10)
      DIMENSION SLUSH(10,10,10), QX(10,10,10)
      DIMENSION QY(10,10,10),QZ(10,10,10),RK33(10,10,10)
C
      COMMON /DATA1/ IRRAD,ABSORB,XMAX,YMAX,ZMAX,NUMX,NUMY,NUMZ,
     &RK1MAX,RK2MAX,RHOMIN,CPMIN,HABLAT,TIMEMX,TINITL,SAFE
      COMMON /DATA2/ RADIUS, XFLUX, YFLUX, TPYRO ,ALPHA,ITYPE,IPRN,
     &IXOUT,IYOUT,IZOUT,OUTFILE,LABTXT
C
C*******************************************************************************
C*******************************************************************************
C
C     ENTER DATA DIALOG TO READ LAST RUNS DATA INPUT, AND ALLOW
C     ANY CHANGES DESIRED
```

```
C
      WRITE(*,*) 'ENTER 0 TO CONTINUE WITH FILE DATA, 1 TO ENTER CORREC
     &T DATA INTERACTIVELY'
      READ(*,'(I1)') LOOP

C
      CALL DATALK(LOOP)
      CALL FLXTLK(LOOP)
C*********************************************************************
C     OPEN FILE TO OUTPUT DATA TO, BLANK FILE NAME FORCES DOS TO
C     PROMPT FOR IT, UNIX NEEDS EXPLICIT NAME
C*********************************************************************
C
      OPEN (UNIT=12,FILE = OUTFILE ,STATUS='NEW')
      WRITE(12,'(A70)') LABTXT
C
C*********************************************************************
C*********************************************************************
C
C     START COMPUTING INITIALLY NEEDED QUANTITIES
C     CHANGE XMAX, IN CENTIMETERS, TO METERS
C*********************************************************************
C*********************************************************************
C
      DX = XMAX / (100.0*FLOAT(NUMX) )
      DY = YMAX / (100.0*FLOAT(NUMY) )
      DZ = ZMAX / (100.0*FLOAT(NUMZ) )
      VOL = DX*DY*DZ
      PI = 4.000*ATAN(1.000)
      ALPHA = ALPHA*PI/180.00
      NGONE = 0
      T = 0.00
C
C*********************************************************************
C     NOTE, CASE SPECIFIC STATEMENTS FOLLOW:.....
C     THE MAXIMUM CONDUCTIVITY FOR STABILITY PURPOSES IS BEING
C     COMPUTED FOR THE SPECIFIC CASE OF K22 = K33, AND ASSUMING THE
C     MAXIMUM SUM OF K(1i) IS ALWAYS LESS THAN THE TRACE OF THE
C     CONDUCTIVITY MATRIX.  THEREFOR , THE MAXIMUM IS BEING SET TO
C     THE TRACE OF THE MATRIX, AND K22=K33.
C*********************************************************************
C
      CONMAX = (RK1MAX + 2.0*RK2MAX)/3.0
      DT = (AMIN1(DX,DY,DZ)**2)*RHOMIN*CPMIN/(2.00*SAFE*CONMAX)
      NTIME = IFIX (TIMEMX/ DT )
C*********************************************************************
C     THE FOLLOWING SUBROUTINE WILL INITIALIZE THE STACKING SEQUENCE OF
C     THE PLYS, TO DICTATE THE ROTATION OF EACH PLY IN THE GLOBAL COORD
C     SYSTEM
C*********************************************************************
C
      CALL STACKR(NSTACK)
C
```

```
C*************************************************************************
C     INITIALIZE THE TEMPERATURE AND PROPERTIES ARRAYS
C     CHANGE HABLAT,kJ/gm, TO J/kg BY MULTIPLYING BY 10**6
C*************************************************************************
C
      DO 99, I = 1, NUMX+2

      DO 99, J = 1, NUMY+2
      DO 99, K = 1, NUMZ+2
           TEMP(I,J,K) = TINITL
99    CONTINUE
C
      DO 101, I = 2, NUMX+1
      DO 102, J = 2, NUMY+1
      DO 103, K = 2, NUMZ+1
C
           CALL COND11( TEMP(I,J,K), RK1)
           CALL COND22( TEMP(I,J,K), RK2,IMETAL)
           CALL DENS  ( TEMP(I,J,K), RHO(I,J,K))
           CALL HEATCP( TEMP(I,J,K), SPECHEAT(I,J,K))
      SLUSH(I,J,K) = HABLAT*1.0E+06*RHO(I,J,K)*VOL
      FLAG(I,J,K) = 1
C
C*************************************************************************
C     NOW ROTATE THE CONDUCTIVITY TENSOR TO PLACE EACH LAYERS PROPER
C     TENSORIAL QUANTITIES INTO ITS ARRAY INITIALLY
C
      CALL ROTATE( RK11(I,J,K), RK22(I,J,K), RK12(I,J,K), RK33(I,J,K),
     & NSTACK(K), RK1,RK2, ALPHA, IMETAL)



103   CONTINUE
102   CONTINUE
101   CONTINUE
C
C*************************************************************************
C*************************************************************************
C     NEXT, INITIALIZE THE FLUX DISTRIBUTION ON THE SAMPLE; THIS
C     IS AGAIN CASE SPECIFIC, AND IS DETERMINED BY THE SUBROUTINE
C     LINKED AS 'MAKEFLUX', WHICH GETS ITS VALUES FROM THE COMMON
C     BLOCKS
C*************************************************************************
C*************************************************************************
C
      CALL MAKEFLUX (FLUX)
C
C*************************************************************************
C*************************************************************************
C     NOW ITS TIME TO ACTUALLY INCREMENT THE TIME AND LOOP THRU
C     THE REGION, SUMMING HEAT BALANCES ON EACH CUBE DX*DY*DZ
C
```

```
C     NOTE!!!!!!!

C     IF ANY INDEX IS 1 or ?MAX, THE TEMP THERE IS SET EQUAL TO
C     INDEX=2 OR ?MAX-1, SO THAT NO FLUX, I.E. INSULATED BOUNDARY,
C     IS ENFORCED.
C
C     NOTE ALSO, THE FLUXES ARE SET TO ZERO IF THE NODE CALCULATED
C     HAS ABLATED OR MELTED AWAY,  OR IF THE CELL INTO WHICH IT'S
C     HEAT WOULD PASS IS MISSING!!!!!!
C*********************************************************************

C*********************************************************************
C
      DO 200, N = 1, NTIME
      T = FLOAT(N) * DT
C*************************
      DO 201, I = 1, NUMX+1
      DO 202, J = 1, NUMY+1
      DO 203, K = 1, NUMZ+1
C
           QX(I,J,K) = FLOAT(FLAG(I,J,K)*FLAG(I+1,J,K))*((RK11(I,J,K)*
     &     (TEMP(I,J,K) - TEMP(I+1,J,K))*DY*DZ/DX ) + ( RK12(I,J,K)*
     &     (TEMP(I,J,K) - TEMP(I,J+1,K)) * DZ ))
C
           QY(I,J,K) = FLOAT(FLAG(I,J,K)*FLAG(I,J+1,K))*((RK12(I,J,K)*
     &     (TEMP(I,J,K) - TEMP(I+1,J,K)) * DZ ) + ( RK22(I,J,K) *
     &     (TEMP(I,J,K) - TEMP(I,J+1,K)) * DZ*DX/DY))
C
           QZ(I,J,K) = FLOAT(FLAG(I,J,K)*FLAG(I,J,K+1))*( RK33(I,J,K)*
     &     (TEMP(I,J,K) - TEMP(I,J,K+1)) * DY*DX/DZ )
C
203   CONTINUE
202   CONTINUE
201   CONTINUE
C
C*********************************************************************
C*********************************************************************
C*********************************************************************
C     NOW LOOP OVER THE INTERIOR OF THE ENTIRE MATERIAL CUBE, WHICH
C     EXCLUDES THE PEREPHERIAL NODES, WHICH ONLY EXIST TO ENFORCE THE
C     BCs.
C     THE INTERIOR, HOWEVER, SIMPLY IS THE CONDUCTION PROBLEM,
C     UNLESS CELLS ARE REMOVED AND THEN LASER FLUX IS APPLIED TO THE
C     CELL WHICH USED TO BE BENEATH IT.
C*********************************************************************
C*********************************************************************
C
      DO 210, I = 2, NUMX+1
      DO 211, J = 2, NUMY+1
      DO 212, K = 2, NUMZ+1
C
      EIN = FLUX(I,J,K)*DX*DY + QX(I-1,J,K) - QX(I,J,K) + QY(I,J-1,K)
     &     -QY(I,J,K) + QZ(I,J,K-1) - QZ(I,J,K)
```

```
C
      DELTAT = EIN*DT/ (RHO(I,J,K) * SPECHEAT(I,J,K)* VOL)
      TEMP(I,J,K) = TEMP(I,J,K) + DELTAT
C
212   CONTINUE
211   CONTINUE
210   CONTINUE
C
C*************************************************************************
C*************************************************************************
C     NOW GO AROUND EACH BOUNDARIES AND SET THE TEMPERATURE ON EACH
C     EDGE NODE EQUAL TO THE TEMPERATURE JUST INSIDE FROM IT, SO

C     THAT ON SUCH BOUNDARIES, THERE WILL BE NO FLUX THROUGH
C     TO THE INTERIOR
C*************************************************************************
C
      DO 220, I = 1, NUMX+2
      DO 221, J = 1, NUMY+2
           TEMP(I,J,1) = TEMP(I,J,2)
           TEMP(I,J,NUMZ+2) = TEMP(I,J,NUMZ+1)
221   CONTINUE
220   CONTINUE
C
      DO 230, I = 1, NUMX+2
      DO 231, K = 1, NUMZ+2
           TEMP(I,1,K) = TEMP(I,2,K)
           TEMP(I,NUMY+2,K) = TEMP(I,NUMY+1,K)
231   CONTINUE
230   CONTINUE
C
      DO 240, J = 1, NUMY+2
      DO 241, K = 1, NUMZ+2
           TEMP(1,J,K) = TEMP(2,J,K)
           TEMP(NUMX+2,J,K) = TEMP(NUMX+1,J,K)
241   CONTINUE
240   CONTINUE
C*************************************************************************
C*************************************************************************
C
C     NOW THAT THE NEW TEMPERATURES HAVE BEEN COMPUTED, RECALCULATE
C     THE PROPERTIES IN THE REGION
C     AGAIN, IF IMETAL IS 1, SKIP ANISOTROPIC TENSOR, SET
C     RK11=RK1=RK22=RK33 AND RK12=0
C*************************************************************************
C*************************************************************************
      DO 301, I = 2, NUMX+1
      DO 302, J = 2, NUMY+1
      DO 303, K = 2, NUMZ+1
C
           CALL COND11( TEMP(I,J,K), RK1)
           CALL COND22( TEMP(I,J,K), RK2,IMETAL)
           CALL DENS  ( TEMP(I,J,K), RHO(I,J,K))
```

```
           CALL HEATCP( TEMP(I,J,K), SPECHEAT(I,J,K))
C
      CALL ROTATE( RK11(I,J,K), RK22(I,J,K), RK12(I,J,K), RK33(I,J,K),
     & NSTACK(K), RK1,RK2, ALPHA, IMETAL)
C
C*************************************************************************
C     IF THIS NODE IS NOT AT THE PYROLYSIS TEMPERATURE, GO ON TO THE
C     NEXT NODE.  IF IT IS AT PYROLYSIS TEMPERATURE, INCREMENT THE
C     'COUNTER' KEEPING TRACK OF THE ABLATION ENERGY BEING DUMPED INTO
C     THE CELL, AND RESET THE TEMPERATURE OF THE CELL BACK DOWN TO THE
C     PYROLYSIS TEMPERATURE, TPYRO.
C*************************************************************************
C*************************************************************************
C

      IF (TEMP(I,J,K) .LE. TPYRO) GOTO 303
C
      SLUSH(I,J,K) = SLUSH(I,J,K) - RHO(I,J,K)*SPECHEAT(I,J,K)*
     &(TEMP(I,J,K)-TPYRO)*VOL
      TEMP(I,J,K) = TPYRO
C*************************************************************************
C     IF THE 'SLUSH' ENERGY, I.E. ENERGY TO ABLATE THE WHOLE CELL
C     HASN'T BEEN REACHED, GO ON TO NEXT CELL.  IF IT HAS, REMOVE IT
C     PLACE IT'S FLUX ON THE NEXT CELL
C*************************************************************************
C
      IF (SLUSH(I,J,K) .GT. 0.00) GOTO 303
           FLAG(I,J,K) = 0
           FLUX(I,J,K+1) = FLUX(I,J,K)
           FLUX(I,J,K) = 0.000
           TEMP(I,J,K) = 0.000
C*************************************************************************
C     INCREMENT COUNTER TO SEE HOW MANY CELLS ARE REMOVED
C*************************************************************************
      NGONE = NGONE + 1
C*************************************************************************
C     LINES TO OUTPUT TO FILE AND TO THE SCREEN
C
C*************************************************************************
C
      WRITE(12,800) 'CR',I,J,K,T
      WRITE(*,800) 'CR',I,J,K,T
C
C
303   CONTINUE
302   CONTINUE
301   CONTINUE
C*************************************************************************
C
      IF ( MOD (N,IPRN) .EQ. 0) THEN

      WRITE(12,'(''TI'',F10.5)') T
```

```
      DO 310, I = 2, NUMX+1, IXOUT
      DO 310, J = 2, NUMY+1, IYOUT
      DO 310, K = 2, NUMZ+1, IZOUT
C
      Y = 100.0*DY* FLOAT(J-2)
      X = 100.0*DX* FLOAT(I-2)
      Z = 100.0*DZ* FLOAT(K-2)
      WRITE(12,'(1X,3F10.4,F8.0)') X,Y,Z,TEMP(I,J,K)
C
310   CONTINUE
      END IF
c
c
      IF ( MOD (N,ITYPE) .EQ. 0) THEN
      WRITE(*,803) T
      WRITE(*,801) (100.0*FLOAT(J-2)*DY, J=NUMY+1,2,-IYOUT)

      DO 410, K = 2, NUMZ+1,IZOUT
      WRITE(*,*) 'PLY LAYER # ',K,' DEPTH= ', 100.0*FLOAT(K-2)*DZ,'CM'
      DO 411, I = 2, NUMX, IXOUT
      X = 100.0*FLOAT(I-2)*DX
      WRITE(*,802) X,(TEMP(I,J,K), J = NUMY+1,2,-IYOUT)
411   CONTINUE
410   CONTINUE
      END IF
C*******************************************************************************
C
C
200   CONTINUE
C
      CALL DENS (TINITL, RHOMAX)
      DELTAM = RHOMAX * VOL * NGONE * 1.0E03
      WRITE(*,*) 'RHOMAX,VOL,NGONE = ' , RHOMAX,VOL,NGONE
      WRITE(*,*) 'MASS LOSS IS ', DELTAM
C
      WRITE(12,*) 'NGONE = ',NGONE
      WRITE(12,*) 'MASS REMOVED = ', DELTAM
800   FORMAT (1X,A2,3I4,F10.5,'CELL IJK REMOVED AT TIME T')
801   FORMAT(1X,'X / Y>',100F7.2)
802   FORMAT(1X,F5.1,100F7.1)
803   FORMAT('1','TIME IS ',F10.6,' SECONDS')

      STOP
      END
```

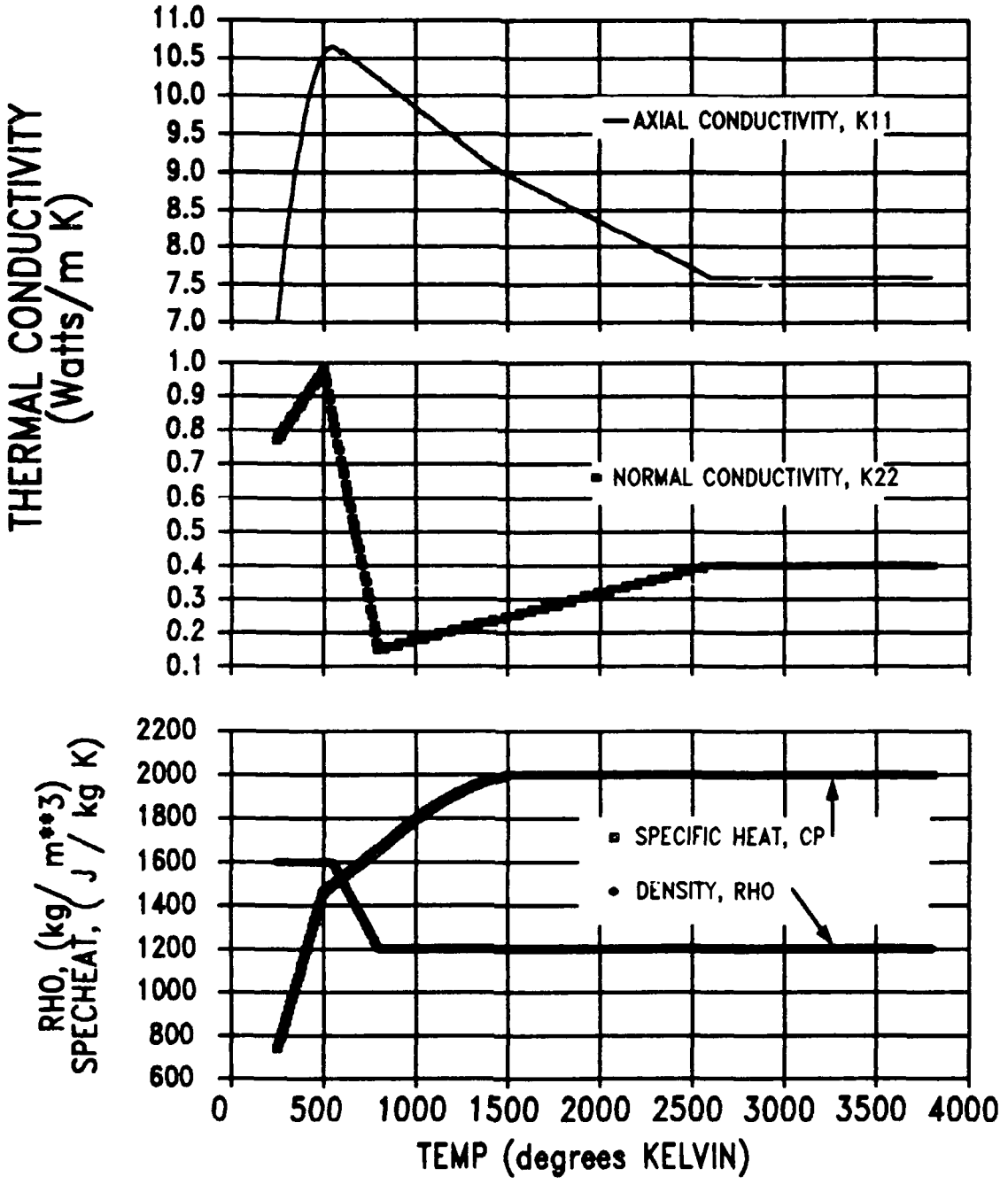

Figure A2. Values of Thermal Properties Used in MELT3D.FOR

```
      SUBROUTINE COND11(T, RK1)
C*****************************************************************************
C     SUBROUTINE TO COMPUTE PRINCIPLE (AXIAL) CONDUCTIVITY, K11, AS A
C     FUNCTION OF TEMPERATURE,T, IN DEGREES KELVIN, BETWEEN 250K AND
C     3800K.  CONDUCTIVITY, K11 IS RETURNED IN WATTS/M*K
C*****************************************************************************
C*****************************************************************************
      IF (T .GE. 2600) THEN
           RK1 = 7.6
      ELSE IF (T .GE. 1400) THEN
           RK1 = 10.85  -  1.25E-03 * T
      ELSE IF (T .GE. 600) THEN
           RK1 = 11.725  -  1.875E-03 * T
      ELSE IF (T .GE. 250) THEN
           RK1 = -1.46101 + T*(.04390889-3.982522E-05*T)
      ELSE IF (T .LT. 250) THEN
           RK1 = 7.0
           IERR = 1
      END IF
      RETURN
      END
C*****************************************************************************
      SUBROUTINE COND22 (T, RK2, METAL)
C*****************************************************************************
C     SUBROUTINE TO COMPUTE PRINCIPLE (NORMAL) CONDUCTIVITY, K22, AS A
C     FUNCTION OF TEMPERATURE,T, IN DEGREES KELVIN, BETWEEN 250K AND
C     3800K.  CONDUCTIVITY, K22 IS RETURNED IN WATTS/M*K
C*****************************************************************************
      IF (T .GE. 2600) THEN
           RK2 = 0.4
      ELSE IF (T .GE. 800) THEN
           RK2 = 3.888888889E-02 + 1.38888889E-04 * T
      ELSE IF (T .GE. 500) THEN
           RK2 = 2.363333333 -  2.76666667E-03 * T
      ELSE IF (T .GE. 250) THEN
           RK2 = 0.56 + 8.4E-04*T
      ELSE IF (T .LT. 250) THEN
           RK2 = 0.77
           IERR = 1
      END IF
C
      METAL = 0
      RETURN
      END
C*****************************************************************************
      SUBROUTINE DENS(T,P)
C*****************************************************************************
C     SUBROUTINE TO COMPUTE DENSITY, P, AS A FUNCTION OF TEMPERATURE,T,
C     IN DEGREES KELVIN, BETWEEN 250K AND 3800K.  DENSITY, P,  IS
C     RETURNED IN kg/m**3
C*****************************************************************************
      IF (T .LE. 550) THEN
```

```
            P = 1600.0
        ELSE IF (T .GE. 800) THEN

            P = 1200.0
        ELSE IF (T .GT. 550) THEN
            P = 2480.0 - 1.6 * T
        END IF
        RETURN
        END
C*******************************************************************************
        SUBROUTINE HEATCP(T,CP)
C*******************************************************************************
C       SUBROUTINE TO COMPUTE HEAT CAPACITY, CP, AS A FUNCTION OF
C       TEMPERATURE,T,IN DEGREES KELVIN, BETWEEN 250K AND 3800K.
C       HEAT CAPACITY, CP IS RETURNED IN JOULES / kg K
C*******************************************************************************
        IF (T .GE. 1500) THEN
            CP = 2000.0
        ELSE IF (T .GE. 850) THEN
            CP = 741.825 + T*(1.484103 - 4.316507E-04*T)
        ELSE IF (T .GE. 500) THEN
            CP =  1131.4286 + 0.657142857 * T
        ELSE IF (T .LT. 500) THEN
            CP = 20.0 + 2.88 * T
        END IF
        RETURN
        END
C*******************************************************************************
C*******************************************************************************
        SUBROUTINE STACKR(NSTACK)
        DIMENSION NSTACK(100)
        COMMON /DATA1/ IRRAD,ABSORB,XMAX,YMAX,ZMAX,NUMX,NUMY,NUMZ,
       &RK1MAX,RK2MAX,RHOMIN,CPMIN,HABLAT,TIMEMX,TINITL,SAFE
C*******************************************************************************
C       FOR A [0, +/- ALPHA]nS LAYUP, 0 MEANS 0, +1 MEANS +ALPHA,
C       -1 MEANS - ALPHA
C*******************************************************************************
        NPLYS = NUMZ
        DO 10, I = 2, (NPLYS/2)+1
            IF (MOD(I-2,3) .EQ. 0) THEN
                NSTACK(I) = 0
            ELSE IF (MOD(I-2,3) .EQ. 1 ) THEN
                NSTACK(I) = 1
            ELSE IF (MOD(I-2,3) .EQ. 2) THEN
                NSTACK(I) = -1
            END IF
10      CONTINUE
C
        DO 20, I = NPLYS/2 + 2, NPLYS+1
            J = (I - (NPLYS/2 +1) )*2 - 1
            NSTACK(I) = NSTACK(I-J)
20      CONTINUE
        RETURN
```

```
      END
C*********************************************************************
      SUBROUTINE FLXTLK (LOOP)
C
      CHARACTER*70 LABTXT
      CHARACTER*10 OUTFILE
      COMMON /DATA1/ IRRAD,ABSORB,XMAX,YMAX,ZMAX,NUMX,NUMY,NUMZ,
     &RK1MAX,RK2MAX,RHOMIN,CPMIN,HABLAT,TIMEMX,TINITL,SAFE
C
      COMMON /DATA2/ RADIUS, XFLUX,YFLUX, TPYRO, ALPHA,ITYPE,IPRN,
     &IXOUT, IYOUT, IZOUT,OUTFILE,LABTXT
C
      OPEN (UNIT=11,FILE='3DINPUT2.DAT',STATUS='OLD')
      READ (11,*) RADIUS, XFLUX, YFLUX, TPYRO, ALPHA,ITYPE,IPRN,IXOUT,
     &IYOUT,IZOUT
      READ (11,'(A10,A70)') OUTFILE,LABTXT
C
      DX = XMAX / (100.0*FLOAT(NUMX) )
      DY = YMAX / (100.0*FLOAT(NUMY) )
      DZ = ZMAX / (100.0*FLOAT(NUMZ) )
      CONMAX = (RK1MAX + 2.0*RK2MAX)/3.0
      DT = (AMIN1(DX,DY,DZ)**2)*RHOMIN*CPMIN/(2.00*SAFE*CONMAX)
      NTIME = IFIX (TIMEMX/ DT )
C
      IF (LOOP .EQ. 0) THEN
           GO TO 999
      END IF
C
017   CONTINUE
      WRITE(*,*) ' '
      WRITE(*,*) 'THE TIME STEP IS ',DT,'  SECONDS'
      WRITE(*,*) 'BROKEN INTO      ',NTIME,'  INCREMENTS'
      WRITE(*,*) ' '
      WRITE(*,*) ' '
      WRITE(*,*) '1  RADIUS OF CIRCULAR BEAM IS ',RADIUS,' CENTIMETERS'
      WRITE(*,*) '2  X COORD OF BEAM CENTER IS   ',XFLUX,' CENTIMETERS'
      WRITE(*,*) '3  Y COORD OF BEAM CENTER IS   ',YFLUX,' CENTIMETERS'
      WRITE(*,*) '4  ABLATION OR MELT TEMP  IS   ',TPYRO,' DEG KELVIN'
      WRITE(*,*) '5  + AND - WRAP ANGLE OF LAYUP IS ',ALPHA,' DEGREES'
      WRITE(*,*) '6  INTEGER FREQUENCY TO TYPE RESULTS TO CRT IS',ITYPE
      WRITE(*,*) '7  INTEGER FREQUENCY TO SEND RESULTS TO DISK IS',IPRN
      WRITE(*,*) '8  DISK FILE TO OUTPUT TO IS(lowercase) ', OUTFILE
      WRITE(*,*) '9  LABEL TO INSERT AT TOP OF DISKFILE IS'
      WRITE(*,'(A70)') LABTXT
      WRITE(*,*) '10  FREQUENCY TO SEND X DATA TO DISK', IXOUT
      WRITE(*,*) '11  FREQUENCY TO SEND Y DATA TO DISK', IYOUT
      WRITE(*,*) '12  FREQUENCY TO SEND Z DATA TO DISK', IZOUT
      WRITE(*,*) ' '
      WRITE(*,*) 'Enter an integer # of variable to change, or 0 to
     &continue'
      WRITE(*,*) ' '
      WRITE(*,*) ' '
```

```
      READ(*,*) NSWER
C
C     IF NSWER ISN'T A PERMISSIBLE # (1-9), PROMPT AGAIN
C
      IF ((NSWER .LT. 1 .OR. NSWER.GT.12).AND. NSWER.NE.0) THEN
           WRITE(*,*) 'REPLY MUST BE 0 OR 1 thru 12, PLEASE TRY AGAIN'

           GOTO 017
      END IF
C
      GOTO (1,2,3,4,5,6,7,8,9,10,11,12), NSWER
C*************************************************************************
C     IF ANSWER IS 0, JUMP OUT OF LOOP AND WRITE NEW VARIABLES TO DATA
C     FILE, BY JUMPING TO LINE #100
C*************************************************************************
      GOTO 100
001   WRITE(*,*)'NEW RADIUS, CENTIMETERS, IS?'
      READ(*,*)  RADIUS
      GOTO 017
002   WRITE(*,*)'NEW X COORD OF CENTERLINE, IN CENTIMETERS, IS?'
      READ(*,*) XFLUX
      GOTO 017
003   WRITE(*,*)'NEW Y COORD OF CENTERLINE, IN CENTIMETERS, IS?'
      READ(*,*) YFLUX
      GOTO 017
004   WRITE(*,*)'NEW PYRO OR MELT TEMP, IN KELVIN, IS?'
      READ(*,*) TPYRO
      GOTO 017
005   WRITE(*,*)'NEW WRAP ANGLE, DEGREES, IS?'
      READ(*,*) ALPHA
      GOTO 017
006   WRITE(*,*)'INTEGER FOR SCREEN OUTPUT ?'
      READ(*,*) ITYPE
      GOTO 017
007   WRITE(*,*)'INTEGER FOR DISKFILE OUTPUT ?'
      READ(*,*) IPRN
      GOTO 017
008   WRITE(*,*)'NAME FOR DISK FILE ?'
      READ(*,'(A10)') OUTFILE
      GOTO 017
009   WRITE(*,*)' LABEL FOR DESCRIBING DISK FILE ?'
      READ(*,'(A70)') LABTXT
      GOTO 017
010   WRITE(*,*)'INTEGER FOR X DISKFILE OUTPUT ?'
      READ(*,*) IXOUT
      GOTO 017
011   WRITE(*,*)'INTEGER FOR Y DISKFILE OUTPUT ?'
      READ(*,*) IYOUT
      GOTO 017
012   WRITE(*,*)'INTEGER FOR Z DISKFILE OUTPUT ?'
      READ(*,*) IZOUT
      GOTO 017
C
```

```
100   CONTINUE
      REWIND 11
      WRITE(11,*) RADIUS, XFLUX, YFLUX, TPYRO, ALPHA, ITYPE, IPRN,IXOUT
     &,IYOUT,IZOUT
      WRITE(11,'(A10,A70)') OUTFILE,LABTXT
999   CONTINUE
      CLOSE (11)
      RETURN
      END
C*******************************************************************************
C*******************************************************************************
      SUBROUTINE DATALK (LOOP)
      REAL IRRAD
      COMMON /DATA1/ IRRAD,ABSORB,XMAX,YMAX,ZMAX,NUMX,NUMY,NUMZ,
     &RK1MAX,RK2MAX,RHOMIN,CPMIN,HABLAT,TIMEMX,TINITL,SAFE
C
      OPEN (UNIT=10,FILE='3DINPUT.DAT',STATUS='OLD')
      READ (10,*) IRRAD,ABSORB,XMAX,YMAX,ZMAX,NUMX,NUMY,NUMZ
      READ (10,*) RK1MAX,RK2MAX,RHOMIN,CPMIN,HABLAT,TIMEMX,TINITL,SAFE
C
      IF (LOOP .EQ. 0) THEN
          GO TO 999
      END IF
C
017   CONTINUE
      DX = XMAX / (100.0*FLOAT(NUMX) )
      DY = YMAX / (100.0*FLOAT(NUMY) )
      DZ = ZMAX / (100.0*FLOAT(NUMZ) )
      CONMAX = (RK1MAX + 2.0*RK2MAX) / 3.0
      DELTAT = (AMIN1(DX,DY,DZ)**2)*RHOMIN*CPMIN/(2.0*SAFE*CONMAX)
      WRITE(*,*) ' '
      WRITE(*,*) ' '
      WRITE(*,*) ' '
      WRITE(*,*) '1  IRRADIANCE INCIDENT IS    ',IRRAD,'       W/cm**2'
      WRITE(*,*) '2  SURFACE ABSORBTIVITY IS    ',ABSORB
      WRITE(*,*) '3  LENGTH(X) OF SPECIMEN IS   ',XMAX,' CENTIMETERS'
      WRITE(*,*) '4  YMAX (Y) OF SPECIMEN IS   ',YMAX, ' CENTIMETERS'
      WRITE(*,*) '5  THICKNESS(Z) SPECIMEN IS   ',ZMAX, '.CENTIMETERS'
      WRITE(*,*) '6  NUMBER OF X NODES IS        ',NUMX
      WRITE(*,*) '7  NUMBER OF Y NODES IS        ',NUMY
      WRITE(*,*) '8  NUMBER OF Z NODES IS        ',NUMZ
      WRITE(*,*) '9  MAX AXIAL CONDUCTIVITY IS ',RK1MAX,'      W/mK'
      WRITE(*,*) '10 MAX NORMAL CONDUCTIVITY IS',RK2MAX,'      W/mK'
      WRITE(*,*) '11 MINIMUM DENSITY  IS       ',RHOMIN,'      kg/m**3'
      WRITE(*,*) '12 MINIMUM Cp IS             ',CPMIN,'       J/ kg K'
      WRITE(*,*) '13 THERMOCHEM HEAT OF ABLATION ',HABLAT,'    kJ/gm'
      WRITE(*,*) '14 MAXIMUM TIME DURATION IS    ',TIMEMX,'    SECONDS'
      WRITE(*,*) '15 INITIAL SAMPLE TEMPERATURE  ',TINITL,'    KELVIN'
      WRITE(*,*) '16 SAFETY FACTOR FOR TIME INCREMENT',SAFE
      WRITE(*,*) 'DT will b    ',DELTAT,' Seconds'
      WRITE(*,*) 'Enter an integer # of variable to change, or 0 to
     &continue'
      WRITE(*,*) ' '
```

```
      WRITE(*,*) ' '
      READ(*,*) NSWER
C
C     IF NSWER ISN'T A PERMISSIBLE # (1-16), PROMPT AGAIN
C
      IF ((NSWER .LT. 1 .OR. NSWER.GT.16).AND. NSWER.NE.0) THEN
           WRITE(*,*) 'REPLY MUST BE 0 OR 1 thru 16, PLEASE TRY AGAIN'
           GOTO 017
      END IF

      GOTO (1,2,3,4,5,6,7,8,9,10,11,12,13,14,15,16), NSWER
C*********************************************************************
C     IF ANSWER IS 0, JUMP OUT OF LOOP AND WRITE NEW VARIABLES TO DATA
C     FILE, BY JUMPING TO LINE #100
C*********************************************************************
      GOTO 100
001   WRITE(*,*)'NEW IRRAD, W/cm**2, IS?'
      READ(*,*) IRRAD
      GOTO 017
002   WRITE(*,*)'NEW SURFACE ABSORBTIVITY (0.0 to 1.0)?'
      READ(*,*) ABSORB
      GOTO 017
003   WRITE(*,*)'NEW LENGTH, CM, IS?'
      READ(*,*) XMAX
      GOTO 017
004   WRITE(*,*)'NEW WIDTH, CM, IS?'
      READ(*,*) YMAX
      GOTO 017
005   WRITE(*,*)'NEW THICKNESS, CM, IS?'
      READ(*,*) ZMAX
      GOTO 017
006   WRITE(*,*)'NEW NUMBER OF X NODES, IS?'
      READ(*,*) NUMX
      GOTO 017
007   WRITE(*,*)'NEW NUMBER OF Y NODES, IS?'
      READ(*,*) NUMY
      GOTO 017
008   WRITE(*,*)'NEW NUMBER OF Z NODES, IS?'
      READ(*,*) NUMZ
      GOTO 017
009   WRITE(*,*)'NEW MAXIMUM AXIAL CONDUCTIVITY, W/ m K, IS?'
      READ(*,*) RK1MAX
      GOTO 017
010   WRITE(*,*)'NEW MAXIMUM NORMAL CONDUCTIVITY, W/ m K, IS?'
      READ(*,*) RK2MAX
      GOTO 017
011   WRITE(*,*)'NEW MINIMUM DENSITY, kg/m**3, IS?'
      READ(*,*) RHOMIN
      GOTO 017
012   WRITE(*,*)'NEW MINIMUM SPECIFIC HEAT(Cp), J/kg K, IS?'
      READ(*,*) CPMIN
      GOTO 017
013   WRITE(*,*)'NEW THERMOCHEM HEAT OF ABLATION, kJ / gm, IS?'
```

```
      READ(*,*) HABLAT
      GOTO 017
014   WRITE(*,*)'NEW MAXIMUM TIME,SECONDS, IS?'
      READ(*,*) TIMEMX
      GOTO 017
015   WRITE(*,*)'NEW INITIAL TEMPERATURE, deg KELVIN, IS?'
      READ(*,*) TINITL
      GOTO 017
016   WRITE(*,*)'NEW SAFETY FACTOR IS?'
      READ(*,*) SAFE
      GOTO 017

100   CONTINUE
      REWIND 10
      WRITE(10,*)IRRAD,ABSORB,XMAX,YMAX,ZMAX,NUMX,NUMY,NUMZ
      WRITE(10,*) RK1MAX,RK2MAX,RHOMIN,CPMIN,HABLAT,TIMEMX,TINITL,SAFE
999   CONTINUE
      CLOSE (10)
      RETURN
      END
C*******************************************************************************
      SUBROUTINE MAKEFLUX(FLUX)
C*******************************************************************************
C     INITIALIZES A CIRCULAR BEAM OF UNIFORM INTENSITY, IRRAD*ABSORB
C     CENTERED ON THE FACE OF REGION
C*******************************************************************************
      CHARACTER*70 LABTXT
      CHARACTER*10 OUTFILE
      REAL IRRAD
      DIMENSION FLUX(10,10,10)
      COMMON /DATA1/ IRRAD,ABSORB,XMAX,YMAX,ZMAX,NUMX,NUMY,NUMZ,
     &RK1MAX,RK2MAX,RHOMIN,CPMIN,HABLAT,TIMEMX,TINITL,SAFE
      COMMON /DATA2/ RADIUS, XFLUX, YFLUX, TPYRO, ALPHA,ITYPE,IPRN,
     &IXOUT,IYOUT,IZOUT,OUTFILE,LABTXT
C
      DO 100, I = 1, NUMX+2
      DO 101, J = 1, NUMY+2
      DO 102, K = 1, NUMZ+2
           FLUX(I,J,K) = 0.0
102   CONTINUE
101   CONTINUE
100   CONTINUE
C
      NXCL =  NINT ( FLOAT(NUMX) / (XMAX/XFLUX))
      NYCL =  NINT ( FLOAT(NUMY) / (YMAX/YFLUX))
      DX = XMAX / FLOAT((NUMX) )
      DY = YMAX / FLOAT((NUMY) )
C
      DO 200, I = 1, NUMX+2
      DO 201, J = 1, NUMY+2
C
      XSQUAR=( DX * FLOAT( IABS(NXCL-I)) )**2.0
      YSQUAR=( DY * FLOAT( IABS(NYCL-J)) )**2.0
```

```
      PNTRAD=XSQUAR+YSQUAR
      DIFF=PNTRAD - (RADIUS*RADIUS + (0.5*(DX*DX + DY*DY) ))
C
      IF (DIFF .LT. 0.0)  THEN
C*************************************************************************
C     CHANGE FLUX FROM WATTS/CM**2 TO WATTS/M**2 BY MULTIPLYING BY
C     10000.0
C*************************************************************************
           FLUX(I,J,2)= IRRAD*ABSORB*10000.0
      END IF
C
201   CONTINUE
200   CONTINUE

C
      DO 300, I = 1, NUMX
      WRITE(*,900) (FLUX (I,J,2), J=1,NUMY)
300   CONTINUE
C
900   FORMAT(1X,100F4.0)
      RETURN
      END
C*************************************************************************
      SUBROUTINE ROTATE(R11,R22,R12,R33, NSTAK, RK1, RK2, ALPHA,
     &IMETAL)
C*************************************************************************
C     SUBROUTINE TO ROTATE CONDUCTIVITIES TO MAKE TENSOR OUT OF THEM
C     IF IMETAL IS 1, SKIP ANISOTROPIC TENSOR, SET RK11=RK1=RK22=RK33
C     AND RK12=0
C*************************************************************************
      IF (IMETAL .EQ. 1) THEN
      R11 = RK1
      R22 = RK1
      R33 = RK1
      R12 = 0.000
      GOTO 104
      END IF
C
      IF (NSTAK .EQ. 0) THEN
           R11 = RK1
           R22 = RK2
           R12 = 0.000
           R33 = RK2
C
      ELSE IF (NSTAK .EQ. 1) THEN
           R33 = RK2
           R11 = RK1*COS(ALPHA)*COS(ALPHA) +
     &               RK2*SIN(ALPHA)*SIN(ALPHA)
           R22 = RK2*COS(ALPHA)*COS(ALPHA) +
     &               RK1*SIN(ALPHA)*SIN(ALPHA)
           R12 = COS(ALPHA)*SIN(ALPHA)*(RK1-RK2)
C
      ELSE IF (NSTAK .EQ. -1) THEN
```

```
            R33 = RK2
            R11 = RK1*COS(ALPHA)*COS(ALPHA) +
     &                RK2*SIN(ALPHA)*SIN(ALPHA)
            R22 = RK2*COS(ALPHA)*COS(ALPHA) +
     &                RK1*SIN(ALPHA)*SIN(ALPHA)
            R12 = COS(ALPHA)*SIN(-ALPHA)*(RK1-RK2)
          END IF
C
C*************************************************************************
C     JUMP DOWN TO HERE IF ISOTROPIC MATERIAL
C*************************************************************************
104   CONTINUE
      RETURN
      END
```

Appendix B: Formulation of Beam Equations on an Elastic Foundation

An elastic beam in flexure on a foundation with a finite modulus is modeled as a simple Bernoulli-Euler beam element subject to a distributed loading. This loading will be broken into two distinct parts: p(x), the normal transverse loading component, and q(x), the reaction of the elastic foundation. If the foundation is assumed to be linearly elastic, $q(x) = k \cdot w(x)$. The differential equation of the beam in Figure B1 becomes

$$EI\, w'''' + kw = -p(x) \qquad \text{(B1)}$$

The homogenous solution to this equation (7:4) is

$$w(x) = e^{\beta x}(A'\cos\beta x + B'\sin\beta x) \cdot + e^{-\beta x}(C'\cos\beta x + D'\sin\beta x) \qquad \text{(B2)}$$

where $\beta^4 = k/4EI$.

Without any loading p(x), the portion of the beam from B to C will obey the homogenous solution. Since the fibers are very long compared to to their diameter, the fiber may be considered to be semi-infinite in length.

The requirement for the displacement and slope of the fiber to vanish at large x ($w = dw/dx = 0;\ x \to \infty$) dictates that the coefficients of $e^{+\beta x}$ must vanish...

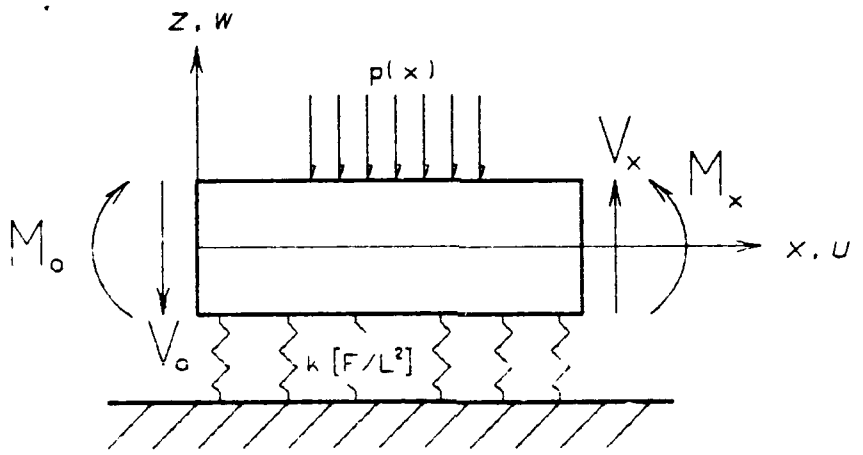

Figure B1. Beam Element on Elastic Foundation

$$w_{BC}(x) = e^{-\beta x}\left[C'\cos\beta x + D'\sin\beta x\right] \qquad \text{(B3a)}$$

$$w'_{BC}(x) = \beta e^{-\beta x}\left[(-C'+D')\cos\beta x + (-C'-D')\sin\beta x\right] \qquad \text{(B3b)}$$

$$w''_{BC}(x) = 2\beta^2 e^{-\beta x}\left[-D'\cos\beta x + C'\sin\beta x\right] \qquad \text{(B3c)}$$

$$w'''_{BC}(x) = 2\beta^3 e^{-\beta x}\left[(C'+D')\cos\beta x + (-C'+D')\sin\beta x\right] \qquad \text{(B3d)}$$

The thermal gradient across the portion of the beam from A to B would induce, in a beam element entirely free to rotate, a curvature of $1/\rho_t$ where ρ_t is the radius of curvature (Figure B2).

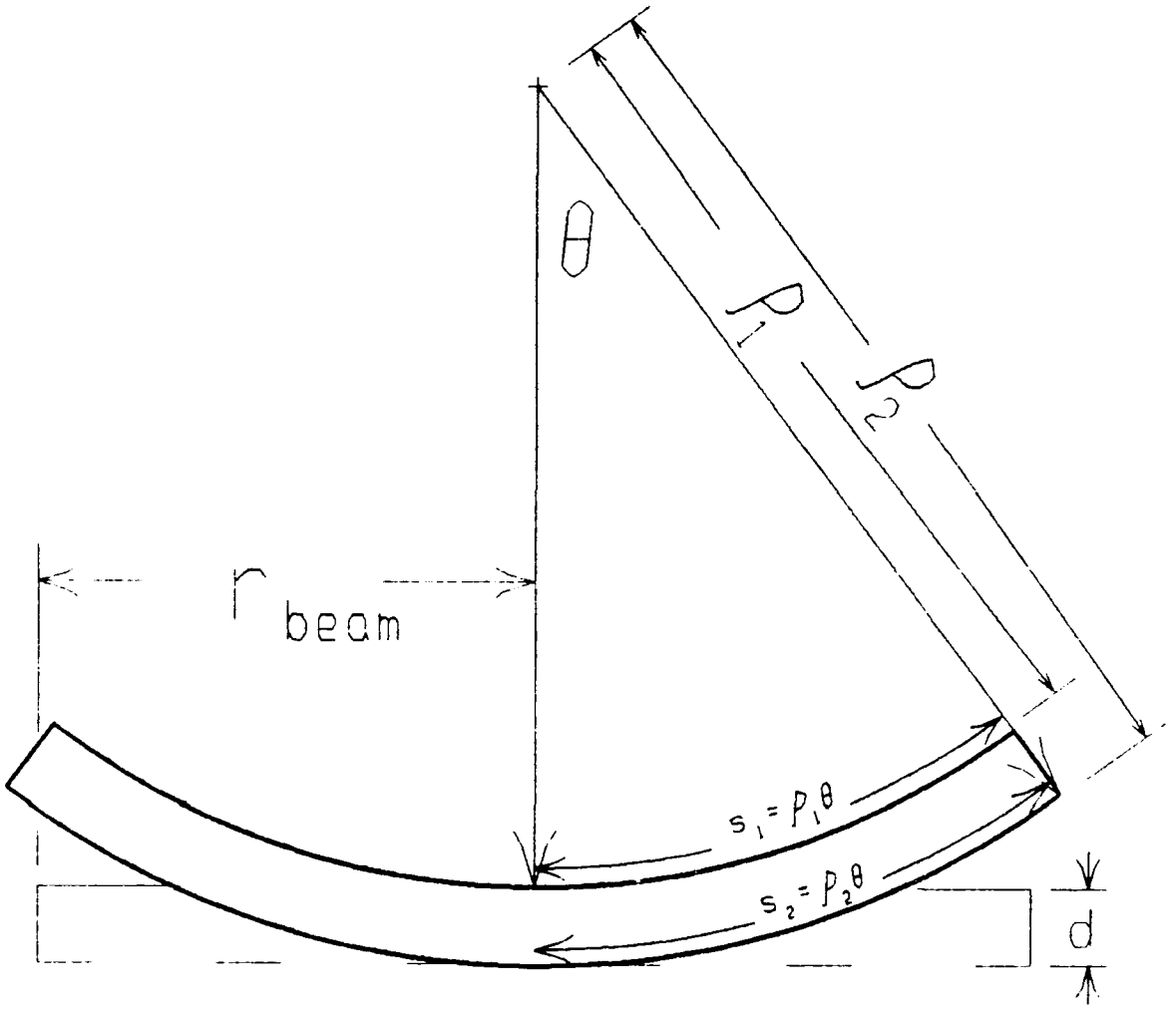

Figure B2. Thermal Curvature of Free Beam with a Temperature Gradient

$S_1 = r + \Delta u_U = \rho_1 \theta$ where Δu_U is the displacement of the top edge of the fiber

$S_2 = r + \Delta u_L = \rho_2 \theta$ where Δu_U is the displacement of the lower edge of the fiber

$$\theta = \frac{r + \Delta u_U}{\rho_1} = \frac{r + \Delta u_L}{\rho_1 + d} = \frac{r + \Delta u_L}{d + \frac{r + \Delta u_U}{\theta}}$$

$$\theta = \frac{\Delta u_L - \Delta u_U}{d} = \frac{r\alpha_1 T_L - r\alpha_1 T_U}{d}$$

$$\rho_1 = \rho_t = \frac{r + \Delta u_U}{\theta}$$

$$\rho_t = \frac{d\left[1 + \alpha_1 T_U\right]}{\alpha_1 \Delta T} \qquad \text{(B4)}$$

However, the section AB is not free to rotate, but instead has a curvature (assumed constant) equal to the sum of thermal curvature, $1/\rho_t$ plus the curvature due to the bending moment M_B applied at the ends of section AB (4:406). If the matrix resin (elastic foundation) is removed by pyrolysis at 700°K and the fiber remains intact, at temperatures above 700°K the heated section AB may be considered to be constrained as shown in Figure B3, with curvature given by

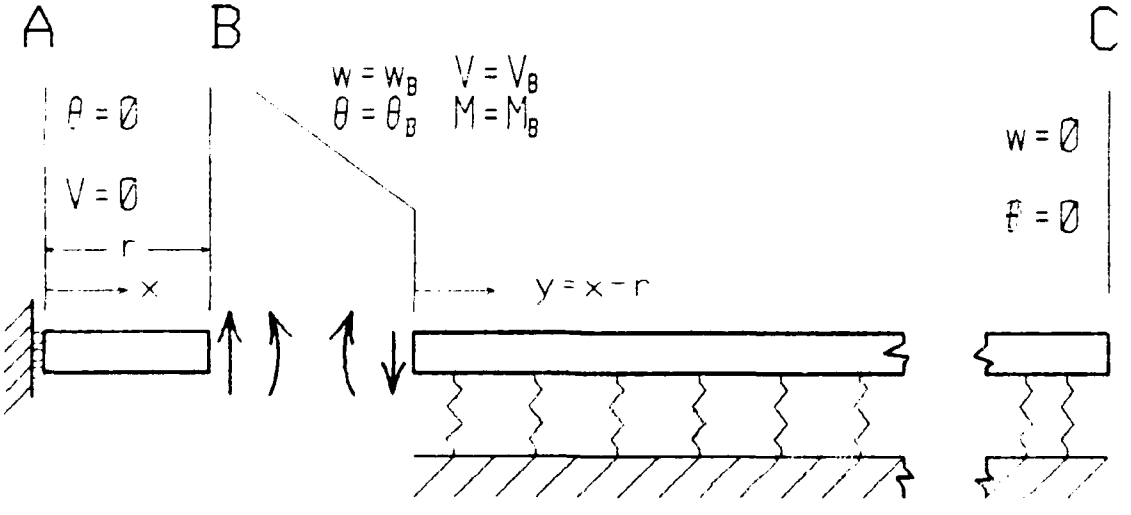

Figure B3. End Conditions for Beams AB and BC

$$w''_{AB}(x) = w''_{homogeneous} + w''_{thermal}$$

$$= \frac{M_B}{EI} + \frac{1}{\rho_t}$$

Two integrations with respect to x yields

$$w_{AB}(x) = \left[\frac{1}{\rho_t} + \frac{M_B}{EI}\right] * \frac{x^2}{2} + Ax + B \qquad \text{(B5)}$$

Symmetry of the fiber about x=Ø requires that w'(Ø) = Ø and V(0) = EIw'''(0) = 0. Continuity at point B (x=r) is required of the deflection, slope and moment. The substitution y = x-r will be made in Equation (B3) so that section BC may be thought of as a semi-infinite beam starting at y=0. This yields the following system to be solved...

$$w_{AB}(x) = \left[\frac{1}{\rho} + \frac{M_B}{EI}\right] * \frac{x^2}{2} + Ax + B \qquad \text{(B6)}$$

$$w_{BC}(y) = e^{-\beta y}\,(C'\cos\beta y + D'\sin\beta y) \qquad \text{(B7)}$$

subject to

$$w'_{AB}(Ø) = Ø \qquad \text{(B8a)}$$

$$w'''_{AB}(Ø) = Ø \qquad \text{(b)}$$

$$w_{AB}(x=r) = w_{BC}(y=Ø) \qquad \text{(c)}$$

$$w'_{AB}(x=r) = w'_{BC}(y=\emptyset) \qquad (d)$$

$$M_B = EI\, w''_{BC}(y=\emptyset) \qquad (e)$$

where M_B, A, B, C', D' are to be determined from Equations (B8).

$$(B8a),\ (B6) \rightarrow \left[\frac{1}{\rho_t} + \frac{M_B}{EI}\right] \cdot 0 + A = 0 \rightarrow A = 0$$

$$(B8c) \rightarrow \left[\frac{1}{\rho_t} + \frac{M_B}{EI}\right] * \frac{r^2}{2} + B = C' \qquad (B9)$$

$$(B8d) \rightarrow \left[\frac{1}{\rho_t} + \frac{M_B}{EI}\right] * r = \beta(-C' + D') \qquad (B10)$$

$$(B8e) \rightarrow M_B = EI\ (-2\beta^2 D') \rightarrow D' = \frac{-M_B}{2\beta^2 EI} \qquad (B11)$$

Since $w'''_{AB} \equiv 0$, Equation (B8b) is solved identically. However, equlibrium of forces in the z direction requires that $V(x=r) = 0 = V(y=0)$. This leads to

$$0 = 2\beta^2(C' + D') \rightarrow C' = -D' \qquad (B12)$$

(B10),(B11),(B12) →

$$\left[\frac{1}{\rho_t} + \frac{M_B}{EI}\right] r = 2\beta D'$$

$$= 2\beta\left[\frac{-M_B}{2\beta^2 EI}\right]$$

$$\frac{r}{\rho_t} = \frac{-M_B}{\beta EI} - \frac{M_B r}{EI}$$

$$M_B = \frac{-rEI}{\left[\frac{1}{\beta} + r\right]\rho_t} \qquad \text{(B13)}$$

(B11),(B13) → $$D' = \frac{-M_B}{2\beta^2 EI}$$

$$= \frac{rEI}{\rho_t \left[\frac{1}{\beta} + r\right] 2\beta^2 EI}$$

$$= \frac{r}{2\rho_t \beta^2 \left[\frac{1}{\beta} + r\right]} \qquad \text{(B14)}$$

(B12),(B14) → $$C' = -D'$$

$$= \frac{-r}{2\rho_t \beta^2 \left[\frac{1}{\beta} + r\right]} \qquad \text{(B15)}$$

(B9),(B13),(B15) →

$$B = C' - \frac{r^2}{2}\left[\frac{1}{\rho_t} + \frac{M_B}{EI}\right]$$

$$B = \frac{-r}{2\rho_t \beta^2 \left(\frac{1}{\beta} + r\right)} - \frac{r^2}{2\rho_t} - \frac{M_B r^2}{2EI}$$

$$= \frac{r}{2\rho_t} \left[\frac{r^2}{\gamma} - r - \frac{1}{\beta^2 \gamma}\right] \qquad \text{(B16)}$$

where $\gamma \equiv \frac{1}{\beta} + r$

Note two interesting limits on these constants;

$$\lim_{\beta \to \infty} M_B = \frac{-EI}{\rho_t}$$

which is the solution for a double-fixed beam subjected to a temperature gradient (4:406). This agrees with the intuitive observation that a beam section BC on an infinitely stiff foundation will act like a fixed wall to the section AB.

Also, $\lim_{\beta \to \infty} \gamma = r$, which implies $\lim_{\beta \to \infty} B = \frac{r}{2\rho_t} \left[r - r - \emptyset\right] = 0.$

This also agrees with the solution for a double fixed beam.

The reduction in bending moment in the section AB can be seen most easily by defining a quantity

$$M^* \equiv \frac{M_B}{-EI/\rho_t} = \frac{r}{\gamma} \tag{B17}$$

$M^*=1$ implies the bending moment in AB is identical to that of a fixed wall beam. The effect of laser beam radius r and foundation stiffness β is shown in Figure B4, which clearly shows that for spot sizes and foundation stiffnesses seen in the experimental setup, $M \approx 1$.

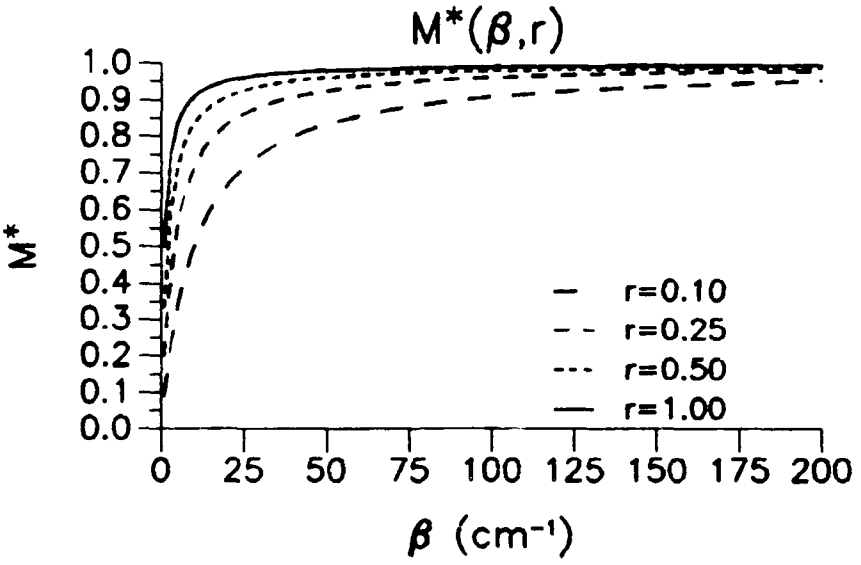

Figure B4. M^* versus β and r

To estimate β, first estimate the foundation modulus k, which is the ratio of beam loading per unit length to the deflection (7). As shown in Figure B5, for a length of beam L with force p on it, the pressure on the foundation of modulus E_m will be $\sigma = \frac{p}{dL}$. This will also be the stress in the foundation which causes strain $\varepsilon = \delta/h$, where h is the thickness of the foundation.

$$\varepsilon = \frac{\sigma}{E_m} = \frac{\delta}{h} = \frac{p}{d\ L\ E_m}$$

Since $k = \frac{p}{L\ \delta}$, we get

$$k = \frac{p}{L} \frac{d\ L\ E_m}{ph}$$

$$= \frac{d\ E_m}{h}$$

Assuming a foundation of epoxy resin as thick as the distance between fibers (assumed equal to a fiber diameter)

$$k \approx \frac{d\ E_m}{h} = \frac{8\text{x}10^{-4}\text{cm} \cdot 2.4\text{x}10^{7}\ \text{N cm}^{-2}}{8\text{x}10^{-4}\ \text{cm}}$$

Therefore,

$$\beta^4 = \frac{k}{4\ E\ I} = \frac{k}{4E\ \frac{\pi}{64}\ d^4}$$

$$= \frac{2.4\text{x}10^{7}\text{N cm}^{-2}}{4\text{x}2.35\text{x}10^{7}\text{Ncm}^{-2}\ \frac{\pi}{64}\ \left(8\text{x}10^{-4}\text{cm}\right)^4}$$

$$\beta \approx 1890\ \text{cm}^{-1} >> 200\ \text{cm}^{-1}$$

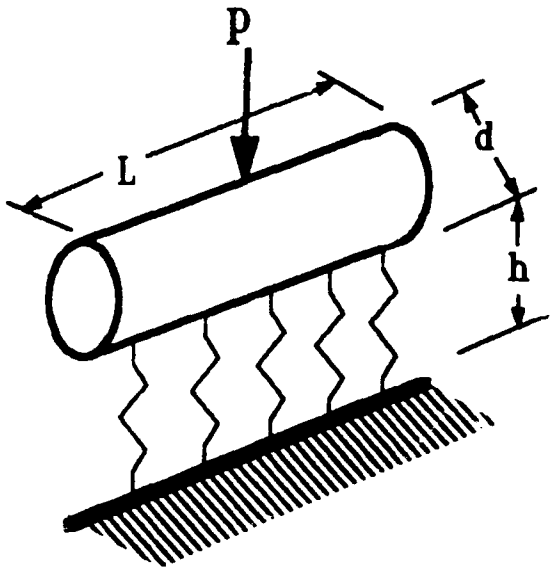

Figure B5. Estimation of Foundation Modulus

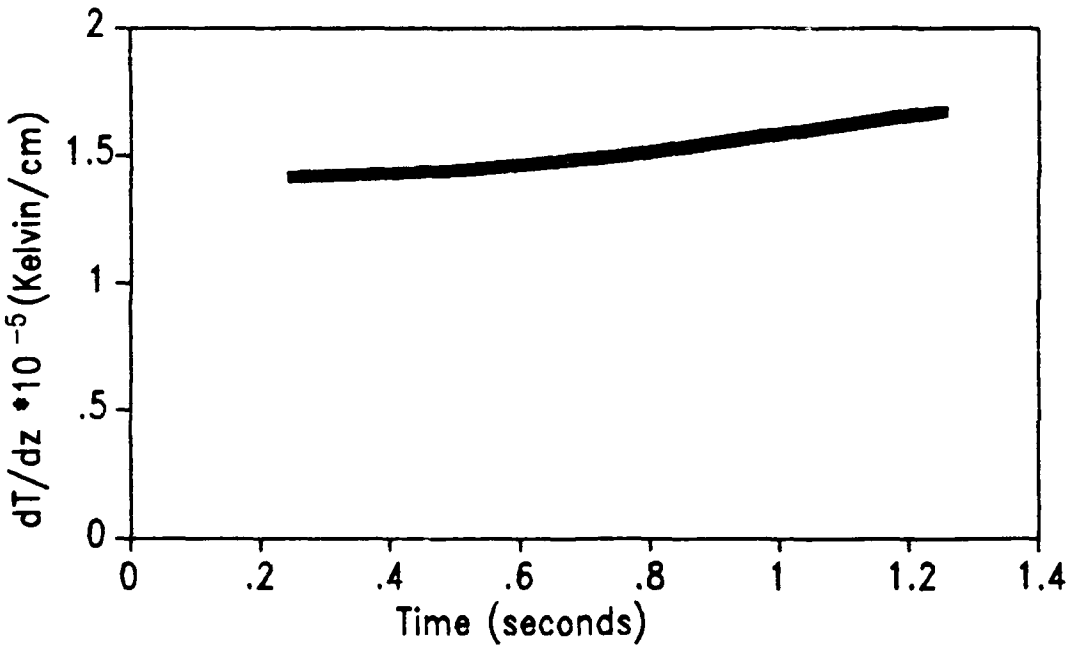

Figure B6. Temperature Gradient in Graphite/Epoxy at 10kW/cm^2 via MELT3D.FOR

For a laser beam radius of r=1.0 cm and $\beta >> 200\ cm^{-1}$, $M_B \approx EI/\rho_t$.

The maximum axial stress from M_B will be

$$\sigma_{x_M} = \frac{M\,y}{I} = \frac{M(d/2)}{I}$$

$$\therefore \sigma_{x_M} = \frac{E\,I}{\rho_t}\,\frac{(d/2)}{I} \qquad \text{(B18)}$$

From MELT3D.FOR, the magnitude of the thermal gradient at $10 kW/cm^2$ is < 200,000 °K/cm (Figure B6). Across the first surface fiber, the temperature difference is $\Delta T \approx 150°K$.

From Chapter III,

$$\rho_t = \frac{d\left[1 + \alpha\, T_U\right]}{\alpha\, \Delta\, T} \qquad \text{(B19)}$$

$$= \frac{8\times10^{-4}cm\left[1-3.3\times10^{-7}\ °K^{-1}\cdot\ 3800°K\right]}{-3.3\times10^{-7}\cdot\ 150°K}$$

$$= -16.1\ cm$$

Therefore from Equation (B18) and Equation (B19)

$$\sigma_{x_M} \approx \frac{E\ (d/2)}{\rho_t}$$

$$\approx \frac{2.4\times10^{7}\ Ncm^{-2}\ \cdot\ \frac{8\times10^{-4}cm}{2}}{-16.1\ cm}$$

$$\approx -600\ N\ cm^{-2} = -6\ MPa$$

But σ_{ult} = 3795 MPa, so

$$\left| \frac{\sigma_{x_M}}{\sigma_{ult}} \right| = \frac{6}{3795} = 0.16\%.$$

But $\sigma_{x_{axial}} = E_1 \varepsilon_1$. When loaded to 2/3 fracture load, $\varepsilon_1 = \frac{2\varepsilon_{ult}}{3}$.

$$\sigma_{x_{axial}} = \frac{2\ \varepsilon_{ult}}{3}\ E_1$$

$$\sigma_{x_{axial}} = \frac{2\ (0.0148)}{3}\ 235 \times 10^9\ \text{Pa}$$

$$= 2.31\ \text{GPa}$$

$$\frac{\sigma_{x_{axial}}}{\sigma_{ult}} = \frac{2.31\ \text{GPa}}{3.795\ \text{GPa}} = 61\%$$

$$\frac{\sigma_{x_M}}{\sigma_{x_{axial}}} = \frac{6\text{MPa}}{2310\ \text{MPa}} = 0.26\%$$

Therefore, bending stresses are appropriately negligible.

Appendix C: Fabrication of AS4/3502 Graphite/Epoxy Test Specimens

The graphite/epoxy (GE) specimens tested in this program were laid up, cured and cut to size by the Structures Survivability/Supportability Group of the Flight Dynamics Laboratory, Wright Research and Development Center (WRDC/FIBCA). Specimen specifications described in Figure C1 were given to the thesis sponsor, and fabricated as described in this appendix.

Layup of the panels was performed by a vacuum bag process as shown in Figure C2.

After the panels are laid up and sealed under vacuum (Fig C2a) they are cured in an autoclave in a manner similar to that suggested in Reference 6:20 (Figure C3).

1. Pull 20 in. (508mm) minimum vacuum on part.
2. Place in autoclave.
3. Raise temperature to 275°F(135°C) at 3-5°F/minute (2-3°C/minute).
4. Hold for 15 minutes at 275°F(135°C) under vacuum pressure only.
5. Pressurize autoclave to 85psi(586 kPa).
6. Hold at 275°F(135°C), 85psi(586 kPa), and vacuum on the part for 45 minutes.
7. Raise temperature to 350°F(177°C) at 3-5°F/minute (2-3°C/minute).
8. Hold for 2 hours.
9. Cool part to 150°F(66°C) in not less than 45 minutes, maintain pressure and vacuum.
10. Remove from autoclave and unbag.

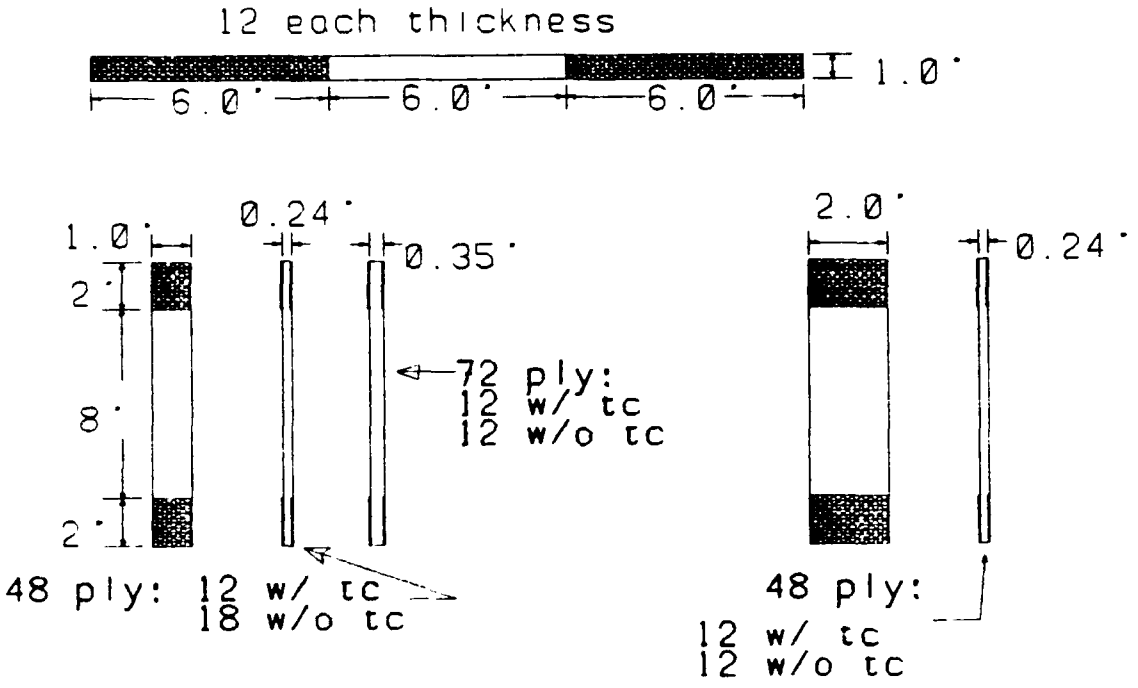

(a) Tenstle Specimens

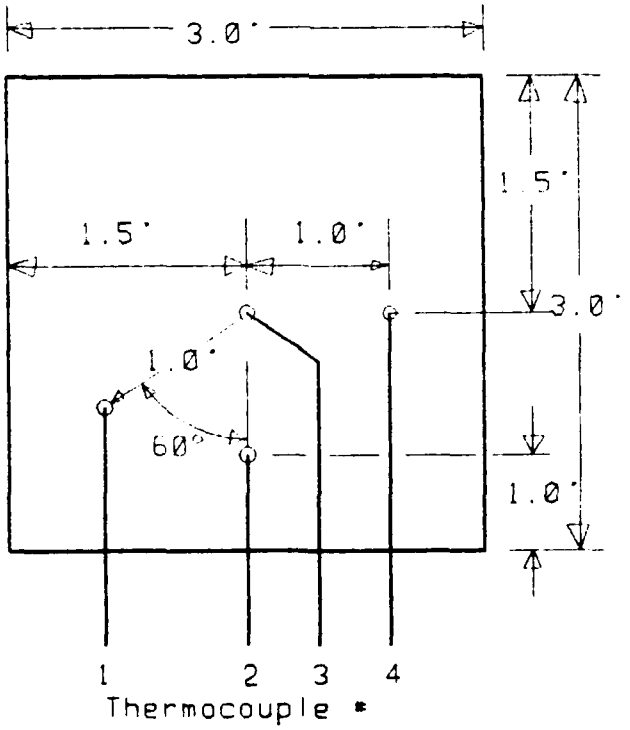

(b) Unloaded Specimens

Figure C1. Test Specimen Specifications

TYPICAL ACCEPTANCE PANEL FABRICATION SEQUENCE

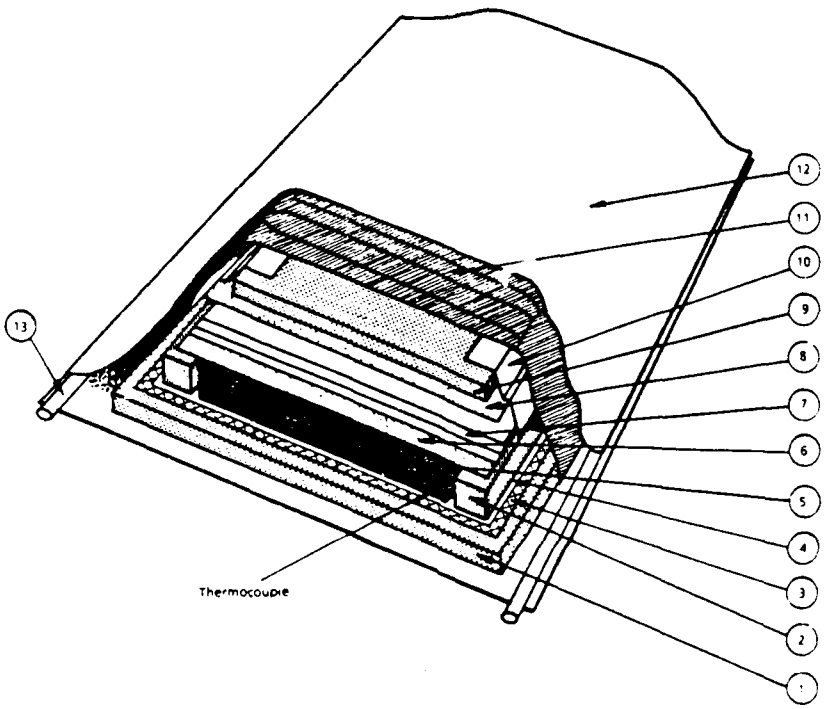

1. Base plate: Aluminum 1/4 to 1/2 in. thick
2. Cork dam: Cork 1/8 x 1 in. with pressure-sensitive adhesive backing (Corprene) or equivalent
3. Release film: Teflon, nonperforated 0.001-0.004 in. thick
4. Release fabric: Fabric enfab TX 10-40 release (porous) or equivalent
5. Prepreg layup
6. Release fabric: Fabric enfab TX 10-40 release (porous)
7. Resin bleeders: Cloth, fiberglass No. 120 (as per calculation on following page)
8. Release film: Teflon, nonperforated 0.001-01.004 in. thick
9. Caul plate: Aluminum, 0.030 in. minimum
10. Tape: Pressure-sensitive, green polyester silicone
11. Air bleeder: Style 1581 glass or equivalent
12. Vacuum bag: Film capron 80, hi-temp nylon, 0.002 in. thick
13. High temperature sealant: Schnee Morehead

Mold release: Frekote-33 or equivalent

(a) Typical Vacuum Bag Layup (6:23)

Figure C2. Fabrication of Test Samples

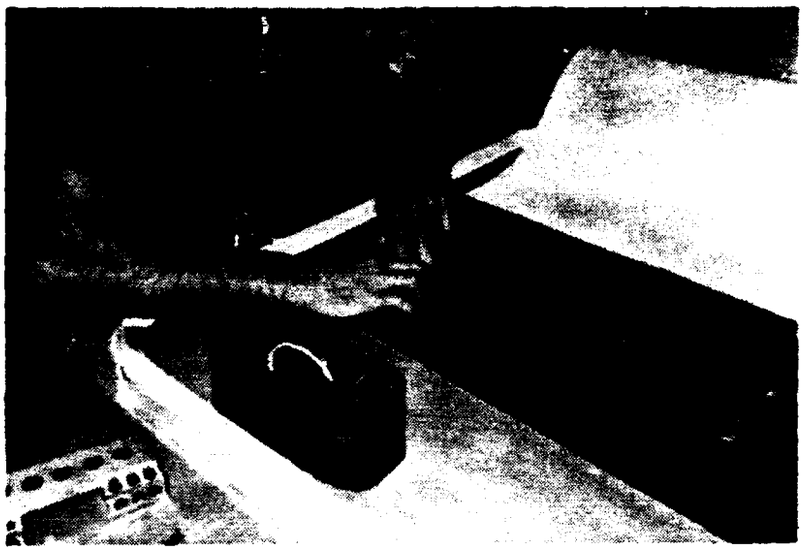

(b) Layup Process

(c) Layup Process (Continued)
Figure C2. (Continued)

(d) Layup Process (Concluded)
Figure C2. (Concluded)

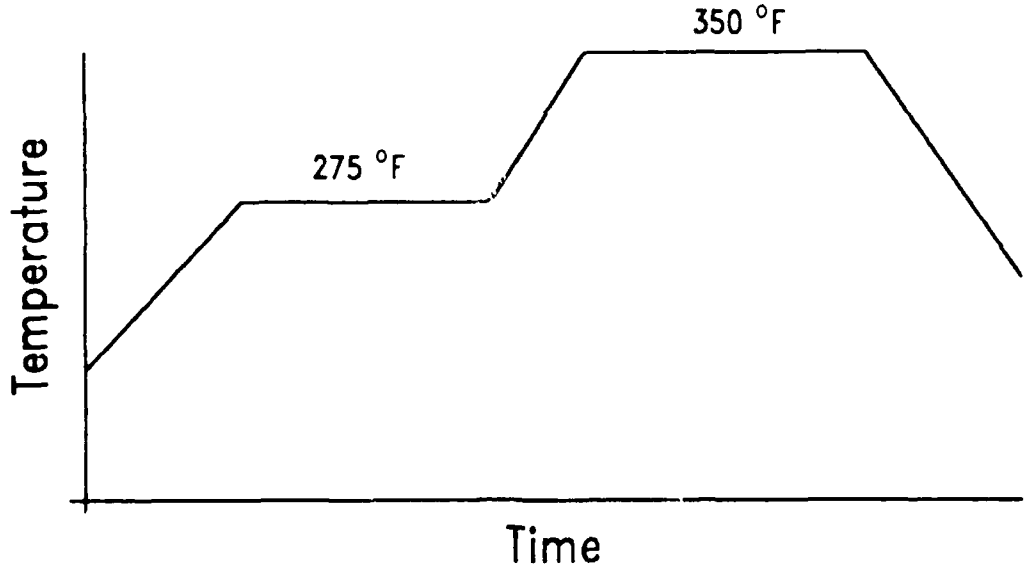

Figure C3. Hercules Suggested Cure Cycle for AS4/3502 (6:20)

The cured panels were examined by computerized axial tomography (CAT) scan to reveal any areas of incomplete interply bonding. Panels fabricated with thermoccuple wire embedded in them were x-rayed to discern any shifting of the thermocouple positions that may have occurred. No flaws were visible to either of these techniques.

Evidence that the structural integrity of the specimens was as high as practically achievable was also found in post mortem inspection of a failed specimen. One sample was tested in tension to failure (Figure C4). At 87% of the predicted strength, failure occured at the grip fixture (note step in output created by delay in switching the amplifier gain as strain gauge output changed scales).

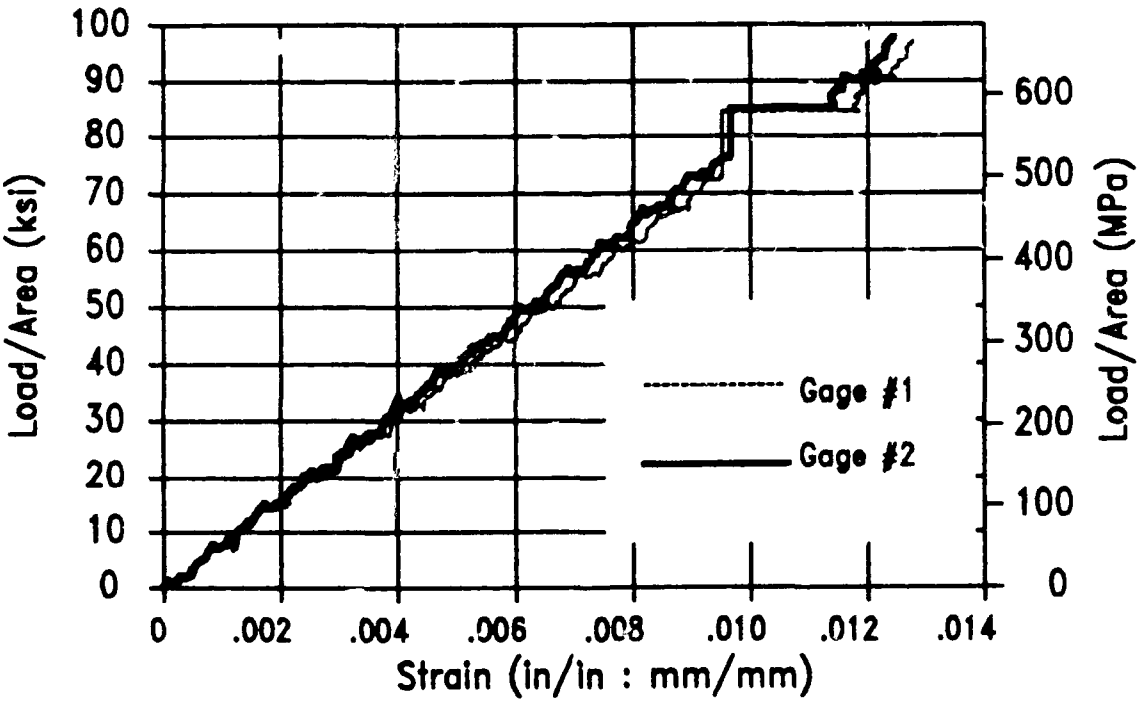

Figure C4. Load versus Strain Gage Output for Sample JH13189-4 #3

Failure was limited to the immediate area of the fracture. Virtually no delamination was observed except in the midplane of the specimen, where the failure remained between the intially separated ply. The strong bonding of fibers to matrix which prevented this delamination from running into other plys, and the nearly intact fracture surface show that the lamination process in this specimen was very sucessful (Figures C5-C8).

Lastly, fiberglass end tabs were attached to specimens intended for tensile testing, and panels were cut to size using a diamond saw.

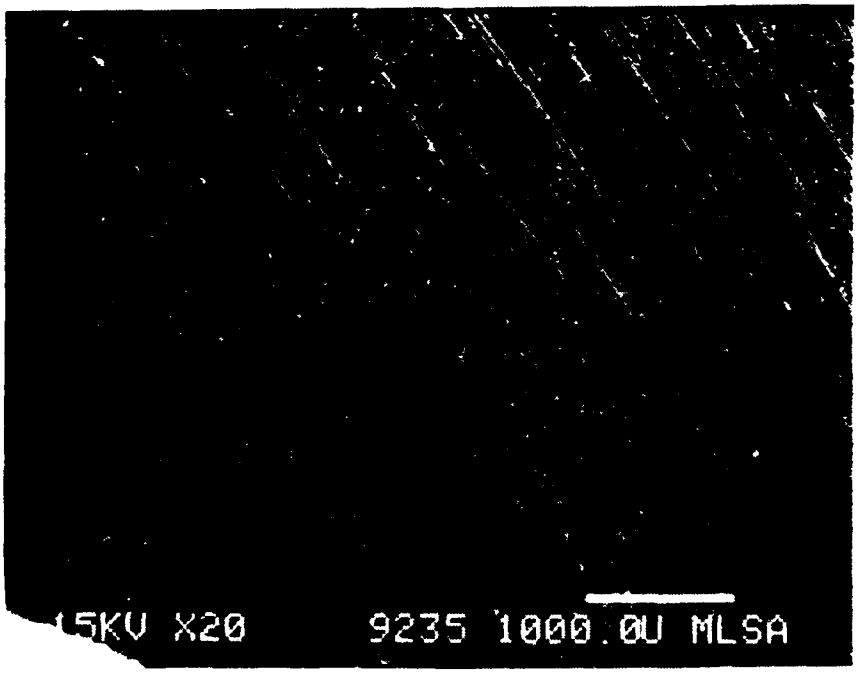

Figure C5. Sample JH13189-4 #3, Delamination Surface (20X)

Figure C6. Sample JH13189-4 #3, Fracture Surface (20X)

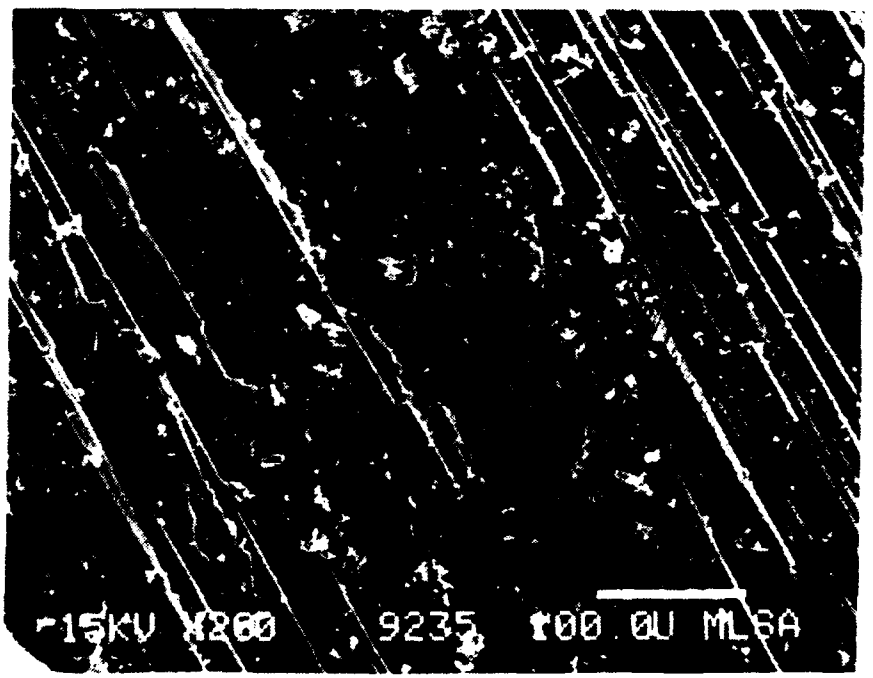

Figure C7. Sample JH13189-4 #3, Delamination Surface (200X)

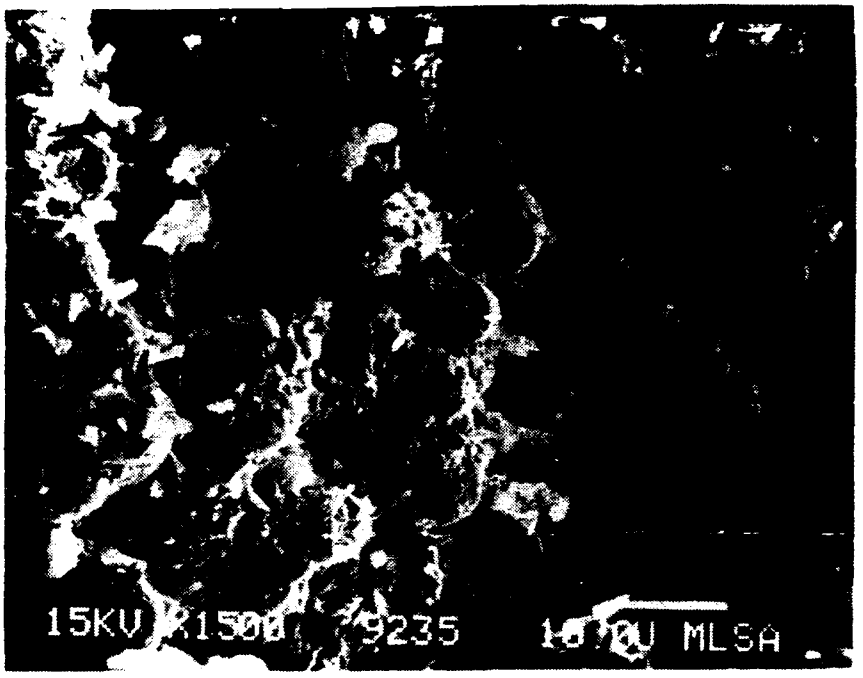

Figure C8. Sample JH13189-4 #3, Fracture Surface (1500X)

Appendix D: Test Results from LHMEL-1

To verify the plausibility of exploring a decrease in effective ablation enthalpy for graphite/epoxy, initial tests were conducted using the 15 kW Laser Hardened Materials Evaluation Laser-1 (LHMEL-1). These were cursory tests with very limited objectives. The only results intended were to see if graphite/epoxy did indeed ablate faster when loaded in tension than when unloaded. These data are shown in Figure D1. The number labeling the data points are intensities at which each was taken. Some data on temperature rise in the center of sample #CH13989-4#12 was also collected (Figure 3). This sample was 2.0 inches (5.08 cm) wide and 0.244 inches (0.620 cm) thick the thermocouple plotted in Figure 3 was in the center of the sample. It was exposed to 1700 kW/cm^2 (11 kW power over 6.53 cm^2 area) for 6.0 seconds. These parameters were input to MELT3D.FOR to generate the data plotted in the figure.

Table III.
LHMEL-1 Test Results

Power (kW)	Area (cm^2)	Intensity (kW/cm^2)	Time (sec)	Mass Loss (gm)	Q*eff (kJ/gm)	LOAD (lbf)	(N)	Stress Ratio
11.5	1.54	7.5	2.00	0.65	35.3	12000	53379	0.33
11.5	1.54	7.5	1.19	0.40	34.2	0	0	0.00
11.5	2.18	5.3	2.18	0.75	33.4	12000	53379	0.50
11.5	2.18	5.3	3.00	0.90	38.3	6000	26689	0.25
11.5	2.18	5.3	2.20	0.60	42.1	9000	40034	0.37
11.5	2.18	5.3	6.50	1.88	39.7	0	0	0.00

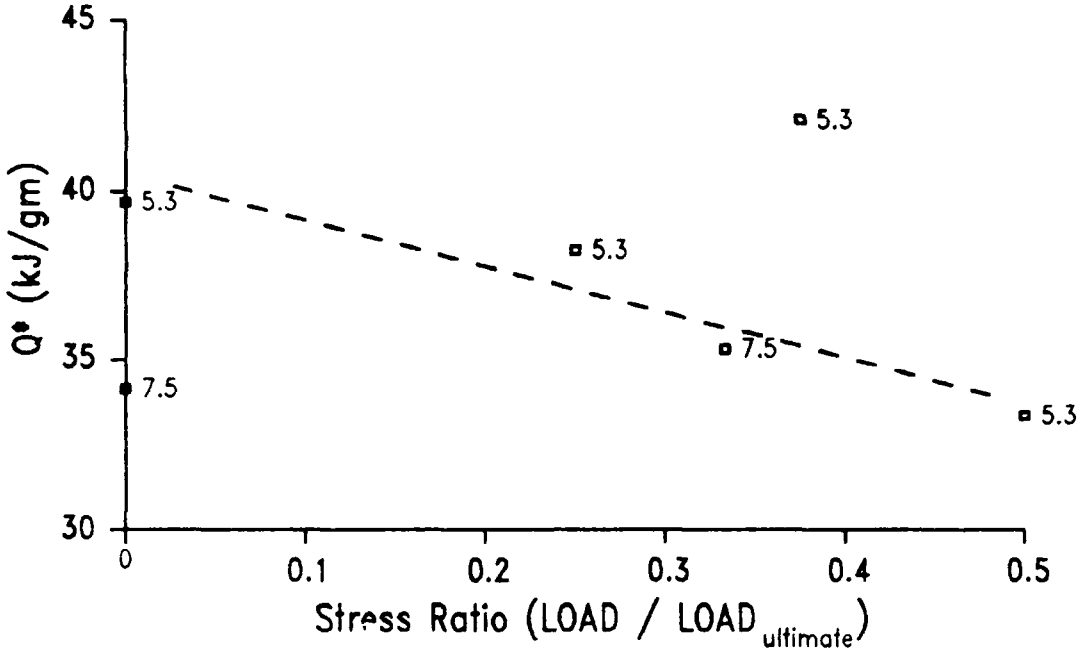

Figure D1. LHMEL-1 Preliminary Results

Bibliography

1. Broek, David, Elementary Engineering Fracture Mechanics, 4th Rvsd Ed, Martinus Nijhoff, Dordrecht, Netherlands, 1986

2. Cozzens, Robert F., Particle Collection Data and Observations, WSMR HI-I Series Summer 1986, Internal Report, Naval Research Laboratory, Washington, DC, September 1986

3. CRC Press, Handbook of Chemistry and Physics, 53rd ed., Chemical Rubber Co., Cleveland, OH, 1972

4. Gere, James M., Timoshenko, Stephen P.,Mechanics of Materials, 2nd Ed, Brooks/Cole Engineering Division, Belmont, CA, 1984

5. Griffis, C. A. et al. Thermal Response of Graphite Epoxy Composite Subjected to Rapid Heating, Naval Research Laboratory, Washington, DC., March 1981 (AD-A096898).

6. Hercules Aerospace Products Group, Magnamite AS4/3502 Graphite Prepreg Tape and Fabric Module, Product Brochure, Magna, UT, 84044, July 1985

7. Hetenyi, Miklos, Beams on Elastic Foundation, University of Michigan Press, Ann Arbor, MI, 1946

8. High Temperature Materials - Mechanical, Electronic and Thermophysical Properties Information Analysis Center (HTMIAC) online database; Center for Information and Numerical Data Analysis and Synthesis (CINDAS), Purdue University; 2595 Yeager Road, West Lafayette, IN 47906

9. Jones, Robert M., Mechanics of Composite Materials, New York: Hemisphere Publishing Corp., 1975.

10. Özişik, M. Necati. Heat Conduction, New York: John Wiley and Sons, 1980.

11. Saada, Adel S., Elasticity: Theory and Applications, Krieger, Malabar, FL, 1987

12. Sendeckyj, George P., "Surface Notches in Composites," Fracture of Composite Materials: Proceedings of the Second USA-USSR Symposium, held at Lehigh University, Bethlehem, PA March 9-12, 1981. 115-127. The Hague, Netherlands: Martinus Nijhoff Publishers, 1982.

13. Torvik, Peter J., A Numerical Procedure for Two Dimensional Heating and Melting Calculations, with Applications to Laser Effects, AFIT-TR-72-2. School of Engineering, Air Force Institute of Technology (AU), Wright-Patterson AFB, OH, March 1972.

14. ----- On the Generation of Stress and Deformation in Elastic Solids by High Powered Lasers, AFIT-TR-80-6. School of Engineering, Air Force Institute of Technology (AU), Wright-Patterson AFB, OH, September 1980

15. ----- Some Further Numerical Studies of Laser Induced Melting and Vaporization, AFIT-TR-73-1. School of Engineering, Air Force Institute of Technology (AU), Wright-Patterson AFB, OH, January 1973

16. ----- Thermal Response Calculations and Their Role in the Design of Experiments, AFIT-TR-73-1. School of Engineering, Air Force Institute of Technology (AU), Wright-Patterson AFB, OH, December 1973

17. Phone conversation with Mr. Jorge Beraun, Air Force Weapons Laboratory (WL/TALE), Kirtland AFB, NM, 13 November 1989.

18. Phone conversations with Dr. Robert F. Cozzens, George Mason University, Washington, DC, February-July 1989

19. Phone conversation with Dr. William Laughlin, Physical Sciences, Inc., Andover, MA, 15 November 1989.

Vita

Captain Joseph Leon Hamrick, II [redacted]. He attended high school in Tucker County, WV until the 11th grade. He dropped out to accept early admission in the Freshman Honors Program at the University of Delaware in 1980. He earned the degree of Bachelor of Mechanical Engineering on 2 June 1984, and was commissioned into the USAF through AFROTC Detachment 128. He reported to the Air Force Weapons Laboratory in July 1984 were he was a Project Engineer involved in researching the lethality of Directed Energy Weapons against aerospace systems. While at the Weapons Laboratory, he received two AF Achievement Medals and an AF Commendation Medal for his efforts in projects to demonstrate High Energy Laser effectiveness against various targets. He was selected to enter the School of Engineering, Air Force Institute of Technology in May 1988.

[redacted]

UNCLASSIFIED
SECURITY CLASSIFICATION OF THIS PAGE

REPORT DOCUMENTATION PAGE

Form Approved
OMB No. 0704-0188

1a. REPORT SECURITY CLASSIFICATION UNCLASSIFIED	1b. RESTRICTIVE MARKINGS
2a. SECURITY CLASSIFICATION AUTHORITY	3. DISTRIBUTION/AVAILABILITY OF REPORT Approved for Public Release; Distribution Unlimited
2b. DECLASSIFICATION/DOWNGRADING SCHEDULE	
4. PERFORMING ORGANIZATION REPORT NUMBER(S) AFIT/GAE/ENY/89D-12	5. MONITORING ORGANIZATION REPORT NUMBER(S)
6a. NAME OF PERFORMING ORGANIZATION School of Engineering 6b. OFFICE SYMBOL (*If applicable*) AFIT/ENY	7a. NAME OF MONITORING ORGANIZATION
6c. ADDRESS (*City, State, and ZIP Code*) Air Force Institute of Technology (AU) Wright-Patterson AFB, Ohio 45433-6583	7b. ADDRESS (*City, State, and ZIP Code*)
8a. NAME OF FUNDING/SPONSORING ORGANIZATION Hardened Materials Branch 8b. OFFICE SYMBOL (*If applicable*) WRDC/MLPJ	9 PROCUREMENT INSTRUMENT IDENTIFICATION NUMBER
8c. ADDRESS (*City, State, and ZIP Code*) Wright Research and Development Center (AFSC) Wright-Patterson AFB, Ohio 45433-6533	10. SOURCE OF FUNDING NUMBERS PROGRAM ELEMENT NO. 63211F; PROJECT NO. 2135; TASK NO 00; WORK UNIT ACCESSION NO 03
11. TITLE (*Include Security Classification*) THE EFFECT OF LOADING ON THE LASER ABLATION OF GRAPHITE/EPOXY COMPOSITE MATERIAL	
12. PERSONAL AUTHOR(S) Joseph L. Hamrick,II, Captain USAF	
13a. TYPE OF REPORT MS Thesis 13b. TIME COVERED FROM _____ TO _____ 14. DATE OF REPORT (*Year, Month, Day*) 1989 December 15. PAGE COUNT 119	
16. SUPPLEMENTARY NOTATION	

17. COSATI CODES		
FIELD	GROUP	SUB-GROUP
11	04	

18. SUBJECT TERMS (*Continue on reverse if necessary and identify by block number*)
Laser Damage; Laser Target Interactions
Carbon Reinforced Composites; Carbon Dioxide Lasers

19. ABSTRACT (*Continue on reverse if necessary and identify by block number*)

Thesis Advisor: Peter J. Torvik
Professor and Head
Department of Aeronautics and Astronautics

20. DISTRIBUTION/AVAILABILITY OF ABSTRACT ☒ UNCLASSIFIED/UNLIMITED ☐ SAME AS RPT. ☐ DTIC USERS	21. ABSTRACT SECURITY CLASSIFICATION UNCLASSIFIED
22a. NAME OF RESPONSIBLE INDIVIDUAL Peter J. Torvik, Prof.& Head, Dept Aero & Astro	22b. TELEPHONE (*Include Area Code*) (513) 255-2362 22c. OFFICE SYMBOL AFIT/ENY

DD Form 1473, JUN 86 *Previous editions are obsolete.*

SECURITY CLASSIFICATION OF THIS PAGE
UNCLASSIFIED

19. Abstract

An investigation was conducted to quantify the effect structural loading of a graphite/epoxy member has upon the mass removal rate during laser ablation. An effective heat of ablation (Q^*_{eff} = energy absorbed / mass removed) was used as a measure of this efficiency. A simple physical model of the important factors affecting the graphite/epoxy was developed, and predictions were made of the effect of loading on Q^*_{eff}.

A three-dimensional finite difference heat transfer code was written to predict the temperature distribution in the composite while modeling the orthotropic nature of the thermal conductivity tensor.

The effect of thermal and mechanical loads upon the stress distribution in a single fiber was calculated. A hypothesis was formed that fracture of individual fibers, a process linearly dependent upon applied stress, will remove a fraction of the composite independent of the absorption of laser energy. A coefficient of increasing ablation efficiency, η_d, was postulated to increase linearly with axial stress, leading to a linear decrease in Q^*_{eff} with increasing stress.

Uniaxial tensile coupons were fabricated from AS4/3502 graphite/epoxy prepreg, in balanced, symmetric layups ([0/±60]nS). These were placed under tensile loads between 0% and 50% of the laminate's ultimate strength. While loaded, they were irradiated with the EDCL-II 10.6 um device at irradiances between 5 and 26 kW/cm^2.

Linear regression of data taken at 15 kW/cm^2 showed η_d = 0.013 kJ/gm + 1.74 (kJ/gm)/GPa x σ. At 26 kW/cm^2, η_d = 0.087 kJ/gm + 3.36 (kJ/gm)/GPa x σ.

It is concluded that axial fiber stress does linearly decrease the 10.6 um laser energy needed to ablate AS4/3502 graphite/epoxy. A decrease of less than 20 percent was seen in the tests reported here.